



Publicly Accessible Penn Dissertations


2017

Mechanisms And Modifiers Of Protein Misfolding And Toxicity Associated With Multisystem Proteinopathy

Alice Flynn Ford

University of Pennsylvania, aliceford24@gmail.com

Follow this and additional works at: <https://repository.upenn.edu/edissertations>

 Part of the [Biology Commons](#), [Family, Life Course, and Society Commons](#), and the [Neuroscience and Neurobiology Commons](#)

Recommended Citation

Ford, Alice Flynn, "Mechanisms And Modifiers Of Protein Misfolding And Toxicity Associated With Multisystem Proteinopathy" (2017). *Publicly Accessible Penn Dissertations*. 2285.
<https://repository.upenn.edu/edissertations/2285>

This paper is posted at ScholarlyCommons. <https://repository.upenn.edu/edissertations/2285>
For more information, please contact repository@pobox.upenn.edu.

Mechanisms And Modifiers Of Protein Misfolding And Toxicity Associated With Multisystem Proteinopathy

Abstract

Multisystem proteinopathy (MSP) is a degenerative syndrome incorporating features of inclusion body myopathy (IBM), Paget's disease of bone (PDB), frontotemporal dementia (FTD), and amyotrophic lateral sclerosis (ALS) that is currently incurable and ultimately fatal. Missense mutations in the prion-like domains (PrLDs) of the genes encoding the RNA-binding proteins (RBPs) heterogeneous nuclear ribonucleoprotein (hnRNP) A1 (D262V) and hnRNPA2 (D290V) cause MSP. These MSP-linked mutations introduce a potent steric zipper into the PrLD and accelerate spontaneous hnRNPA1 and hnRNPA2 fibrillogenesis. However, the mechanism by which these variants of hnRNPA1 and hnRNPA2 cause disease is unknown. Here, we employ *Saccharomyces cerevisiae* as a model system to recapitulate the cellular phenotype seen in MSP patients and map the determinants of hnRNPA1 and hnRNPA2 toxicity and misfolding. We have also utilized a candidate gene approach and an unbiased gene deletion screen to identify genetic modifiers of hnRNPA1 and hnRNPA2 toxicity. Using a series of deletion and truncation constructs, we have determined that hnRNPA1 and hnRNPA2 require at least one intact RNA-recognition motif and a portion of the low complexity PrLD to confer toxicity. Thus, we propose a mechanism of toxicity that requires RNA binding and formation of cytoplasmic inclusions by hnRNPA1 or hnRNPA2. hnRNPA1 and hnRNPA2 form self-templating fibrils *in vitro*, which cannot occur in the absence of the PrLD. We identified forty gene deletions that suppressed the toxicity of hnRNPA1 and hnRNPA2, including RNP (ribonucleoprotein)-granule components (Sbp1, Lsm6, and Lsm7), molecular chaperones (Hsc82, Sti1, Sse1, and Ydj1), and spliceosome proteins (Lsm6, Lsm7, Prp18, and Bud31). In all cases, genetic suppressors of hnRNPA1 toxicity also suppressed hnRNPA2 toxicity, indicating mechanistic convergence. Importantly, only five genes from this list are known modifiers of FUS or TDP-43 toxicity in yeast. TDP-43 and FUS are also RBPs with PrLDs implicated in the pathogenesis of neurodegenerative disease. This lack of overlap in genetic modifiers suggests important mechanistic differences in the underpinnings of cellular toxicity mediated by hnRNPA1 and hnRNPA2 versus TDP-43 or FUS. By contrast, engineered variants of a protein disaggregase, Hsp104, that possess potentiated disaggregase activity suppressed the toxicity of TDP-43 and FUS in addition to hnRNPA1, hnRNPA2, and both MSP-linked mutant hnRNPs. Potentiated Hsp104 variants, therefore, represent a possibly broadly efficacious therapeutic that could be developed to combat a range of neurodegenerative phenotypes caused by RBPs with PrLDs. The toxicity suppressors that we have identified may ultimately have therapeutic implications for not only MSP patients, but also patients with sporadic ALS, FTD, IBM, and PDB. Future work should include investigation of existing small-molecule inhibitors, for example Hsp90 or Hsp70 inhibitors, that mimic the genetic deletions we have uncovered for potential therapeutic use.

Degree Type

Dissertation

Degree Name

Doctor of Philosophy (PhD)

Graduate Group

Neuroscience

First Advisor
James Shorter

Second Advisor
Kelly L. Jordan-Sciutto

Subject Categories
Biology | Family, Life Course, and Society | Neuroscience and Neurobiology

MECHANISMS AND MODIFIERS OF PROTEIN MISFOLDING AND TOXICITY ASSOCIATED
WITH MULTISYSTEM PROTEINOPATHY

Alice Flynn Ford

A DISSERTATION

in

Neuroscience

Presented to the Faculties of the University of Pennsylvania

in

Partial Fulfillment of the Requirements for the

Degree of Doctor of Philosophy

2017

Supervisor of Dissertation

James Shorter, M.A., Ph.D.
Associate Professor of Biochemistry and Biophysics

Graduate Group Chairperson

Joshua I. Gold, Ph.D.
Professor of Neuroscience

Dissertation Committee

Kelly L. Jordan-Sciutto, Ph.D., Professor of Pathology (Chair)

James H. Eberwine, Ph.D., Elmer Holmes Bobst Professor of Pharmacology

Edward B. Lee, MD, Ph.D., Assistant Professor of Pathology and Laboratory Medicine

Kristen W. Lynch, Ph.D., Professor of Biochemistry and Biophysics

Jeremy E. Wilusz, Ph.D., Assistant Professor of Biochemistry and Biophysics

MECHANISMS AND MODIFIERS OF PROTEIN MISFOLDING AND TOXICITY ASSOCIATED
WITH MULTISYSTEM PROTEINOPATHY

COPYRIGHT

2017

Alice Flynn Ford

This work is licensed under the
Creative Commons Attribution-
NonCommercial-ShareAlike 3.0
License

To view a copy of this license, visit

<https://creativecommons.org/licenses/by-nc-sa/3.0/us/>

For Neil.

ACKNOWLEDGMENTS

Thank you, first, to my advisor, Dr. Jim Shorter, for four years of invaluable mentorship, guidance, advice, and patience. You have helped me grow as a writer, thinker, and scientist. Thank you to past and present members of the Shorter lab, whose friendship has made coming to work a pleasure, and whose willingness to answer questions and discuss ideas has been immensely helpful in the completion of this work. I am especially grateful to Dr. Lin Guo, Dr. Mike Soo, Olivia Zhou, Zamia Diaz, Katie Critelli, Lina Bader, Emily Scarborough, and Annie Chen for experimental contributions to this work.

Thank you to Dr. Aaron Gitler and members of the Gitler lab, in particular Dr. Julien Couthouis and Dr. Maria Armakola who directly contributed to this work, for collaboration and valuable discussions. Thank you to Dr. Andrea Stout and the CDB Microscopy Core for assistance with confocal microscopy experiments. Thank you also to Dr. F. Bradley Johnson, Dr. Frank Luca, and Dr. Roy Parker for generously sharing reagents.

I am extremely thankful for funding support from the Center for Neurodegenerative Disease Research T32 Training Grant (NIH/NIA AG00255) and an F31 fellowship from NINDS (F31NS087676).

Thank you to the members of my thesis committee for sharing your thoughts, suggestions, and expertise throughout my thesis work. Thank you to the Penn MSTP, especially Dr. Skip Brass and Maggie Krall, and the Neuroscience Graduate Group, especially Dr. Josh Gold and Christine Clay, for giving me the opportunity to learn at this institution and for offering support and guidance at every stage of training.

Thank you to Dr. Joe Schall at the University of Vermont for teaching me what it means to be a scientist, and for sharing your knowledge and contagious enthusiasm with me during my first four years of bench science.

Thank you to my family, my parents and brothers, for a lifetime of love and support that allowed me to pursue anything I chose. And finally, thank you to my husband, Neil, who, more than anyone else, has made every day of my thesis work so much better and easier than it would have been without him.

ABSTRACT

MECHANISMS AND MODIFIERS OF PROTEIN MISFOLDING AND TOXICITY ASSOCIATED WITH MULTISYSTEM PROTEINOPATHY

Alice Flynn Ford

James Shorter, M.A., Ph.D.

Multisystem proteinopathy (MSP) is a degenerative syndrome incorporating features of inclusion body myopathy (IBM), Paget's disease of bone (PDB), frontotemporal dementia (FTD), and amyotrophic lateral sclerosis (ALS) that is currently incurable and ultimately fatal. Missense mutations in the prion-like domains (PrLDs) of the genes encoding the RNA-binding proteins (RBPs) heterogeneous nuclear ribonucleoprotein (hnRNP) A1 (D262V) and hnRNPA2 (D290V) cause MSP. These MSP-linked mutations introduce a potent steric zipper into the PrLD and accelerate spontaneous hnRNPA1 and hnRNPA2 fibrillogenesis. However, the mechanism by which these variants of hnRNPA1 and hnRNPA2 cause disease is unknown. Here, we employ *Saccharomyces cerevisiae* as a model system to recapitulate the cellular phenotype seen in MSP patients and map the determinants of hnRNPA1 and hnRNPA2 toxicity and misfolding. We have also utilized a candidate gene approach and an unbiased gene deletion screen to identify genetic modifiers of hnRNPA1 and hnRNPA2 toxicity. Using a series of deletion and truncation constructs, we have determined that hnRNPA1 and hnRNPA2 require at least one intact RNA-recognition motif and a portion of the low complexity PrLD to confer toxicity. Thus, we propose a mechanism of toxicity that requires RNA binding *and* formation of cytoplasmic inclusions by hnRNPA1 or hnRNPA2. hnRNPA1

and hnRNPA2 form self-templating fibrils *in vitro*, which cannot occur in the absence of the PrLD. We identified forty gene deletions that suppressed the toxicity of hnRNPA1 and hnRNPA2, including RNP (ribonucleoprotein)-granule components (Sbp1, Lsm6, and Lsm7), molecular chaperones (Hsc82, Sti1, Sse1, and Ydj1), and spliceosome proteins (Lsm6, Lsm7, Prp18, and Bud31). In all cases, genetic suppressors of hnRNPA1 toxicity also suppressed hnRNPA2 toxicity, indicating mechanistic convergence. Importantly, only five genes from this list are known modifiers of FUS or TDP-43 toxicity in yeast. TDP-43 and FUS are also RBPs with PrLDs implicated in the pathogenesis of neurodegenerative disease. This lack of overlap in genetic modifiers suggests important mechanistic differences in the underpinnings of cellular toxicity mediated by hnRNPA1 and hnRNPA2 versus TDP-43 or FUS. By contrast, engineered variants of a protein disaggregase, Hsp104, that possess potentiated disaggregase activity suppressed the toxicity of TDP-43 and FUS in addition to hnRNPA1, hnRNPA2, and both MSP-linked mutant hnRNPs. Potentiated Hsp104 variants, therefore, represent a possibly broadly efficacious therapeutic that could be developed to combat a range of neurodegenerative phenotypes caused by RBPs with PrLDs. The toxicity suppressors that we have identified may ultimately have therapeutic implications for not only MSP patients, but also patients with sporadic ALS, FTD, IBM, and PDB. Future work should include investigation of existing small-molecule inhibitors, for example Hsp90 or Hsp70 inhibitors, that mimic the genetic deletions we have uncovered for potential therapeutic use.

TABLE OF CONTENTS

ABSTRACT	VI
LIST OF TABLES.....	XI
LIST OF ILLUSTRATIONS	XII
LIST OF ABBREVIATIONS	XV
CHAPTER 1: INTRODUCTION—RNA-BINDING PROTEINS WITH PRION-LIKE DOMAINS IN HEALTH AND DISEASE	1
1.1 Protein misfolding unites diverse neurodegenerative diseases.....	1
1.2 ALS and FTD are related disorders	2
1.3 Prions are self-replicating protein conformers	4
1.4 Human RBPs with PrLDs cause neurodegenerative diseases.....	5
1.4.1 Transactivation response element DNA-binding protein 43.....	6
1.4.2 Fused in sarcoma	8
1.4.3 TATA-binding protein-associated factor 15 and Ewing sarcoma breakpoint region 1 .	11
1.5 hnRNP A1 and hnRNP A2B1 cause multisystem proteinopathy.	13
1.6 MSP-linked <i>hnRNP A1</i> and <i>hnRNP A2B1</i> mutations enhance protein aggregation.....	17
1.7 Disease-associated RBPs are involved in the formation of RNP granules.....	21
1.8 Phase transitions underpin RNP granule formation and misregulation	27
1.9 Therapeutic protein disaggregases to counter aberrant phase transitions.....	30
1.10 <i>S. cerevisiae</i> as a tool for modeling neurodegeneration.....	32
1.11 Goals of Thesis	32
CHAPTER 2: MECHANISMS AND MODIFIERS OF PROTEIN MISFOLDING AND TOXICITY FOR MULTISYSTEM PROTEINOPATHY-LINKED HNRNP A1 AND HNRNP A2.....	34

2.1 Introduction	34
2.2 Results	37
2.2.1 RRM2 and PrLD determinants enable maximal hnRNPA1 toxicity.....	37
2.2.2 Other ALS-associated hnRNPA1 variants are toxic and form foci in <i>S. cerevisiae</i>	41
2.2.3 hnRNPA1 constructs with RRM1 <i>and</i> RRM2 or the PrLD aggregate in yeast.....	42
2.2.4 The hnRNPA1 PrLD is critical for fibrillization <i>in vitro</i>	46
2.2.5 RRM1, RRM2, and PrLD determinants enable maximal hnRNPA2 toxicity	49
2.2.6 PrLD determinants are critical for hnRNPA2 aggregation in yeast.....	52
2.2.7 The hnRNPA2 PrLD is critical for fibrillization <i>in vitro</i>	55
2.2.8 Disruption of RRM-RNA interactions suppressed hnRNPA1 ^{D262V} , hnRNPA2 ^{D290V} , and TDP-43 toxicity.....	57
2.2.9 Potentiated Hsp104 variants suppress hnRNPA1 ^{D262V} and hnRNPA2 ^{D290V} toxicity	62
2.2.10 hnRNPA1 and hnRNPA2 colocalize with a stress granule marker	65
2.2.11 Overexpression of Tif2, but not Pab1, reduces hnRNP toxicity	70
2.2.12 hnRNPA1 and hnRNPA2 colocalize with a P-body marker	74
2.2.13 Deletion of Lsm7, but not Pub1 or Pbp1, is protective against hnRNPA1 and hnRNPA2 toxicity.....	79
2.2.14 Overexpression of U6 snRNA does not suppress hnRNPA1 or hnRNPA2 toxicity.	82
2.2.15 Deletion of DBR1 does not protect against hnRNPA1 or hnRNPA2 toxicity.....	83
2.2.16 A deletion screen reveals novel suppressors of hnRNPA1 and hnRNPA2 toxicity. ..	85
2.2.17 Overexpression of Hsp82 does not suppress hnRNPA1 or hnRNPA2 toxicity.....	98
2.3 Discussion.....	99
2.4 Materials and Methods.....	110
2.4.1 Yeast strains, plasmids, and media	110
2.4.2 Yeast transformation and spotting assay	111
2.4.3 Immunoblotting	111

2.4.4 Sedimentation analysis of yeast lysates	112
2.4.5 Fluorescence Microscopy	113
2.4.6 SDD-AGE.....	113
2.4.7 Confocal microscopy.....	114
2.4.8 Protein Purification.....	114
2.4.9 Sedimentation analysis of hnRNPA1 fibrillization	115
2.4.12 Genetic deletion screen for toxicity modifiers	116
CHAPTER 3: CONCLUSIONS AND FUTURE DIRECTIONS	117
BIBLIOGRAPHY	124

LIST OF TABLES

Table 1: Functional enrichment of an interaction network incorporating deletion suppressors of hnRNPA1 and hnRNPA2 toxicity and related proteins.....	87
Table 2: A genome-wide deletion screen uncovers suppressors of both hnRNPA1 and hnRNPA2 toxicity.....	93

LIST OF ILLUSTRATIONS

Figure 1: Prions self-replicate conformation by templating the folding of soluble protein to the prion conformation.	5
Figure 2: Mutations that cause ALS and FTD cluster in the PrLD of TDP-43.	8
Figure 3: ALS- and FTD-causing mutations in FUS cluster in LC domains and the PrLD.	11
Figure 4: FET proteins EWSR1 and TAF15 have domain architectures similar to the domain architecture of FUS.	13
Figure 5: MSP-causing mutations affect a conserved aspartate residue in the hnRNPA1 and hnRNPA2 PrLDs.	18
Figure 6: MSP- and ALS-associated mutations are predicted to increase the fibrillization propensity of hnRNPA1 and hnRNPA2.	20
Figure 7: Cytoplasmic RNP granules include stress granules and P bodies.	23
Figure 8: Mapping the domain requirements for hnRNPA1 ^{D262V} aggregation and toxicity in <i>S. cerevisiae</i>	41
Figure 9: ALS-associated hnRNPA1 variants are toxic and form cytoplasmic foci in yeast.	42
Figure 10: The PrLD of hnRNPA1 ^{D262V} forms high-molecular weight, SDS-resistant species and is crucial for the aggregation of the full-length protein.	45
Figure 11: hnRNPA1 ^{D262V} forms ThT positive fibrils and requires the C-terminal PrLD to fibrillize <i>in vitro</i>	48
Figure 12: Mapping the domain requirements for hnRNPA2 ^{D290V} aggregation and toxicity in <i>S. cerevisiae</i>	52

Figure 13: The PrLD of hnRNPA2 is crucial for the aggregation of the full-length protein.	54
Figure 14: hnRNPA2 ^{D290V} forms THT negative fibrils and requires the C-terminal prion-like domain to fibrillize <i>in vitro</i>	57
Figure 15: Disruption of RRM-mediated RNA binding reduces the toxicity of hnRNPA1 ^{D262V} and hnRNPA2 ^{D290V} and alters cytoplasmic aggregation patterns.	59
Figure 16: Disruption of RRM-mediated RNA binding reduces the toxicity of TDP-43 and can restore nuclear localization.	62
Figure 17: Potentiated forms of Hsp104 can suppress the toxicity of hnRNPA1, hnRNPA1 ^{D262V} , hnRNPA2, and hnRNPA2 ^{D290V}	65
Figure 18: A stress granule marker, Pab1, forms foci that colocalize with aggregated hnRNPA1 and hnRNPA1 ^{D262V} , and hnRNPA2, but remains diffuse throughout the cytoplasm when coexpressed with hnRNPA2 ^{D290V}	68
Figure 19: Expression of mCherry-tagged Pab1 does not affect toxicity of hnRNPA1, hnRNPA2, or deletion constructs.	70
Figure 20: Overexpression of Tif2, but not Pab1, reduces the toxicity of hnRNPA1, hnRNPA1 ^{D262V} , hnRNPA2, and hnRNPA2 ^{D290V}	73
Figure 21: Deletion of both RRMs disrupts the colocalization of hnRNPA1 ^{D262V} and hnRNPA2 ^{D290V} with the P-body protein Dcp2.	77
Figure 22: Expression of RFP-tagged Dcp2 does not alter the toxicity of hnRNPA1, hnRNPA2, or deletion constructs.	78
Figure 23: Deletion of LSM7, but not PBP1 or PUB1, reduces the toxicity of hnRNPA1, hnRNPA1 ^{D262V} , hnRNPA2, or hnRNPA2 ^{D290V} in <i>S. cerevisiae</i>	81

Figure 24: Overexpression of U6 snRNA does not reduce hnRNPA1, hnRNPA2, or MSP-linked variant toxicity.....	83
Figure 25: Loss of the lariat-debranching enzyme, Dbr1, does not suppress the toxicity of hnRNPA1, hnRNPA1 ^{D262V} , hnRNPA2, or hnRNPA2 ^{D290V}	84
Figure 26: Deletion suppressors of hnRNPA1 and hnRNPA2 toxicity have little overlap with those uncovered as suppressors of TDP-43 and FUS toxicity.	86
Figure 27: Gene deletions suppress toxicity of hnRNPA1 and hnRNPA1 ^{D262V}	95
Figure 28: Gene deletions that suppress hnRNPA1 toxicity also suppress toxicity of hnRNPA2 and hnRNPA2 ^{D290V}	97
Figure 29: Overexpression of Hsp82 does not affect hnRNPA1 or hnRNPA2 toxicity. ..	99
Figure 30: Proposed mechanisms to explain the suppression of hnRNPA1 and hnRNPA2 toxicity by perturbation of the splicing machinery in yeast.	107

LIST OF ABBREVIATIONS

AD, Alzheimer's disease; ALS, amyotrophic lateral sclerosis; ARE; AU-rich element; ASO, antisense oligonucleotide; CNS, central nervous system; FTD, frontotemporal dementia; FTLD, frontotemporal lobar degeneration; GO, gene ontology; HD, Huntington's disease; hnRNP, heterogeneous nuclear ribonucleoprotein; IBM, inclusion body myopathy; iPSC, induced pluripotent stem cell; LCD, low-complexity domain; LLPS, liquid-liquid phase separation; MD, middle domain; MSP, multisystem proteinopathy; NLS, nuclear-localization signal; NMD, nonsense-mediated decay; P body, processing body; PD, Parkinson's disease; PDB, Paget's disease of bone; PrLD, prion-like domain; RAN, repeat associated non-ATG; RBP, RNA-binding protein; RNP, ribonucleoprotein; RRM, RNA-recognition motif; SCA, spinocerebellar ataxia; SDD-AGE, semi-denaturing detergent agarose gel electrophoresis; siRNA, short interfering RNA; snRNP, small nuclear ribonucleoprotein; ThT, Thioflavin T; UTR, untranslated region; WT, wild typ

CHAPTER 1: INTRODUCTION—RNA-BINDING PROTEINS WITH PRION-LIKE DOMAINS IN HEALTH AND DISEASE

Alice Ford Harrison^{1,2} and James Shorter^{1,2}

¹Department of Biochemistry and Biophysics, Perelman School of Medicine at the University of Pennsylvania, Philadelphia, PA 19104, USA and

²Neuroscience Graduate Group, Perelman School of Medicine at the University of Pennsylvania, Philadelphia, PA 19104, USA

Originally published in *Biochemical Journal* (2017) Apr 7; 474 (8): 1417-1438

1.1 Protein misfolding unites diverse neurodegenerative diseases

The problem of neurodegeneration remains a pressing public health concern and a biologic black box [1,2]. Age-related neurodegenerative diseases like Alzheimer's disease (AD), Parkinson's disease (PD), amyotrophic lateral sclerosis (ALS), frontotemporal dementia (FTD, the clinical disorder resulting from frontotemporal lobar degeneration (FTLD) [3]) and Huntington's disease (HD), lead to cell death within the central nervous system (CNS) and progressive CNS dysfunction [4-9]. ALS pathology also extends to the peripheral nervous system [5,10]. Our lack of understanding of the mechanisms and risk factors governing the development and progression of neurodegenerative diseases has largely precluded the development of disease-

reversing therapeutics [4,11,12]. Symptomatic treatments are available for PD and AD, but the efficacy of these can be modest or limited by problematic side effects, and they do not address the root cause of disease [12,13].

Despite dramatic differences in characteristic age of onset, symptomatology, and regional involvement of CNS tissue, neurodegenerative disorders are united on a cellular and biochemical level by the accumulation of misfolded proteins in the brain [5-7,14-16]. Cytoplasmic inclusions of α -synuclein in the neurons of the substantia nigra pars compacta and other brain regions are a hallmark feature of PD [8,16,17]. In AD, intracellular tangles of misfolded tau protein in conjunction with extracellular plaques of aggregated amyloid- β are defining features found in the neocortex and hippocampus [9,16,18,19]. In HD, a genetic trinucleotide repeat expansion leads to an elongated polyglutamine tract in the protein huntingtin, causing it to form both nuclear and cytoplasmic amyloid inclusions [18,19]. In addition, repeat-associated non-ATG (RAN) translation occurs in several diseases caused by repeat expansions, including spinocerebellar ataxia type 8 (SCA8), myotonic dystrophy type 1, fragile X-associated tremor ataxia syndrome, ALS, and HD [20-23]. RAN translation in HD, which occurs in multiple reading frames from both sense and antisense transcripts, leads to the accumulation of aggregated polyalanine, polyserine, polyleucine, and polycysteine in the brains of HD patients [21].

1.2 ALS and FTD are related disorders

ALS, also known as Lou Gehrig's disease in homage to the prominent baseball player who was diagnosed in 1939 and died two years later, is a devastating neurodegenerative disorder that affects the upper and lower motor neurons of the brain

and spinal cord [5]. The widespread and relentlessly progressive destruction of motor neurons causes muscle weakness and atrophy with hyperreflexia and spasticity, ultimately leading to paralysis and death within 2-5 years of disease onset in most cases [5,24]. FTD is a leading cause of early-onset dementia, second only to AD [25]. It results in the selective degeneration of the frontal and temporal lobes of the brain, which typically manifests as primarily behavioral dysfunction, including changes in personality and executive function or loss of volition, or language deficits [5,25]. It has become increasingly clear that there is significant overlap between ALS and FTD clinically, genetically, and neuropathologically [3,5,10,25,26].

It is now estimated that up to 50% of ALS patients also suffer from cognitive impairment or behavioral changes associated with FTLD, and, while in many cases these symptoms do not reach a clinical severity that meets criteria for dementia, ~15-20% of those with ALS also carry a diagnosis of FTD [3,25,27,28]. Similarly, a study of FTD patients found that ~50% had motor neuron involvement evident via exam or electromyography [3,27]. The idea that purely motor ALS and purely cognitive FTD exist at the two ends of a spectrum of disease is not surprising when it is considered that the two clinical entities are known to share genetic causes in their familial forms and have commonalities in their cellular signatures [15,29]. Like other neurodegenerative disorders, ALS and FTD are characterized by pathologic protein aggregation in the cytoplasm of affected neurons [15,30]. Among the proteins that have been genetically linked to these diseases and identified in cytoplasmic inclusions in patient neurons are several RNA-binding proteins (RBPs) that have low-complexity domains (LCDs), termed

prion-like domains (PrLDs) because of their similarity in amino acid composition to yeast prion domains [31].

1.3 Prions are self-replicating protein conformers

Prions are the cause of devastating human neurodegenerative diseases including Creutzfeldt-Jakob disease, Gerstmann-Sträussler Scheinker syndrome and fatal familial insomnia, but confer heritable traits that can be beneficial in yeast [18,31-36]. Prions are infectious protein conformers capable of self-replication, which occurs as the prion templates the folding of soluble proteins comprised of the same amino acid sequence (Figure 1) [37,38]. In the prion conformation, these proteins typically form stable amyloid fibers that are often sodium dodecyl sulfate (SDS) insoluble and resistant to proteases and heat denaturation [18,37]. Amyloid is a polymeric 'cross- β ' structure in which the strands of the β -sheets run perpendicular to the axis of the fiber [18,35]. The ability of yeast prions to form amyloid is dependent upon a prion domain rich in glycine as well as uncharged polar amino acids, including glutamine, asparagine, tyrosine, and serine [31,39-41]. Deletion of this prion domain precludes access to the prion state [42], and addition of this region to otherwise innocuous proteins is sufficient to confer prion behavior [43-45]. Importantly, randomization of the primary amino acid sequence of the prion domain does not impact prion formation [46,47]. Identification of several prion domains that confer bona fide prion behavior has led to the development of bioinformatics algorithms that scan amino-acid composition to screen the human genome for proteins with PrLDs [31,39,40,48].

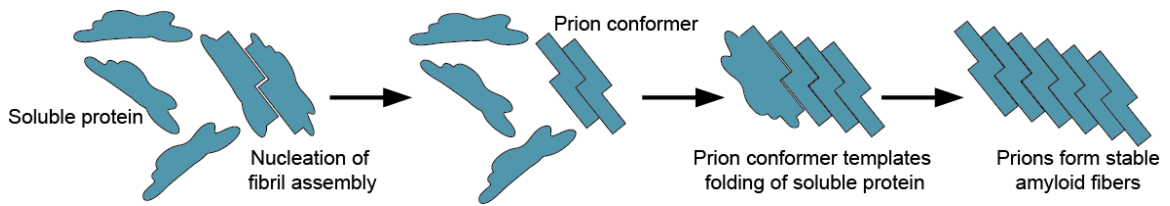


Figure 1: Prions self-replicate conformation by templating the folding of soluble protein to the prion conformation.

Prions are protein conformers that self-replicate by templating the folding of natively folded proteins of the same amino acid sequence to the prion conformation [18,35,49]. Prions typically form stable amyloid fibers with a hallmark ‘cross- β ’ structure in which β -strands run perpendicular to the axis of the fiber [18,35]. These amyloid assemblies are typically resistant to denaturation by heat, proteases, and detergents [18,37,49].

1.4 Human RBPs with PrLDs cause neurodegenerative diseases.

Interestingly, a disproportionate number of the ~240 human proteins with PrLDs are RNA- or DNA-binding proteins, many of which contain a canonical RNA-recognition motif (RRM) [41,50]. Gene ontology (GO) annotations indicate that ~30% of human proteins with PrLDs function in RNA binding and ~33% function in DNA binding [41]. While RRM-containing genes represent only ~1% of the human protein-coding genome, they comprise more than 10% of all genes containing PrLDs [31]. One by one, RNA/DNA-binding proteins with PrLDs are being implicated in neurodegenerative disease [41,50]. This association began with the identification of a trinucleotide repeat expansion in the gene encoding ataxin-1 (*ATXN1*) that leads to a polyglutamine protein product and causes SCA1 [51,52]. The expansion is now recognized to occur within the PrLD and promotes aggregation of ataxin 1 [41,53]. A similar expansion in ataxin 2 (*ATXN2*) causes SCA2 [52,54]. The SCAs are a group of autosomal dominantly inherited disorders characterized by ataxia, tremors, and dysarthria with profound

cerebellar atrophy [52]. It would be almost a decade before the misfolding of another RBP with a PrLD was linked to the pathogenesis of ALS and FTD.

1.4.1 Transactivation response element DNA-binding protein 43

The first of the RRM- and PrLD-containing proteins to be implicated in neurodegeneration was TDP-43 (transactivation response element DNA-binding protein 43, see domain architecture in Figure 2) [29,55]. TDP-43 was identified in 2006 as the predominant protein component of the ubiquitinated inclusions observed in ALS patients and a subset of cases of FTD in which there was no observable tau or α -synuclein aggregation [29,56]. TDP-43 is a primarily nuclear protein that shuttles between the nucleus and the cytoplasm and plays a role in mRNA transport, transcriptional repression, splicing regulation, miRNA biogenesis, stress granule formation, and the stabilization of long intron-containing RNA and long non-coding RNA [57,58]. TDP-43 favors binding to long UG repeats or UG-enriched RNA sequences [59-62]. We now know that TDP-43 is mislocalized to cytoplasmic aggregates in degenerating neurons and glia in roughly 97% of sporadic ALS cases and ~45% of sporadic FTD cases [57,63]. Its mislocalization has been identified as the primary histologic abnormality in cases of inclusion body myositis and a familial form of parkinsonism known as Perry syndrome [29,64]. TDP-43 inclusions are also present in many cases of AD, PD, and HD [29]. Mutations in the gene encoding TDP-43 (*TARDBP*) have been identified in cases of both familial and sporadic ALS, with mutations segregating with disease in the former, further implicating TDP-43 in the pathogenesis of neurodegeneration, [29,65-69]. *TARDBP* mutations are also found in rare instances of FTD [57,70,71].

The vast majority of these observed mutations are found in the C-terminal PrLD of TDP-43 (Figure 2) [72], which is critical for elements of normal protein function [41]. The PrLD facilitates miRNA biogenesis by mediating interactions with the nuclear Drosha complex, which cleaves pri-miRNAs into pre-miRNAs, and the cytoplasmic Dicer complex, which then cleaves these pre-miRNAs into mature miRNAs [73]. The TDP-43 PrLD mediates protein-protein interactions with other splicing factors, including heterogeneous nuclear ribonucleoprotein A1 (hnRNPA1), hnRNPA2B1, and fused in sarcoma (FUS), and is essential for the regulation of splicing of certain mRNA transcripts [41,74,75]. The PrLD is essential for recruitment of TDP-43 to stress granules [76]. The TDP-43 PrLD is also crucial for aberrant protein aggregation *in vitro* and in model systems, and select disease-linked mutations accelerate protein aggregation *in vitro* and *in vivo* [31,77-80]. Deletion of the PrLD eliminates protein toxicity in model organisms, as does disruption of the RNA-binding ability of TDP-43, suggesting roles for both misfolding and RNA engagement in disease pathogenesis [77,78,81,82].

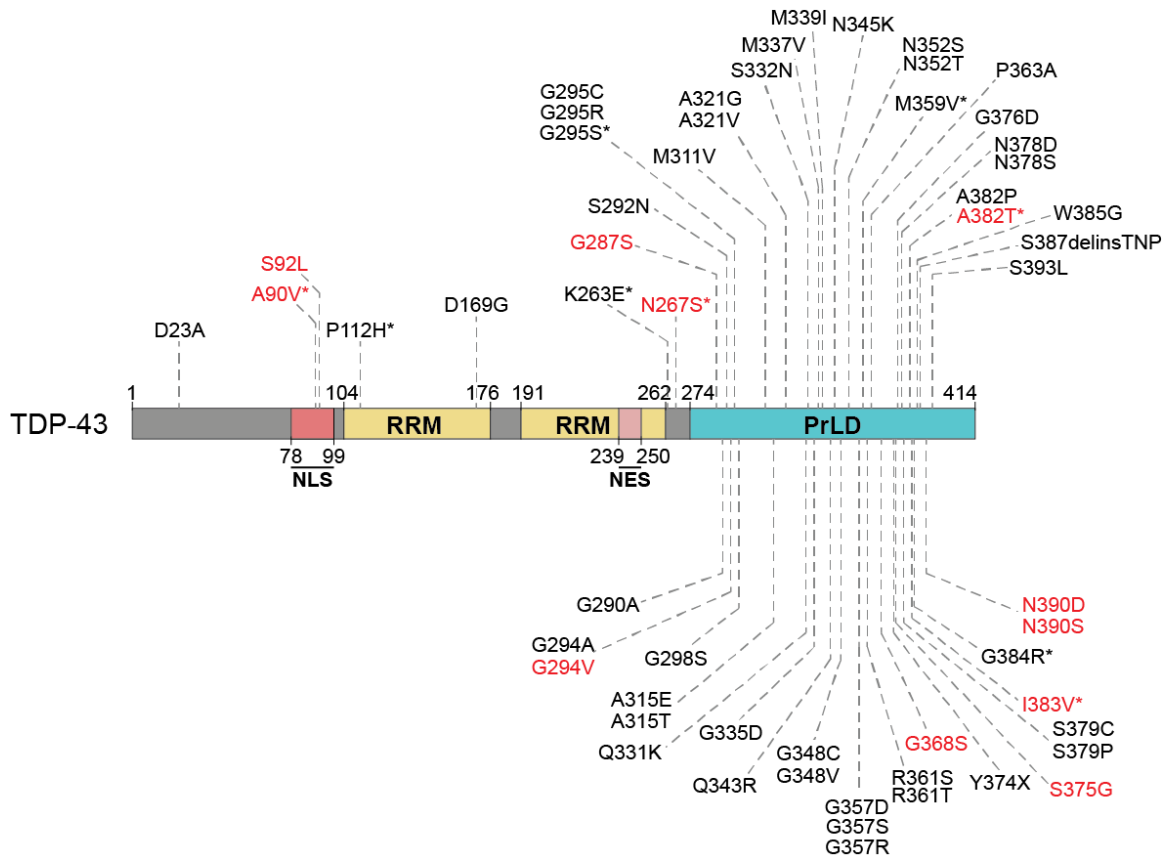


Figure 2: Mutations that cause ALS and FTD cluster in the PrLD of TDP-43. TDP-43 is an RBP with two canonical RRM and a C-terminal PrLD [48,78,79,83]. Mutations that have been identified in patients with ALS and FTD are shown, and cluster in the PrLD [72,83]. Mutations identified in patients reported to have features of FTD, with or without a clinical ALS phenotype, are denoted by an * [70,84-92]. Mutations in red have also been observed in healthy control individuals [91,93-96]. Disease-associated mutations were identified from Buratti [97], Cady et al. [93], Floris et al. [71], Lagier-Tourenne et al. [72], Peters et al. [83], the ALS data browser: <http://alsdb.org> [94], and the ALS Online Genetics Database: <http://alsod.iop.kcl.ac.uk/> [49,98].

1.4.2 Fused in sarcoma

Shortly after the connection was made between TDP-43 and disease, another protein with a canonical RRM and a low-complexity PrLD, FUS (see Figure 3 for domain architecture), was linked to both ALS and FTD. Similar to TDP-43 in many ways, FUS,

also sometimes known as translocated in liposarcoma (TLS), is a primarily nuclear protein that functions in transcriptional regulation, pre-mRNA splicing, and other elements of mRNA processing and metabolism [57,99]. Notably, though, the most common FUS-binding motif is GUGGU, and the repertoires of RNAs bound by TDP-43 and FUS have little overlap [57]. FUS-binding sites are enriched for 5' untranslated region (UTRs), and it has been suggested that FUS also preferentially binds 3'UTRs, and intronic sequences [100,101]. FUS participates in the shuttling of RNA between the nucleus and the cytoplasm, miRNA processing, and the stabilization of long intronic sequences and long noncoding RNAs [57]. FUS interacts with RNA polymerase II and Transcription Factor II D (TFIID), in addition to other transcription factors, and is thought to have both transcriptional activation and repression activity [57,100]. FUS is recruited to sites of DNA damage and plays an essential role in cellular recovery, including the recruitment of other DNA-repair factors [57,100].

Mutations in *FUS* have been linked to sporadic and familial cases of ALS, and these patients demonstrate the accumulation of FUS-positive inclusions in the cytoplasm of degenerating neurons and glia, and decreased nuclear FUS [5,15,30,102-105]. FUS mutations have caused the earliest reported onset of juvenile-onset ALS in children as young as 11 years old [106]. Neuronal and glial FUS aggregates have also been observed in ~9% of FTD cases, and rare mutations in *FUS* have been identified in FTD patients [5,30,57,107-111]. Of note, nuclear FUS inclusions have been identified in patient neurons in cases of polyglutamine diseases including HD, SCA1, and SCA2 without *FUS* mutations [57,72].

Putative pathogenic mutations in *FUS* cluster in the C-terminal proline-tyrosine-nuclear localization signal (NLS), the RGG-rich region, and the PrLD (Figure 3) [57,99,110,112]. Studies in model systems have indicated that RNA-binding is essential for the toxic effect of FUS, as is the case for TDP-43, but in addition to the RRM and PrLD, a portion of the RGG-rich region is crucial for the aggregation and toxicity of FUS [99,110,113]. ALS-linked FUS mutations confer both gain- and loss-of-function phenotypes [114]. FUS interacts with the U1 snRNP (small nuclear ribonucleoprotein) of the spliceosome and the survival motor neuron (SMN) protein, a component of the complex that enables snRNP biogenesis [72,114]. SMN deficiency causes a childhood motor neuron disease known as spinal muscular atrophy, which is characterized by a reduction in nuclear SMN-containing bodies known as Gems [114]. Similarly, ALS-linked mutations in *FUS* increase the association of FUS with SMN, leading to a reduction in the abundance of Gems and altered snRNA levels [114]. These pathologic mutations simultaneously decrease FUS binding to the U1 snRNP, resulting in splicing disruptions that phenocopy a partial loss of FUS activity [114].

overexpression of TDP-43 or FUS in yeast, then filtered based on bioinformatically predicted PrLDs, two proteins, TAF15 (TATA-binding protein-associated factor 15) and EWSR1 (Ewing sarcoma breakpoint region1), emerged with structural and functional similarities to TDP-43 and FUS [31,48]. TAF15 and EWSR1, along with FUS, belong to family of proteins known as FET proteins (see Figure 4 for domain architecture) [31,127,128]. As their names imply, FET proteins were originally described as components of pathogenic fusion oncogenes in certain human cancers [128]. Further investigation identified mutations in *TAF15* and *EWSR1* in patients with sporadic ALS (Figure 4) and revealed that either protein may be found depleted from the nucleus and mislocalized to cytoplasmic neuronal inclusions in ALS and FTD [48,127-129]. Additional evidence for pathogenicity came from *in vitro* studies demonstrating that both proteins are intrinsically aggregation prone and ALS-linked *TAF15* and *EWSR1* mutations accelerate aggregation [48,127]. In addition, both proteins are toxic when overexpressed in the *Drosophila* nervous system and disease-associated *TAF15* mutations cause a more severe phenotype [48,127]. Finally, in cultured mammalian neurons, disease-linked *TAF15* and *EWSR1* mutations induced formation of cytoplasmic TAF15 and EWSR1 inclusions [48,127].

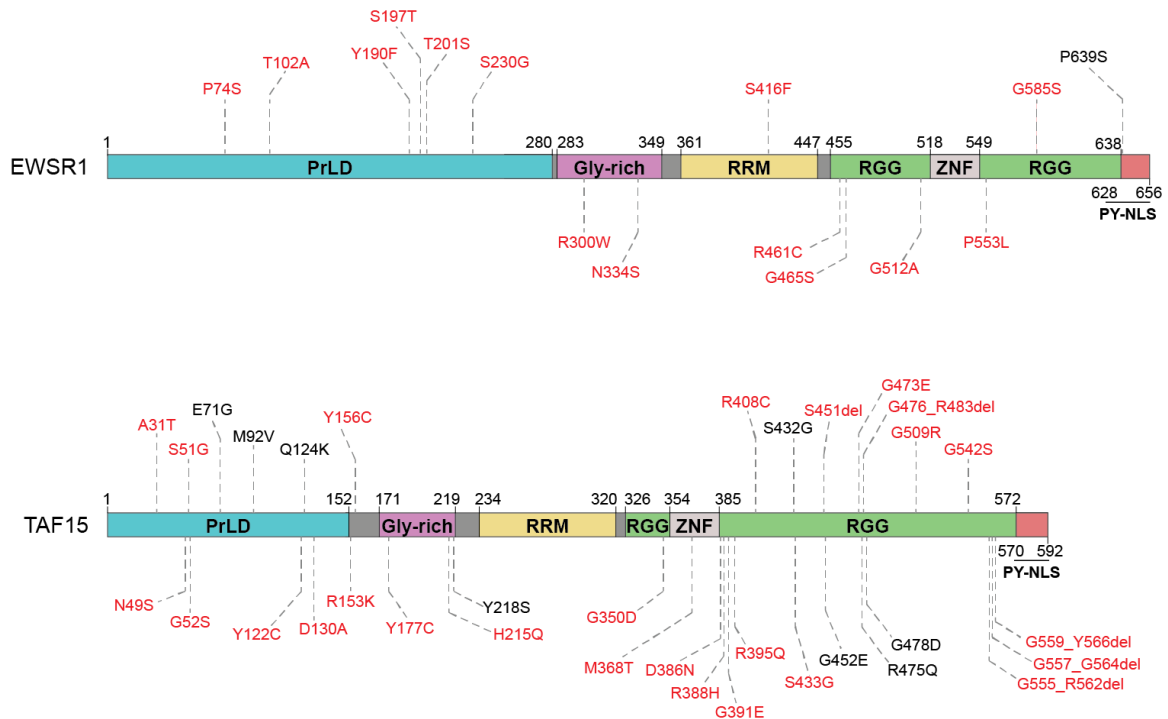


Figure 4: FET proteins EWSR1 and TAF15 have domain architectures similar to the domain architecture of FUS.

FUS, TAF15, and EWSR1 are members of the FET protein family, and are similar in domain structure and function [100,127,128]. Like FUS (Figure 3), EWSR1 and TAF15 each have an N-terminal PrLD, a glycine-rich region, and a single RRM, with C-terminal RGG-rich regions, a zinc-finger domain, and a PY-NLS [31,48,83,127,130-133]. Mutations shown were identified in ALS patients and compiled from Cady et al. [93], Couthouis et al. [48], Couthouis et al. [127], Couthouis et al. [132], Ticozzi et al. [129], and the ALS Data Browser: <http://alsdb.org> [49,94]. Those in red have also been observed in healthy control individuals [93-95,123,127,132].

1.5 hnRNPA1 and hnRNPA2B1 cause multisystem proteinopathy.

More recent information linking LCDs in the context of RBPs to neurodegeneration has emerged from the study of a rare degenerative syndrome known as multisystem proteinopathy (MSP) [134]. This autosomal, dominantly-inherited disorder was formerly known as inclusion body myopathy with Paget's disease of bone, frontotemporal dementia, and amyotrophic lateral sclerosis (IBMPFD/ALS) [134,135].

MSP is a heterogeneous, adult-onset disorder that is characterized by a variable presentation, even within the families that it affects [134-136]. Patients may suffer from degeneration of the muscle, bone, brain, motor neurons, or several of these tissues concurrently [134,137]. The most common feature of disease is inclusion body myopathy (IBM), which occurs in ~80-90% of MSP patients and leads to progressive weakness and atrophy, primarily of proximal muscle groups [136,138]. Roughly half of MSP patients will develop Paget's disease of bone (PDB), a disorder of increased osteoclast activity and bone turnover that is clinically marked by bone pain, pathologic fractures, and skeletal deformities, most often of the skull, vertebrae, and pelvis [136,139]. Cognitive changes and language deficits that define FTD can be observed in a subset of MSP patients, as can the signs of upper and lower motor neuron dysfunction and electromyographic findings that are hallmarks of ALS [136,137].

There are currently three known genetic causes of MSP [137]. The first identified was valosin-containing protein (VCP), a AAA+ protein (ATPase associated with diverse cellular activities) that participates in a number of cellular processes including the cell cycle, DNA damage repair, apoptosis, the proteotoxic stress response, post-mitotic Golgi reassembly, endoplasmic reticulum-associated degradation, and ubiquitin-dependent protein degradation [134,135,137,140]. *VCP* mutations have subsequently been identified in patients with isolated ALS, IBM, and PDB [134,138,139,141]. VCP plays a critical role in the clearance of stress granules via autophagy, and disease-associated VCP variants cause the constitutive formation of stress granules in cell culture, suggesting that aberrant stress granule persistence may contribute to neurodegenerative disease pathogenesis [142].

Exome sequencing and linkage analysis of two MSP-affected families without *VCP* mutations uncovered pathogenic mutations in the genes encoding heterogeneous nuclear ribonucleoproteins (hnRNPs) A1 and A2B1 (hnRNPA1 and hnRNPA2B1), two RBPs with PrLDs [134,137]. MSP can be caused by a D262V substitution in hnRNPA1 or a D290V substitution in hnRNPA2 [134]. hnRNPA1 and hnRNPA2 (the shorter of two hnRNPA2B1 isoforms by 12 amino acids, which constitutes roughly 90% of hnRNPA2B1 expression in most human tissues) share a domain structure consisting of two N-terminal RRM and a PY-NLS-containing C-terminal PrLD (Figure 5) [39,134].

hnRNPA1 is an abundantly and ubiquitously expressed, primarily nuclear RBP that functions widely in nucleic-acid processing [143]. hnRNPA1 binds to promoter sequences or transcription factors to either activate or repress transcription and contributes to the regulation of alternative splicing and splice-site selection, often promoting exon skipping [143-146]. It can shuttle between the nucleus and cytoplasm, facilitating nuclear mRNA export [143]. In addition to showing affinity for specific motifs including UAGGGA, UAGA, UAGG and UGGGGU [143,147,148], hnRNPA1 binds AU-rich elements (AREs) (containing AUUUA motifs) that are known to modulate the stability and degradation of mature mRNA transcripts [143,149]. hnRNPA1 also binds to internal ribosomal entry sites to regulate translation [150,151], is critical for telomere biogenesis and length maintenance [143,152], and participates in miRNA processing [153,154]. Like hnRNPA1, hnRNPA2B1 is one of the most abundantly expressed proteins in the cell, and is predominantly nuclear with the ability to shuttle between the nucleus and cytoplasm [147]. It has functional similarities to hnRNPA1, including roles in the regulation of alternative pre-mRNA splicing and translation [155-157], mRNA stability

[157], and telomere maintenance [158,159]. Distinct from hnRNPA1, hnRNPA2B1 also plays a crucial role in mRNA trafficking in neurons and oligodendrocytes [160,161]. Like hnRNPA1, hnRNPA2B1 has a significant binding preference for UAG motifs [148].

Recent studies of hnRNPA2B1 function in mouse spinal cord, patient fibroblasts, and motor neurons derived from human induced pluripotent stem cells (iPSCs) identified an enriched UAGG binding motif in CNS tissue [157]. hnRNPA2B1 binding sites were particularly enriched in 3'UTRs *in vivo* and in cultured cells, and hnRNPA2B1 was found to contribute to polyadenylation site selection [157]. The importance of hnRNPA2B1 to pre-mRNA splicing was illustrated by altered proportions of the long and short isoforms of the murine protein *Dao* upon depletion of hnRNPA2B1 in the mouse CNS [157]. The human homologue, *DAO*, which encodes D-amino acid oxidase, is highly expressed in the CNS, and has been implicated in familial ALS [157,162,163]. Loss of hnRNPA2B1 expression in the mouse model causes increased proportional expression of a short *Dao* isoform that is degraded by the proteasome and has ~85% less enzymatic activity than the longer isoform [157]. Importantly, the splicing changes that result from the MSP-causing substitution, D290V, in hnRNPA2B1 in patient fibroblasts are distinct from those that occur due to loss of hnRNPA2B1 function [157]. By contrast, the splicing changes caused by the D290V substitution in hnRNPA2B1 have a ~66% overlap with splicing alterations observed in fibroblasts from patients with an MSP-causing mutation in *VCP* [134]. This finding suggests a possible etiology for the shared disease phenotype caused by mutations in *VCP* and *hnRNPA2B1*.

1.6 MSP-linked *hnRNPA1* and *hnRNPA2B1* mutations enhance protein aggregation.

hnRNPA1 and hnRNPA2 have a common domain architecture consisting of two N-terminal RRM domains and a C-terminal PrLD containing a PY-NLS that mediates nuclear import (Figure 5) [134,143]. Interestingly, both MSP-linked mutations involve a valine substitution at a conserved gatekeeper aspartate residue in the PrLD that is computationally predicted, by two separate algorithms, to increase prionogenicity (Figure 5) [39,40,134]. Additionally, an algorithm that scores the ability of hexapeptides to form amyloid fibrils primarily based on structural information rather than amino acid sequence predicts that each of these mutations lies within a “steric-zipper” motif (Figure 6) [134,164]. Steric zippers are defined as two self-complementary beta sheets with the ability to act as the backbone of an amyloid fibril [164]. The aspartate to valine substitution in this region is predicted to strengthen a steric zipper, making the protein more prone to fibrillization (Figure 6) [134]. Indeed, both hnRNPA1 and hnRNPA2 form fibrils *in vitro* that are self-seeding (i.e. can nucleate the aggregation of soluble protein), thereby reducing the lag phase of assembly, and the disease-associated mutations greatly accelerate fibrillization [134,165]. *In vitro*, the mutant proteins are capable of seeding their own assembly as well as the assembly of the corresponding wild-type (WT) protein [134], providing a potential explanation for the genetic dominance of MSP mutations. A heterozygous individual would produce both WT and mutant protein. However, if the presence of the aspartate to valine substitution accelerates the misfolding of the mutant protein, and the misfolding of the mutant protein can nucleate the misfolding of the WT protein, the presence of the WT allele would not be protective against the development of a disease phenotype.

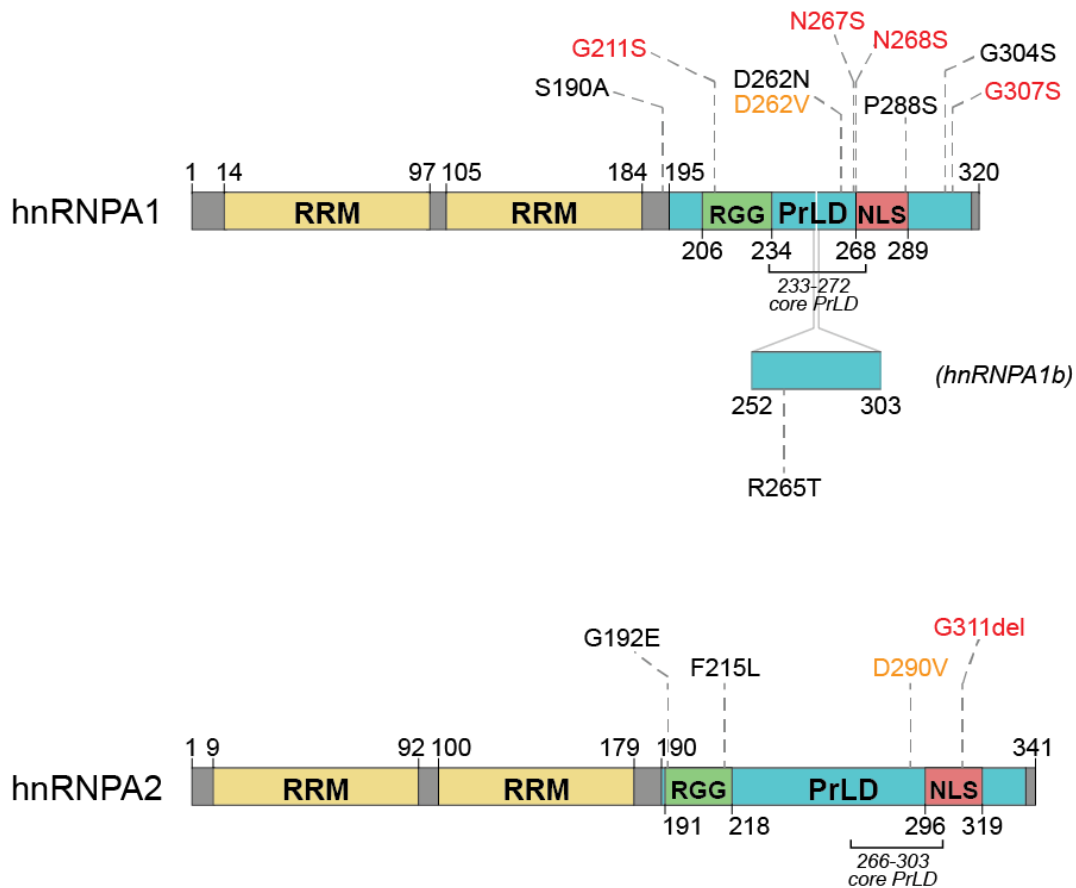


Figure 5: MSP-causing mutations affect a conserved aspartate residue in the hnRNPA1 and hnRNPA2 PrLDs.

hnRNPA1 and hnRNPA2 contain two N-terminal RRM and a C-terminal PrLD [134]. The PrLDs contain an RGG motif and a PY-NLS that mediates nuclear import [134,143,166]. A 52-amino-acid stretch that occurs in the longer isoform of hnRNPA1 (hnRNPA1b) is depicted [167]. Missense mutations in *hnRNPA1* and *hnRNPA2* that cause MSP are noted in orange [134]. All other mutations were identified in patients with sporadic or familial ALS and compiled from Couthouis et al. [132], Kim et al. [134], Liu et al. [168], and the ALS Data Browser: <http://alsdb.org> [49,94]. Those in red have been observed in healthy control individuals [95].

Muscle biopsies from MSP patients with mutations in *VCP*, *hnRNPA1*, or *hnRNPA2B1* share cytopathologic features including the cytoplasmic aggregation of TDP-43, which has also been observed in sporadic IBM in addition to ALS and FTD

[134,136,138,169]. A biopsy from an affected individual in the family harboring the hnRNPA2^{D290V} variant also demonstrated mislocalization of hnRNPA2 from the nucleus to cytoplasmic inclusions, and in muscle fibers obtained from a patient expressing hnRNPA1^{D262V} both hnRNPA1 and hnRNPA2 were cleared from myonuclei and localized to sarcoplasmic inclusions [134]. Motor neurons differentiated from iPSCs from MSP patients with *hnRNPA2*^{D290V} or *VCP*^{R155H} mutations demonstrate nuclear hnRNPA2B1 aggregation [157]. Concurrent mislocalization and partial colocalization of TDP-43 and hnRNPA1 or TDP-43 and hnRNPA2 could be observed in muscle fibers of MSP-affected patients [134]. Cytoplasmic hnRNPA1- and hnRNPA2-positive aggregates have also been identified in sporadic cases of IBM [134,170]. The intersection of protein pathologies in MSP and IBM underscores the fact that there is much to be learned about common degenerative diseases from more rare, familial disorders.

Sequencing efforts to uncover pathogenic mutations in familial and sporadic ALS patients have identified additional mutations in *hnRNPA1* and *hnRNPA2* linked to ALS [94,132,134]. A substitution (D262N) occurring in a familial case of ALS affects the same aspartate residue implicated in the pathogenesis of MSP [134]. The D262N substitution in hnRNPA1 introduces a strong steric zipper and strengthens an existing steric zipper (Figure 6) [134,164]. Similar to the D262V substitution, D262N significantly reduced the lag phase of fibrillization and accelerated hnRNPA1 aggregation *in vitro* [134]. Several other mutations in *hnRNPA1* that have been identified in patients with ALS also introduce or strengthen steric zipper motifs (Figures 5 and 6) [164]. One of these, a mutation in the PY-NLS of hnRNPA1 (P288S) was recently identified as the cause of a familial case of flail-arm ALS (Figure 5) [168]. The location of this mutation suggests that

hnRNPA2^{P288S} may have impaired nuclear import, leading to increased cytoplasmic mislocalization in addition to increased fibrillization propensity.

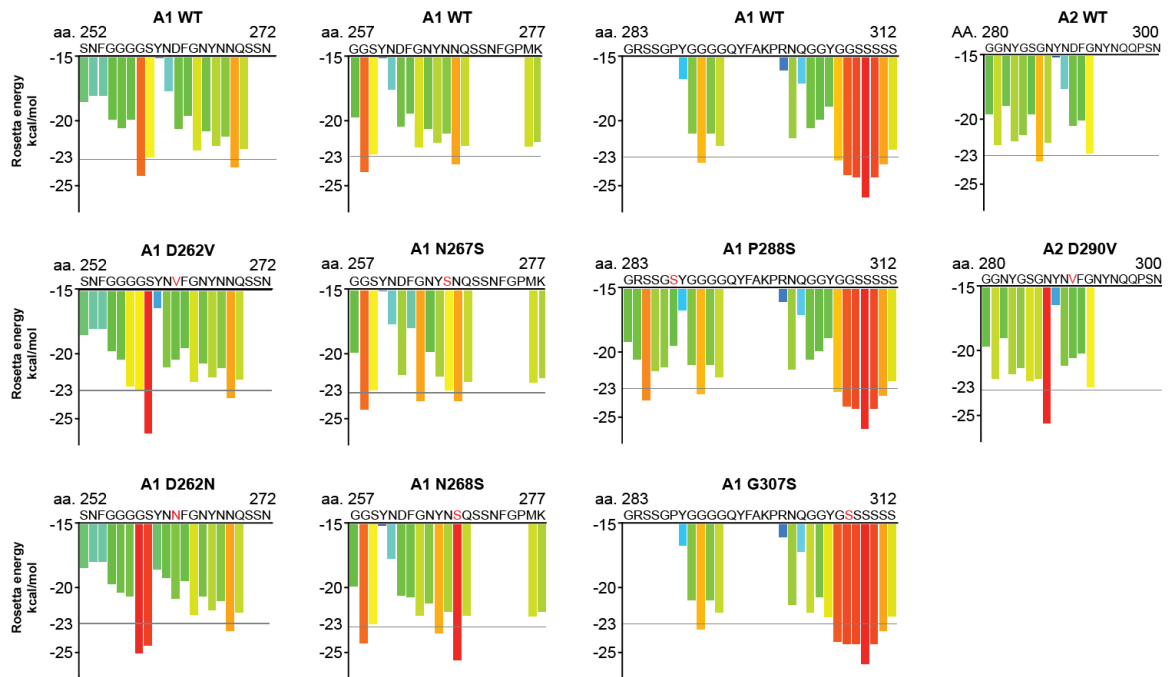


Figure 6: MSP- and ALS-associated mutations are predicted to increase the fibrillization propensity of hnRNPA1 and hnRNPA2.

ZipperDB, a structure-based algorithm, calculates the propensity of hexapeptide fragments to form steric zippers [164]. Steric zippers, which are self-complementary β -sheets that form the backbone of an amyloid fibril, are predicted to form when the Rosetta energy of a hexapeptide is below the empirically determined ‘high fibrillization propensity’ threshold of -23 kcal/mol [164]. Several of the described mutations in *hnRNPA1* and *hnRNPA2* introduce a predicted steric zipper motif or strengthen an existing zipper [49,134,164]. For example, the D262V substitution in hnRNPA1 creates a potent SYNVFG zipper, while the D262N substitution also strengthens the GSYNDF zipper [134,164].

Many questions remain, however, about the extent and prevalence of hnRNPA1 and hnRNPA2 pathology in patients with MSP and sporadic forms of ALS and FTD.

Mislocalized hnRNPA1 and hnRNPA2 inclusions have been observed in muscle fibers of patients with MSP, but can the clearance of these proteins from the nucleus to cytoplasmic foci be observed also in motor neurons of the brain and spinal cord and in the frontal and temporal cortical lobes of these patients? It remains unclear how this disease manifests in such a heterogeneous way among patients with the same mutation, and it would be informative to investigate, via post-mortem biopsy, whether patients that developed muscle and bone pathology, for example, but no clinical dementia demonstrated evidence of asymptomatic protein pathology in the frontal cortex. Also of relevance would be a study of ALS patients with TDP-43 or FUS mutations and pathology to look for co-occurrence of hnRNPA1 or hnRNPA2 pathology. WT TDP-43 aggregates along with hnRNPA1 and hnRNPA2 in MSP [134], suggesting the possibility that WT hnRNPA1 and hnRNPA2 may be present in the inclusions driven by mutations in other RBPs in ALS and FTD patients. A single study of frontal cortex from 10 patients with FTD and TDP-43 pathology showed no mislocalization of hnRNPA1 or hnRNPA2 [171]. Importantly, one of these patients harbored a familial *VCP* mutation [171]. Thus, *VCP* mutations are not always accompanied by hnRNPA1 and hnRNPA2 pathology as they can be in MSP.

1.7 Disease-associated RBPs are involved in the formation of RNP granules.

An important shared feature of ataxin 2, TDP-43, FUS, hnRNPA1, hnRNPA2, EWSR1, and TAF15 is their recruitment to stress granules upon cellular exposure to environmental stresses like heat shock, infection, ischemia, or oxidative stress [50,134,172]. Stress granules are RNP granules that assemble in the cytoplasm in stress conditions and incorporate non-translating polyadenylated mRNA transcripts,

translation initiation factors, small ribosome subunits, and RBPs (Figure 7) [50,173]. They are sites of translation suppression, consisting of stalled translation-initiation complexes and translational-silencing proteins in addition to other regulators of RNA metabolism, and serve to redirect cellular energy and resources towards the production of cytoprotective proteins that will be essential for survival and recovery after stress [50,172,174,175]. Processing bodies (P bodies) are a related class of RNP granules that are constitutively assembled in addition to being induced by cellular stress (Figure 7) [172]. P bodies are cytosolic sites of mRNA decay that interact with stress granules, allowing for possible exchange of mRNAs and proteins between assemblies [50,172,174,176,177]. Crucial to the reversible assembly of RNP granules is the intermolecular association of PrLDs or other LCDs via multiple weak, transient interactions as target RNAs are engaged, primarily via RNA-binding domains [50,134,175,178]. In some cases, as with hnRNPA1, PrLDs can also bind RNA, frequently via RGG motifs [179,180]. In other cases, as with FUS, the PrLD does not bind to RNA directly [181]. The PrLD of the mammalian stress granule protein T-cell intracellular antigen (TIA1) [182] is required for incorporation into chemically-induced stress granules [183]. In yeast, a reduction in the recruitment of prion-like proteins Lsm4 and Pop2 to P-bodies is observed in the absence of their PrLDs [184]. Therefore, despite their propensity for misfolding events, PrLDs have likely been preserved throughout evolution in part because they enable essential protein-protein interactions that provide the fluid architecture of membraneless cellular compartments [41]. In addition to stress granules and P bodies, germ granules are cytoplasmic RNP bodies found in the cytoplasm [185]. Membraneless organelles that contribute to nuclear

organization include nucleoli, paraspeckles, gems, Cajal bodies, and promyelocytic leukemia (PML) bodies [41,158].

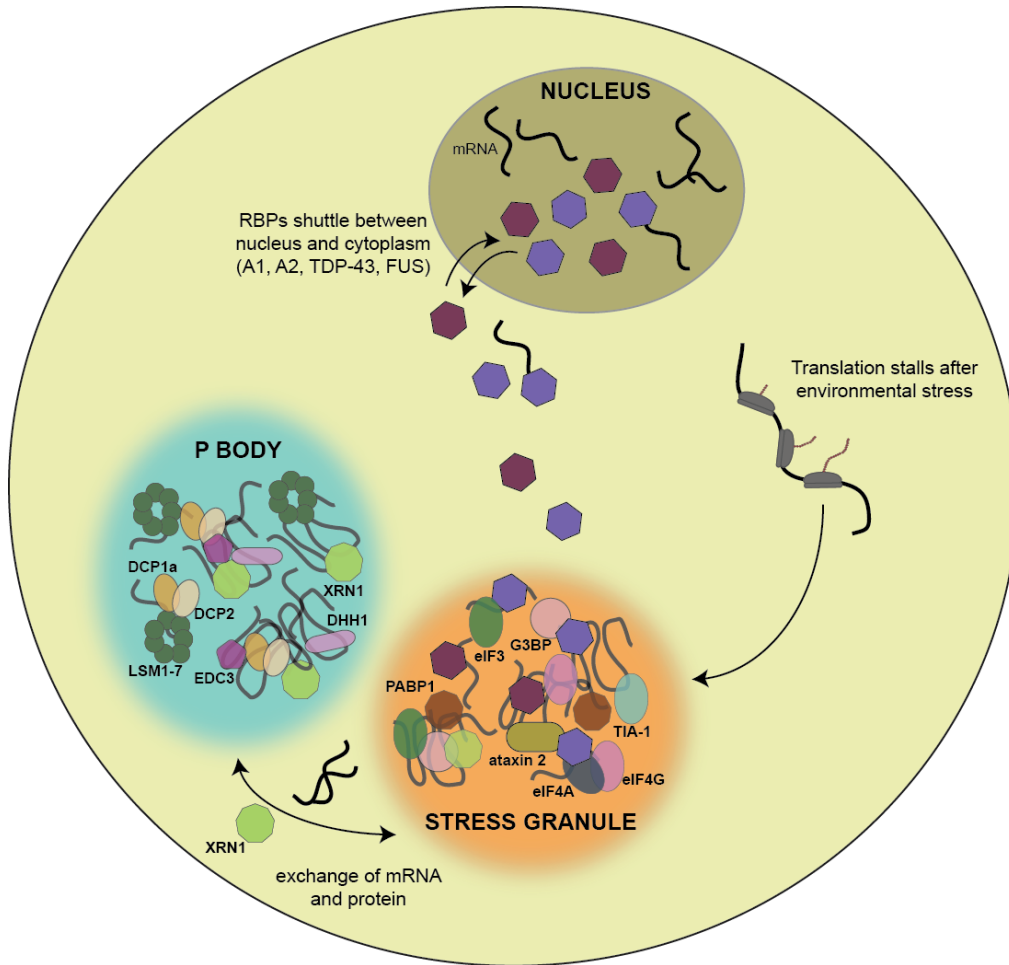


Figure 7: Cytoplasmic RNP granules include stress granules and P bodies. Stress granules are cytoplasmic assemblies that form in response to environmental stress and are sites of stalled translation initiation [50,172,176]. They contain polyadenylated mRNA transcripts, RBPs, translation initiation factors, and small ribosomal subunits [173]. P bodies are constitutively present but also form in response to stressful conditions [172]. They serve as sites of mRNA degradation and are characterized by the elements of the mRNA decapping and decay machinery [50,172]. Shown are a number of protein components of mammalian stress granules and P bodies [49,50,172,176].

Remarkably, a number of RBPs with PrLDs, which have not yet been connected to disease, are emerging as critical scaffolds for the formation of these membraneless organelles. For example, the PrLD of RBM14 (as well as FUS) is critical for paraspeckle formation [186]. Likewise, the PrLD of hnRNPD plays an important role in Sam68 nuclear body formation [187], whereas the PrLD of Xvelo is critical for Balbiani body formation [188,189]. Finally, PrLDs in DAZ1-4 and DAZL are predicted to have important roles in the formation of amyloid-like structures that regulate key meiotic events [190,191]. We anticipate that PrLDs in RNA/DNA-binding proteins will continue to surface as key scaffolds for various membraneless organelles. PrLDs in proteins that do not bind nucleic acids will also likely serve as scaffolds in other contexts. For example, the PrLD of Pin2 can function as a trans-Golgi network retention motif by driving the assembly of higher order complexes [192].

A role for the alteration of RNP granule dynamics in neurodegenerative pathology is suggested by studies showing that disease-associated mutant proteins are recruited differently to RNP granules than their WT counterparts [112,134,173,182,193,194]. Moreover, changes in the expression of RNP granule components modify the effects of toxic neurodegenerative disease RBPs in model systems [195]. hnRNPA1 and hnRNPA2 are nuclear when expressed in HeLa cells but are incorporated into cytoplasmic stress granules upon arsenite stress, and recruitment of hnRNPA1^{D262V} and hnRNPA2^{D290V} occurs more rapidly than relocalization of the WT proteins [134]. The D290V substitution also enhances hnRNPA2 recruitment to stress granules in motor neurons derived from MSP-patient iPSCs [157]. A *VCP* mutation that also causes MSP has the same effect on hnRNPA2 [157]. The fact that these mutations

promote the targeting of RBPs to stress granules, while *VCP* mutations can also decrease stress-granule clearance [142], suggests a model in which MSP can be caused by any perturbation that shifts the equilibrium of dynamic stress-granule formation and dissolution towards granule formation or persistence. In cultured cells, familial ALS mutations cause increased formation of TDP-43 inclusions that are also positive for stress granule markers after exposure to environmental stress [50,182]. *FUS* variants, too, show enhanced association with stress granule markers in cytoplasmic inclusions [50,112,173,193,194]. In a yeast model of TDP-43 proteinopathy, overexpression of several RNP granule components, including *Tis11*, *Hrp1*, *Vts1*, *Kem1*, and *Pbp1*, either enhanced or suppressed the toxicity of TDP-43 expression [195].

Pbp1 is a stress-granule protein that interacts with *Pab1*, also a component of stress granules, and regulates mRNA polyadenylation [81,196]. Interestingly, *Pbp1* is the yeast homologue of human ataxin 2, which bears a polyglutamine expansion in SCA2 [81]. Deletion of *Pbp1* diminishes stress granule formation and suppresses TDP-43 toxicity in yeast, whereas overexpression of *Pbp1* enhances TDP-43 toxicity in yeast [81]. The *Drosophila* homologue, *Atx2*, also has a dose-dependent effect on TDP-43 toxicity in the fly nervous system, with a reduction in *Atx2* expression reducing the toxic TDP-43 phenotype [81]. Further analysis revealed that TDP-43 and ataxin 2 physically interact in yeast and humans in an RNA-dependent manner [81]. Furthermore, ataxin 2 forms abnormal cytoplasmic foci in ALS and FTD patient neurons, and TDP-43 inclusions can be found in cerebellar Purkinje cells and brainstem nuclei in SCA2 [81]. Genetically, mutations in *ATXN2* are the most common known risk factor for ALS [81]. Polyglutamine expansions of >34 repeats cause SCA2, but intermediate-length

expansions from 27 to 33 glutamines in length were found to increase the likelihood of developing ALS by a factor of ~2.8 [81,197-199].

In *Drosophila*, increased expression of the stress granule protein PABP causes more severe TDP-43-induced retinal degeneration [195]. The cytoplasmic human homolog PABPC1 was observed in cytoplasmic inclusions in the motor neurons of ALS patients, despite having a predominantly diffuse pattern of localization in healthy controls [195]. RNP-granule markers have also been found to modify FUS toxicity in model systems [110]. Overexpression of stress granule proteins Pab1, Tif2, Tif3, and Tis11 in a yeast model suppressed the toxic effect of FUS overexpression [110,195,196]. The human homologue of Tif2, EIF4A1, is similarly able to suppress FUS toxicity in cultured mammalian cells [110]. FUS toxicity in yeast is also mitigated by overexpression of the P body protein Edc3 or Sbp1, which localizes to both stress granules and P bodies [110,196,200]. Both Edc3 and Sbp1 promote mRNA decapping prior to 5'-to-3' degradation [196,201]. Deletion of the stress granule protein Pub1 or the P-body protein Lsm7 decreases FUS toxicity in yeast [110,196]. In P bodies, Lsm7 is part of a heteroheptameric complex consisting of Lsm proteins 1-7 [202,203]. The Lsm1-7 proteins activate mRNA decapping and protect mRNA from trimming, a process by which transcripts are shortened by 10-20 nucleotides at the 3' end [202-204]. Lsm7 also participates in pre-mRNA splicing as a component of a nuclear complex consisting of Lsm proteins 2-8 [202,205,206]. This heptamer stabilizes newly synthesized U6 snRNA by binding to its 3' end [202,205,206]. The Lsm2-8 complex also contributes to mRNA degradation in the nucleus by targeting nuclear RNAs for decapping [202,207].

Stress granule formation in yeast is diminished by deletion of Pbp1, the yeast homologue of ataxin 2, or Pub1, which is the yeast homologue of the human protein TIA1 [208]. TIA1 is required for mammalian stress-granule formation, and reduced ataxin 2 expression results in reduced stress-granule assembly [209,210]. TIA1 and another stress-granule marker, eIF3, have been identified in the proteinaceous inclusions in the brain and spinal cord tissue of patients with ALS and FTD [112,182]. TIA1 is a protein containing RRM domains and a PrLD that is essential for stress-granule formation in cultured mammalian cells [50,183]. A mutation in TIA1 causes Welander distal myopathy, and mutant TIA1 expression leads to increased stress-granule abundance in cultured cells, suggesting that altered stress-granule dynamics may underpin this slowly progressive, adult-onset disorder [50,211,212].

1.8 Phase transitions underpin RNP granule formation and misregulation

It is now thought that RNP-granule components coalesce into membraneless compartments through phase transitions that drive the reversible formation of liquid droplets or more solid hydrogel states [41,50,213-215]. Several RNP granules have been shown to have liquid-like properties, including P granules in *C. elegans*, P bodies in *S. cerevisiae*, PML nuclear bodies, and mammalian stress granules and P bodies [216-218]. These compartments are spherical, can fuse with one another and relax into a new sphere, and undergo rapid internal rearrangement as demonstrated by half-bleaching experiments [216,217,219]. Liquid droplets form via liquid-liquid phase separation (LLPS), or the “demixing” of the granule components and the cytoplasm, a process modeled by the separation of standing oil and vinegar [219]. Recent work has shown that the liquid droplet environment promotes certain biochemical reactions,

including the stabilization of RNA hairpins and the unwinding of double-stranded nucleic acids [220]. The liquid interior is therefore a specialized microcosm for certain nucleic-acid remodeling reactions [214]. Liquid droplets create a controlled environment by permitting or restricting entry of proteins based on amino acid sequence [220].

The transition from soluble protein to liquid droplet is characteristically driven by intrinsically-disordered proteins, and can be mediated by a multitude of intermolecular interactions [178,221]. Disordered LCDs, including PrLDs, associate with each other via weak, non-specific interactions in a manner that can be concentration dependent [178,181,222]. RNA-binding via RRM or PrLDs can facilitate additional multivalent interactions, explaining the observation that the protein concentration required for the formation of hnRNPA1 droplets is decreased in the presence of RNA [178,222]. Interactions between disordered regions of the P-granule protein Ddx4 are mediated by electrostatic interactions resulting from patterned blocks of residues of alternating net charge [178,223]. Structural analysis of the LCD of FUS in the liquid phase-separated state demonstrates that it retains a disordered character within droplets, suggesting that interactions among PrLDs within liquid droplets are likely to be transient with frequent reorientations [41,181].

Hydrogels have solid-like properties, a cross-linked structure, a high water content, and water-soluble components [219]. Stress granules in yeast are gel-like, highlighting the biological relevance of this form of protein assembly [178,217]. LCDs can also facilitate the transition to the gel phase [213,224,225]. *In vitro*, the PrLDs of FUS, hnRNPA1 and hnRNPA2 all form hydrogels that are composed of amyloid-like fibrils [41,222,224]. These hydrogel structures are capable of trapping homotypic and

heterotypic LCDs [224]. FUS LCD hydrogels, for example, bind and retain, with varying avidities, soluble FUS LCDs as well as the LCDs of hnRNPA1, hnRNPA2, TDP-43 and TIA1 [224]. The role of hydrogel structures in normal RNP granule assembly in mammalian cells has been controversial [217,226]. One recent model of mammalian stress granules suggests that, rather than being pure liquid droplets, stress granules are composed of a liquid-like exterior containing an internal gel-like core [41,226].

Recent evidence suggests that inappropriate phase transitions nucleated by RNP granules may represent a crucial element of the pathogenesis of neurodegenerative disease [222,227]. *In vitro* experiments exploring LLPS of FUS and hnRNPA1 indicate that, over time, liquid droplets are prone to ‘mature’ and undergo a liquid to solid transition involving protein fibrillization [222,227]. This process is accelerated by pathologic PrLD mutations [222,227]. Mutations in the PrLD of FUS also reduce the reversibility of FUS hydrogel formation [225]. This suggests a model in which disease-causing FUS mutations, which tend to cluster in the PrLD, RGG-rich regions, and NLS [83], enhance fiber formation within droplets via one of two mechanisms. First, PrLD mutations likely serve to directly increase the propensity of FUS liquids to transition into irreversible aggregates [225,227]. Second, NLS mutations, or frameshift mutations that disrupt the NLS (Figure 3), may function to increase cytoplasmic FUS concentration by decreased nuclear import, driving liquid droplet formation, persistence, and maturation to fibrous structures [41,227]. Importantly, though, mutations in the FUS NLS can also directly alter the dynamics of phase transitions [225]. When purified FUS with and without mutations in the PY-NLS was induced by a temperature shift to form liquid droplets *in vitro*, mutant FUS droplets persisted longer than those composed of WT FUS

[225]. Thus, mutations in regions outside the LCD may contribute to pathologic persistence of RNP granules leading to aberrant fibril formation.

The most common cause of ALS and FTD is a hexanucleotide repeat expansion in a noncoding region of *C9ORF72* [228,229]. This expansion leads to the RAN translation of several dipeptide repeat proteins, including poly-(Pro-Arg) (PR) and poly-(Gly-Arg) (GR), which form nuclear and cytoplasmic inclusions in the brain and spinal cord of ALS/FTD patients harboring this expansion [229]. LCDs, such as those contained in hnRNPA1, hnRNPA2, and other RNP granule components, are a preferred binding target of PR and GR, which can disrupt granule dynamics [229,230]. GR₅₀ or PR₅₀ expression in cultured cells caused spontaneous assembly of persistent stress granules [229]. GR₂₀ or PR₂₀ reduced the concentration required for hnRNPA1 LLPS, and led to the formation of droplets with reduced fluidity [229].

1.9 Therapeutic protein disaggregases to counter aberrant phase transitions

A therapeutic agent with the ability to counteract pathologic phase transitions could have tremendous utility across neurodegenerative diseases caused by misfolding events related to RNP granule dysfunction. One approach would be to identify a small molecule or RNA that could preserve the liquid-granule state by preventing the transition to solid aggregates. An agent that could actively reverse the liquid-to-solid phase transition would be especially appealing for patients with active disease. Hsp104 is a hexameric protein disaggregase in the AAA+ ATPase family [231-233]. It is found in yeast and has homologues across eubacteria and eukaryotic species, but no metazoan orthologue exists [231,234]. Hsp104 preserves proteostasis and promotes survival in *S. cerevisiae* by renaturing aggregated proteins and returning them to their native

conformations after exposure to environmental stress [231,234,235]. It also has the ability to rapidly remodel amyloid fibers and prefibrillar oligomers and, in doing so, regulates prionogenesis and the propagation and elimination of yeast prion conformers [232,235-239]. In *S. cerevisiae*, Hsp104 also functions in the dissolution of stress granules and the maintenance of the liquid-like properties of P bodies [217]. Hsp104 contributes to the proper targeting of P body components, which mislocalize to stress granules in its absence [217]. As a potential therapeutic, Hsp104 has shown promise in several models of neurodegenerative disease [8,235,240]. In a rat model of PD, expression of Hsp104 decreased dopaminergic neuron loss and accumulation of α -synuclein aggregates in the substantia nigra of animals expressing a PD-linked α -synuclein variant [8]. Hsp104 increased lifespan and reduced the number of cortical polyglutamine inclusions in a mouse model of HD [240]. Potentiated Hsp104 variants with enhanced ATPase activity reduce protein aggregation and suppress toxicity of TDP-43, FUS, and α -synuclein in *S. cerevisiae* [234,235,241-243]. Enhanced Hsp104 variants also protect against dopaminergic neuron loss in a *C. elegans* model of PD [235]. These studies suggest that Hsp104 has broad activity against neurodegenerative disease substrates, and its substrate repertoire can be expanded or sharpened using engineering strategies.

Finally, it will also be important to determine whether endogenous human protein disaggregases, including Hsp110, Hsp70, Hsp40, and small heat-shock proteins [244-246]; HtrA1 [247]; and NMNAT2 plus Hsp90 [248], also display activity against disease-linked RBPs with PrLDs. These protein-disaggregase systems could also be engineered to possess enhanced disaggregase activity against disease-linked RBPs with PrLDs

[249]. Moreover, small-molecule drugs that enhance the activity of these systems could be useful therapeutics aimed at restoring homeostasis of RBPs with PrLDs [249]. We anticipate that harnessing the power of protein disaggregases could lead to important advances in treating several devastating diseases caused by aberrant phase transitions of RBPs with PrLDs [249].

1.10 *S. cerevisiae* as a tool for modeling neurodegeneration

The budding yeast *S. cerevisiae* has emerged as a powerful tool for studying protein pathology associated with neurodegeneration [1,7]. There is significant conservation of biological pathways from yeast to humans, and the yeast genome is tractable and well-catalogued [1,7,250]. Robust yeast models of TDP-43, FUS, and α -synuclein have been used to identify modifiers of RBP toxicity that have translated to *Drosophila*, *C. elegans*, and mammalian cell culture models [7,110,195,235,251]. A genetic modifier of TDP-43 toxicity in yeast led to the identification of ataxin 2 expansions as a relatively common genetic risk factor for ALS [81]. Yeast also predicted the involvement of TAF15, EWSR1, hnRNPA1, and hnRNPA2 in neurodegenerative disease pathogenesis [48]. We have recently established a yeast model of hnRNPA1 and hnRNPA2 pathology in MSP [134]. This system recapitulates the cytoplasmic hnRNPA1 and hnRNPA2 mislocalization and cellular toxicity caused by hnRNPA1 and hnRNPA2 seen in patients with MSP [134]. This powerful model will provide a useful means for further study of these disease-causing RBPs.

1.11 Goals of Thesis

Our goal was to dissect the mechanism by which hnRNPA1 and hnRNPA2B1 cause MSP by modeling disease pathology in *S. cerevisiae*. We employed a domain-

mapping approach to understand which functional regions of hnRNPA1 and hnRNPA2 are required for protein misfolding and toxicity. We explored the relationship between these RBPs and RNP granules in yeast, and asked whether association with stress granules or P bodies is an essential feature of hnRNPA1 and hnRNPA2 toxicity in yeast. We tested candidate genetic modifiers of hnRNPA1 and hnRNPA2 toxicity and executed an unbiased genetic deletion screen in an effort to identify strategies for reversing their toxic effects. We aimed to understand how hnRNPA1 and hnRNPA2 are similar to and different from each other and other proteins that cause ALS and FTD, including the more well-understood TDP-43 and FUS, by comparing the cellular pathways involved in protein toxicity through genetic modifier studies. This knowledge will be crucial for understanding whether disease-modifying therapeutics should target specific protein dysfunction or a more general pathologic process. Our hope is to gain insight into the underpinnings of cellular degeneration not only in MSP, but also in sporadic ALS, FTD, IBM, and PDB, all of which are closely related and significantly more common disorders. A more in depth comprehension of the ways in which RBPs cause disease will be the first step towards the development of therapeutic strategies of broad efficacy.

CHAPTER 2: MECHANISMS AND MODIFIERS OF PROTEIN MISFOLDING AND TOXICITY FOR MULTISYSTEM PROTEINOPATHY-LINKED hnRNPA1 AND hnRNPA2

2.1 Introduction

The last century has seen a dramatic increase in human life expectancy, and with an aging population comes an increased prevalence of age-related neurodegenerative diseases [252]. The financial and emotional burden of disorders like AD, PD, ALS and FTD will continue to grow at the societal and individual levels as modes of prevention, therapeutic strategies, and effective cures remain elusive [252]. The development of clinical interventions will demand a detailed understanding of the pathogenic mechanisms underlying these disorders, which are unified by protein misfolding and the presence of pathologic proteinaceous aggregates in affected tissues [19,29,78,253].

Interestingly, a number of proteins implicated in neurodegeneration are RBPs with PrLDs—protein domains rich in uncharged polar amino acids and glycine and of similar amino acid composition to prion domains that enable yeast prions to self-replicate and form stable amyloid [31,39,40]. TDP-43, FUS, TAF15, and EWSR1 have RRM and PrLDs, and are found in the hallmark protein inclusions of ALS and FTLD [15,29,31,48,56,72,128]. Moreover, mutations in TDP-43 and FUS can cause these diseases, and TAF15 and EWSR1 variants have been identified in sporadic ALS patients [29,48,127,129,132]. These observations, and a growing list of RBPs with

PrLDs associated with various neurodegenerative pathologies, imply a possible role for protein misfolding mediated by PrLDs in age-related degeneration [31,50].

Recent genetic studies revealed that specific missense mutations in the PrLDs of hnRNPA1 and hnRNPA2, cause familial inclusion body myopathy with Paget's disease of bone, frontotemporal dementia, and amyotrophic lateral sclerosis [134]. This rare age-related degenerative disease, also known as MSP, has a heterogeneous presentation characterized by early degeneration of muscle, bone, brain tissue, and motor neurons, and is untreatable and ultimately fatal [134,136]. Interestingly, additional missense mutations in the PrLD of hnRNPA1 have been identified in familial and sporadic ALS [134,168]. All five identified mutations are predicted, by two separate algorithms, to enhance the natural prionogenicity of these RBPs [39,40,134].

ZipperDB, an algorithm that scores amyloidogenicity, predicts that these amino acid substitutions create hexapeptides with an increased propensity to form "steric zippers," self-complementary beta sheets that constitute the backbone of amyloid fibrils [164]. These findings suggest that the PrLDs of hnRNPA1 and hnRNPA2 can assume an ordered fibrillar structure and are more likely to do so when harboring these disease-linked missense mutations. *In vitro* experiments confirm that purified WT hnRNPA1 and hnRNPA2 form self-seeding fibrils, a process that is accelerated in the disease-linked variants [134]. This observation provides a possible mechanism for the pathogenicity of the mutant hnRNPs and a connection between the aggregation-prone nature of PrLDs and neurodegeneration. More recently, it has been established that aberrant fibrillization may occur in the context of RNP granules that form via liquid-liquid demixing driven by transient interactions of the LCDs of RBPs [178,213,214,222,227]. Disease-linked

mutations in hnRNPA1 and FUS promote the transition of these liquid droplet-like compartments to more solid, fibrillar structures [222,227].

As a first step toward understanding how the mutant proteins hnRNPA1^{D262V} and hnRNPA2^{D290V} cause pathology in MSP we determined which functional domains govern misfolding and toxicity. We have asked whether the two are intrinsically linked—whether hnRNPA1 and hnRNPA2 misfolding is always cytotoxic, and whether protein toxicity can occur in the absence of protein misfolding. As we search for therapeutic options for patients with MSP and more common degenerative disorders, such as isolated ALS or FTLN, it will be important to understand whether the mechanism of cell death is variable based on the identity of the disease-causing protein. We aimed to draw comparisons among hnRNPA1, hnRNPA2 and the well-studied disease causing proteins TDP-43 and FUS to identify mechanistic similarities and distinctions. We also asked whether known suppressors of TDP-43 and FUS toxicity could mitigate the toxicity of hnRNPA1 and hnRNPA2, which would present opportunities for broadly efficacious therapeutics.

We have conducted our studies using *Saccharomyces cerevisiae*, which has proven to be a powerful tool for answering similar questions in the context of other neurodegenerative diseases associated with protein misfolding including AD, PD, HD, in addition to ALS and FTLN [78,110,254-257]. Budding yeast offer an efficient system with an easily manipulated, well-understood and highly conserved genome [1]. The conservation of cellular pathways from yeast to humans allows us to study perturbations due to the misfolding and accumulation of neurodegeneration-associated proteins and draw mechanistic conclusions that can be applied to human pathology [1,7]. Yeast were, in fact, used to predict that hnRNPA1 and hnRNPA2 were likely to be connected with

neurodegenerative disease [48]. In MSP patients, even in the absence of mutations in hnRNPA1 and hnRNPA2, muscle atrophy is accompanied by the mislocalization of these proteins to cytoplasmic inclusions in muscle tissue [134,137,258]. Overexpression of hnRNPA1 and hnRNPA2 in a yeast model of MSP recapitulates this cytoplasmic protein accumulation and cytotoxicity [134,258]. Here, we map the domain requirements for hnRNPA1 and hnRNPA2 toxicity and aggregation in yeast. We define striking similarities but also important differences in how hnRNPA1 and hnRNPA2 aggregate and confer toxicity in yeast, which also distinguish them from other ALS-linked RBPs with PrLDs, including FUS and TDP-43. These differences will likely help inform potential therapeutic strategies.

2.2 Results

2.2.1 RRM2 and PrLD determinants enable maximal hnRNPA1 toxicity

The domain architecture of hnRNPA1 consists of two N-terminal RRMs (RRM1 and RRM2) that engage RNA [259,260] as well as a C-terminal glycine-rich region (Figures 5, 8A) [130,134]. The C-terminal glycine-rich region has been identified as a PrLD (residues 195-317), while another algorithm predicts that a shorter sequence within the PrLD, referred to as the “core” PrLD (residues 233-272), will have prion-like properties [39,40,134]. The PrLD also contains a RGG box (residues 206-234), and contributes to the RNA binding and remodeling activity of hnRNPA1 [166,179,261]. A PY- NLS (or M9 sequence) resides in the PrLD [130,180]. However, the yeast nuclear import machinery does not decode the hnRNPA1 PY-NLS [262,263]. Thus, expression of WT hnRNPA1 in yeast recapitulates the cytoplasmic mislocalization of WT hnRNPA1 that occurs in forms of MSP caused by mutations in hnRNPA2 or VCP [134]. Both WT

hnRNPA1 and hnRNPA1^{D262V} were highly toxic when expressed in *S. cerevisiae* (Figure 8B) [48,134]. We created a series of deletion and truncation constructs to determine the functional domain requirements for this toxicity (Figure 8A-C). All of these constructs were robustly expressed (Figure 8C). Thus, variations in the toxicity of hnRNPA1^{D262V} constructs could not be attributed to altered protein expression levels.

The MSP-linked D262V substitution introduces an amyloidogenic hexapeptide (residues 259-264) that increases the aggregation propensity of the PrLD of hnRNPA1 [134]. Indeed, deletion of this hexapeptide greatly retards hnRNPA1 fibril formation *in vitro* [134]. Intriguingly, this hexapeptide is not critical for toxicity in yeast, as neither deletion of this enhanced “steric zipper” motif nor deletion of the core PrLD containing this hexapeptide (residues 233-272) affected toxicity (Figure 8A, B, constructs Δ 259-264 and Δ 233-272). In the absence of this crucial steric zipper, hnRNPA1 is unable to fibrillize, but retains the ability to undergo liquid-liquid phase separation, forming protein-rich droplets with liquid properties [134,222]. Our results suggest that liquid hnRNPA1^{D262V} droplets may represent a toxic species in yeast. These surprising results led us to question whether the PrLD was required at all for hnRNPA1 toxicity in yeast. Deletion of the entire PrLD spanning residues 195-317, preserving only the RRMs resulted in decreased toxicity (Figure 8A, B, construct 1-195), demonstrating that PrLD determinants contribute to toxicity. Moreover, RRM1 alone was not toxic (Figure 8A, B, construct 1-97). Nonetheless, the mild toxicity of the RRM1 plus RRM2 construct, 1-195, differentiates hnRNPA1 from TDP-43 and FUS, where deletion of the PrLD eliminates toxicity [78,110].

Next, we added back progressively larger portions of the PrLD (Figure 8A, B, constructs 1-233, 1-272, and 1-289) in an effort to restore maximal toxicity. Remarkably, a very short N-terminal portion of the PrLD corresponding to the RGG box (residues 218-234) [166] was sufficient to restore maximal toxicity (Figure 8A, B). Thus, the RGG box of the PrLD, an RNA-binding portion of this domain [179], plays a critical role in hnRNPA1 toxicity in yeast.

Importantly, the hnRNPA1^{D262V} PrLD construct (Figure 8A, B, construct 195-320) was not toxic, indicating that the appended RRMs are critical for hnRNPA1^{D262V} toxicity. Indeed, deletion of RRM2 reduced but did not eliminate toxicity (Figure 8A, B, constructs Δ 105-184), whereas deletion of RRM1 had no effect on toxicity (Figure 8A, B, construct 105-320). Thus, maximal hnRNPA1 toxicity requires RRM2 as well as determinants within the PrLD.

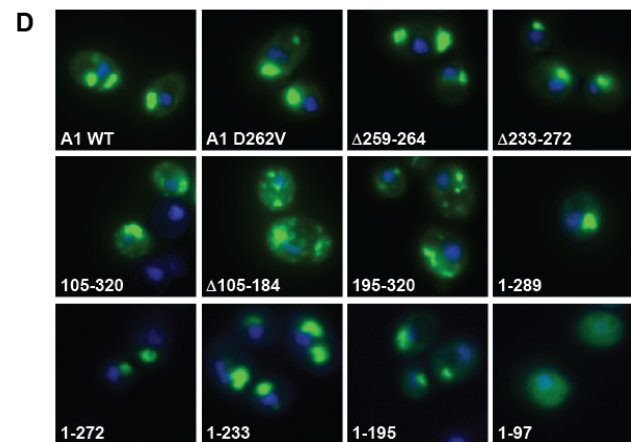
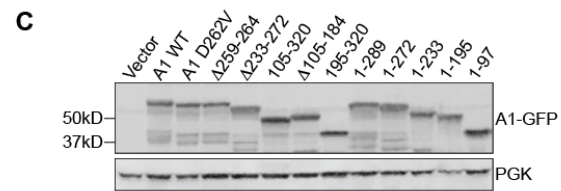
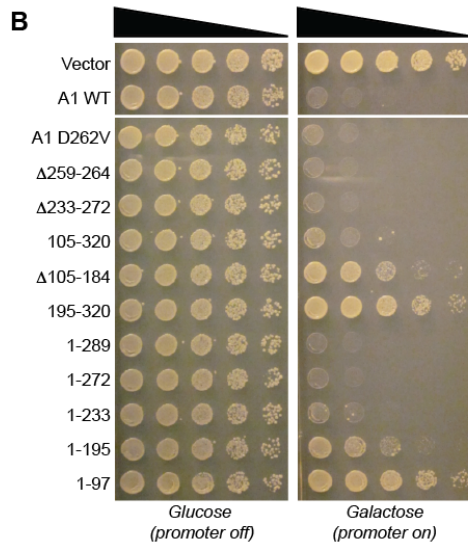
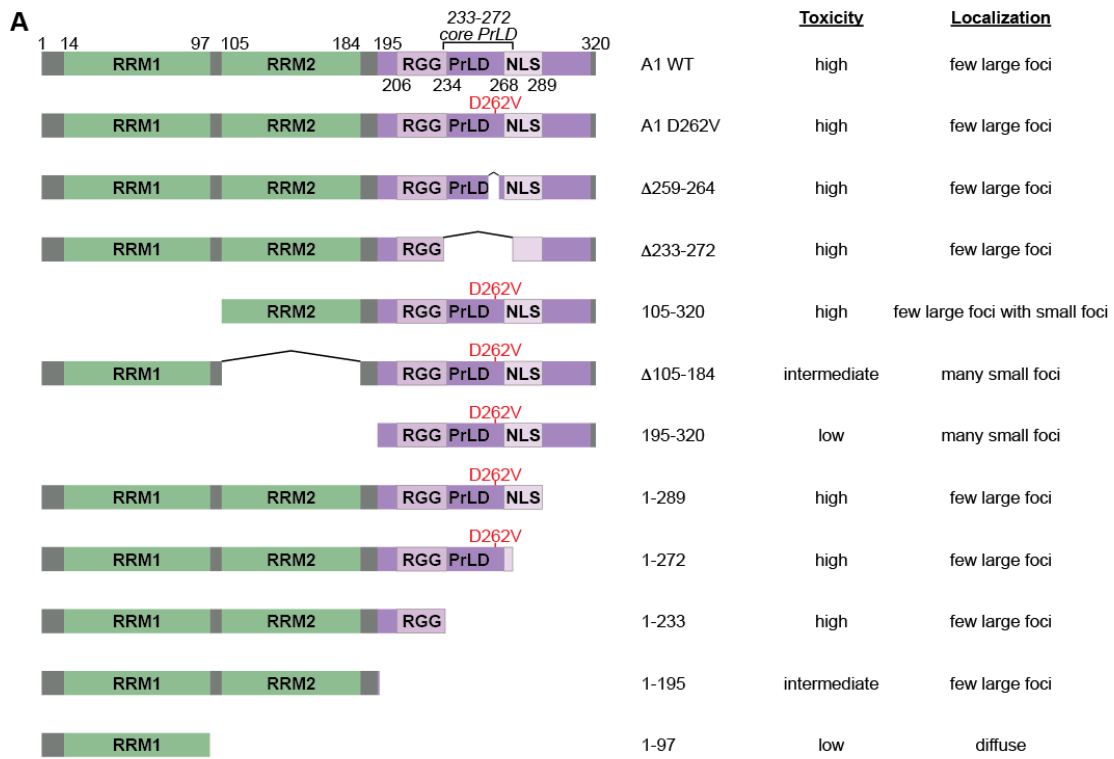


Figure 8: Mapping the domain requirements for hnRNPA1^{D262V} aggregation and toxicity in *S. cerevisiae*.

(A) The domain structure of hnRNPA1 is illustrated, along with a series of hnRNPA1^{D262V} deletion and truncation constructs, which were expressed in *S. cerevisiae*. **(B)** Five-fold serial yeast dilutions were spotted on glucose and galactose. hnRNPA1 and hnRNPA1^{D262V} were highly toxic when expressed in yeast, and RRM2 was important for this toxicity (construct Δ 105-184). A portion of the C-terminal PrLD was also crucial (construct 1-195). Because hnRNPA1 constructs are under the control of the GAL1 promoter, expression is repressed on glucose media but robustly induced on galactose media. **(C)** Immunoblot confirmed expression of all hnRNPA1 protein constructs. **(D)** Fluorescence microscopy illustrates the cellular localization of GFP-tagged hnRNPA1 constructs. The WT protein and all mutant constructs localized to the cytoplasm, with all proteins forming foci except the isolated RRM1 (construct 1-97). RRM2 deletions resulted in smaller, more numerous foci (constructs Δ 105-184 and 195-320). WT, wild type; RRM, RNA-recognition motif; PrLD, prion-like domain; NLS, nuclear localization signal.

2.2.2 Other ALS-associated hnRNPA1 variants are toxic and form foci in *S. cerevisiae*.

We asked whether other ALS-associated hnRNPA1 variants are also toxic when expressed in our yeast model and whether these proteins are similarly localized to cytoplasmic foci. We overexpressed hnRNPA1^{D262N}, which was identified in a patient with familial ALS, and hnRNPA1^{N267S}, which was found in a patient with sporadic ALS, in *S. cerevisiae*. hnRNPA1^{D262N} and hnRNPA1^{N267S} were as toxic as hnRNPA1^{D262V} and hnRNPA1 in yeast (Figure 9A). Both hnRNPA1^{D262N} and hnRNPA1^{N267S} formed large cytoplasmic foci (Figure 9B). Thus, though the cellular phenotype of patients carrying hnRNPA1^{D262N} and hnRNPA1^{N267S} mutations has not been demonstrated, it is likely that our yeast model will have utility in modeling a range of hnRNPA1-associated pathologies.

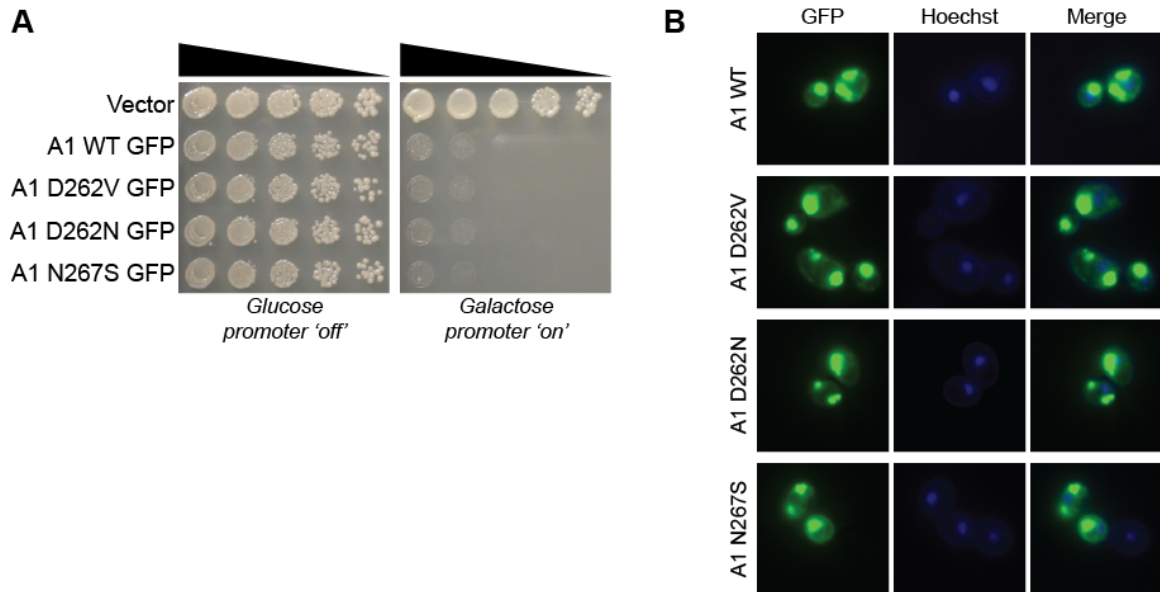


Figure 9: ALS-associated hnRNPA1 variants are toxic and form cytoplasmic foci in yeast.

(A) A spotting assay was used to compare the toxicities of GFP-tagged hnRNPA1 variants. hnRNPA1^{D262N} and hnRNPA1^{N267S} were as toxic as hnRNPA1^{D262V} and hnRNPA1 in yeast. **(B)** GFP-tagged hnRNPA1 WT and three disease-associated mutants, hnRNPA1^{D262V}, hnRNPA1^{D262N}, and hnRNPA1^{N267S} formed large cytoplasmic foci when overexpressed in yeast.

2.2.3 hnRNPA1 constructs with RRM1 and RRM2 or the PrLD aggregate in yeast

hnRNPA1^{D262V} and hnRNPA1 mislocalized to a few, large cytoplasmic foci (Figure 8A, D, Figure 9B) [48,134]. Deletion of the MSP-linked steric zipper from the PrLD did not affect this localization, nor did deletion of the core PrLD (Figure 8A, D, constructs Δ 259-264 and Δ 233-272), indicating that these highly aggregation-prone regions are not required for the formation of cytoplasmic protein foci in yeast. C-terminal deletions in the PrLD also did not affect the localization of hnRNPA1^{D262V} (Figure 8A, D, constructs 1-289, 1-272 and 1-233). By contrast, deletion of one or both RRMs, resulted in more numerous protein foci that were scattered throughout the cytoplasm (Figure 8A,

D, constructs 105-320, Δ 105-184 and 195-320). Thus, formation of distinct, large foci likely depends upon interactions mediated by RRM1 and RRM2. Indeed, RRM1 and RRM2 were sufficient to maintain the distribution of hnRNPA1 to few large cytoplasmic foci in the absence of the PrLD (Figure 8D, construct 1-195). RRM1 alone, however, was diffusely located throughout the cell and did not form foci (Figure 8D, construct 1-97). Thus, the only soluble hnRNPA1 construct was not toxic (Figure 8B, D). However, aggregation per se was not sufficient for toxicity as the PrLD alone aggregated but was not toxic (Figure 8B, D). Indeed, these findings suggest that hnRNPA1 aggregation is only connected with toxicity if the construct bears an intact RRM (Figure 8B, D), indicating that aggregation *and* RRM-mediated RNA binding are required for toxicity.

Next, we asked whether the cytoplasmic foci formed by various hnRNPA1 and hnRNPA1^{D262V} constructs represent bona fide aggregates via sedimentation analysis of yeast lysates [79,235]. As expected, construct 1-97, RRM1 alone, which exhibits diffuse fluorescence (Figure 8D), was confined to the soluble fraction as was the endogenous soluble protein Pgk1 (Figure 10A). Both hnRNPA1 and hnRNPA1^{D262V} partitioned to the insoluble fraction, indicating formation of biochemical aggregates (Figure 10A). Likewise, the PrLD construct hnRNPA1^{D262V} 195-320 also separated primarily into the insoluble fraction (Figure 10A). By contrast, however, the RRM1 and RRM2 construct, 1-195, partitioned to both the soluble and insoluble fractions (Figure 10A), indicating that the large foci formed by hnRNPA1 1-195 in yeast (Figure 8D) likely represent more transient or unstable aggregated structures. Thus, the PrLD enables a greater proportion of hnRNPA1 to form insoluble structures.

Typically, yeast prions form infectious amyloid fibrils that are SDS-resistant [35,37]. For yeast prions, a distinctive prion domain enriched in uncharged polar amino acids and glycine enables prionogenesis [31,39,40]. The PrLD of hnRNPA1 possesses similar amino acid composition to canonical yeast prion domains [31,39,40,50,134,258]. Thus, we assessed whether aggregates formed by various hnRNPA1 constructs were amyloid-like via semi-denaturing detergent-agarose gel electrophoresis (SDD-AGE) [264]. As a positive control, we employed the yeast prion protein Rnq1 [265] tagged with YFP, which as expected formed a smear of large SDS-resistant conformers (Figure 10B) [266]. With the exception of the hnRNPA1^{D262V} PrLD construct, 195-320, none of the hnRNPA1 constructs formed a very high molecular weight smear like Rnq1 in the presence of 2% SDS (Figure 10B). Rather, with the exception of the hnRNPA1^{D262V} PrLD construct, 195-320, all the hnRNPA1 constructs formed two distinct higher-order species above the 250kDa marker (Figure 10B, arrow). These high molecular weight forms likely represent SDS-resistant oligomeric structures or stable RNP particles. These findings distinguish hnRNPA1 from TDP-43, which was resolved entirely as SDS-soluble monomers via SDD-AGE [78]. Intriguingly, the non-toxic hnRNPA1^{D262V} PrLD construct, 195-320, formed a very high molecular weight smear more similar to Rnq1 (Figure 10B). Thus, the hnRNPA1^{D262V} PrLD construct, 195-320, likely forms amyloid-like conformers in yeast, which are non-toxic. Likewise, amyloid forms of Rnq1 are not toxic to yeast [267,268]. Overexpression of soluble Rnq1 is highly toxic to yeast cells bearing Rnq1 prions, i.e. [RNQ⁺] yeast, but toxicity results from SDS-soluble forms of Rnq1 and increased formation of SDS-resistant Rnq1 amyloid is protective [267,268].

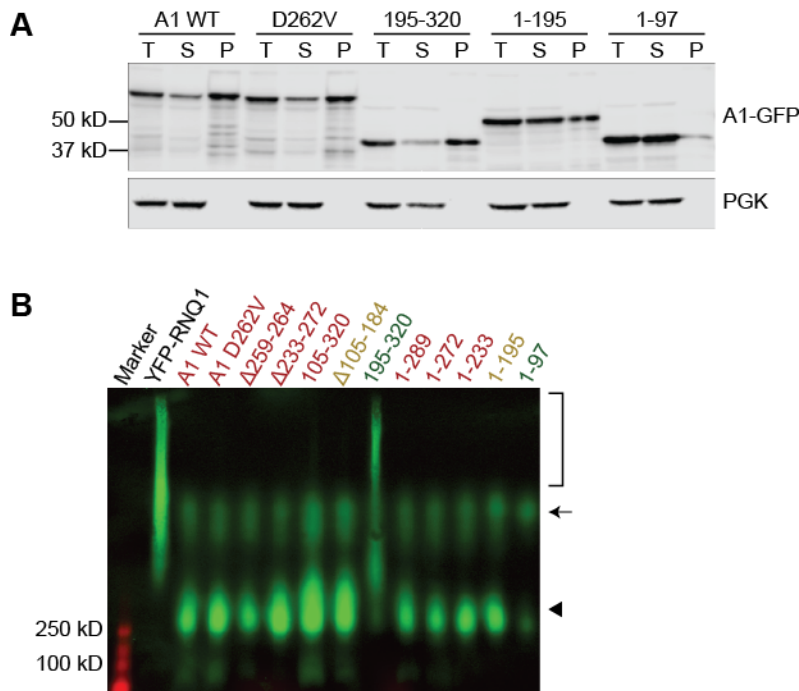


Figure 10: The PrLD of hnRNPA1^{D262V} forms high-molecular weight, SDS-resistant species and is crucial for the aggregation of the full-length protein.

(A) *In vivo* sedimentation was carried out on clarified yeast cell lysates. hnRNPA1, hnRNPA1^{D262V}, and construct 195-320 entered the pellet fraction when lysates were subjected to ultracentrifugation, indicating the formation of biochemical aggregates. Construct 1-97 segregated primarily to the soluble lysate fraction, suggesting a lack of aggregate formation. Construct 1-195 demonstrated both aggregated and soluble species. For all constructs, 10% of each of the total and soluble fractions was run alongside 20% of the pelleted protein fraction. **(B)** Yeast expressing hnRNPA1 and all hnRNPA1^{D262V} constructs were subject to SDD-AGE. A YFP-tagged prion protein, Rnq1, served as a positive control, forming amyloid species that were SDS-insoluble, indicated by a high molecular weight smear (bracket). In 2% SDS, the hnRNPA1^{D262V} PrLD in isolation (construct 195-320) formed a similar high molecular weight smear that was distinct from a secondary higher order species (arrow) formed by all other constructs. A red label indicates a highly toxic construct, yellow denotes intermediate toxicity, and green is used for non-toxic constructs. SDD-AGE experiments were done in collaboration with Michael Y. Soo.

2.2.4 The hnRNPA1 PrLD is critical for fibrillization *in vitro*

The ability of various hnRNPA1^{D262V} constructs to form higher-order, SDS-resistant species in yeast and the ability of the hnRNPA1^{D262V} PrLD construct, 195-320, to form amyloid-like structures of similar size to Rnq1 prions led us to examine whether hnRNPA1 might form amyloid *in vitro*. Previously, we demonstrated that purified, recombinant hnRNPA1 forms self-seeding fibrils, a process that is accelerated by the MSP-linked mutation D262V, but whether these fibrils were amyloid was unclear [134]. We now show that unlike recombinant fibrils formed by full-length FUS or TDP-43 [79,110], these hnRNPA1 fibrils bind Thioflavin T (ThT), a diagnostic amyloid dye (Figure 11A), indicating that they likely adopt an amyloid cross- β structure [222]. hnRNPA1^{D262V} spontaneously assembled into ThT-reactive fibrils more rapidly than hnRNPA1 (Figure 3A). The major difference was a much shorter lag phase prior to assembly for hnRNPA1^{D262V} (~2.5h) compared to hnRNPA1 (~10.5h; Figure 11A). Thus, the D262V mutation enables hnRNPA1 to more rapidly nucleate amyloidogenesis. The ability of hnRNPA1 and hnRNPA1^{D262V} to readily access an amyloid state *in vitro* suggests that the hnRNPA1^{D262V} PrLD construct, 195-320, is likely forming amyloid conformers in yeast (Figure 10B).

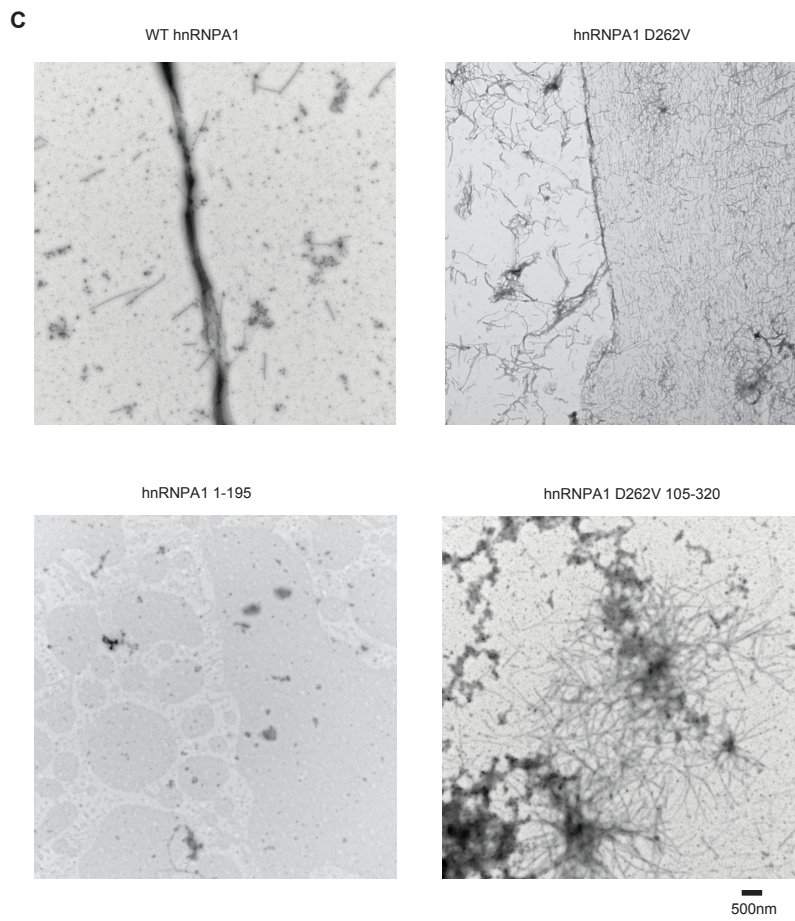
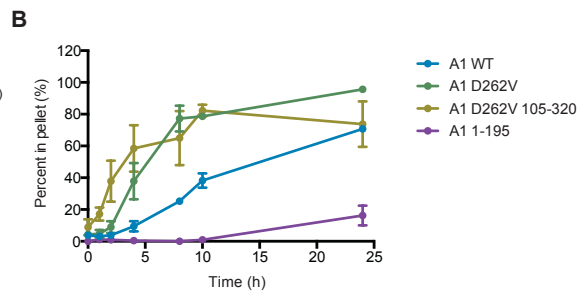
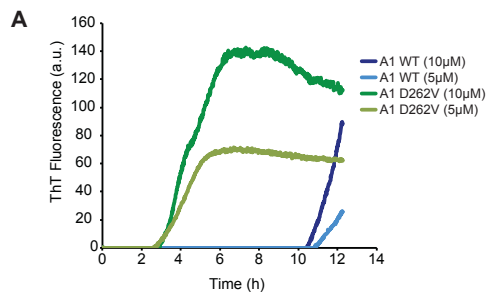


Figure 11: hnRNPA1^{D262V} forms ThT positive fibrils and requires the C-terminal PrLD to fibrillize *in vitro*.

(A) Fluorescence spectroscopy was used to measure ThT fluorescence over 12 hours. hnRNPA1 and hnRNPA1^{D262V} assembled into ThT-positive fibrils. (B) Purified hnRNPA1, hnRNPA1^{D262V}, and construct 1-195 were agitated at 25°C for 24 hours. hnRNPA1^{D262V} 105-320 was agitated at 37°C. Protein aggregation was monitored by sedimentation. Values represent means ± s.e.m. (n=3). Deletion of the PrLD (construct 1-195) abrogated fibril formation. (C) Transmission electron microscopy images taken at 24 hours. hnRNPA1 aggregates were fibrillar and there was a distinct lack of fiber assembly by hnRNPA1 construct 1-195. ThT assays were conducted by Zamia Diaz and Emily Scarborough. Sedimentation and EM were performed by Lin Guo.

Previously, we demonstrated that hnRNPA1 fibrillization is retarded *in vitro* upon making a small deletion of a hexapeptide (residues 259-264) in the PrLD corresponding to the position of the enhanced steric zipper in hnRNPA1^{D262V} [134]. However, in yeast, deletion of this hexapeptide did not affect aggregation (Figure 8D), suggesting a more complex aggregation process *in vivo*, or perhaps the formation of liquid droplets as opposed to protein fibrils [222]. Indeed, the RRM1 and RRM2 protein, 1-195, aggregated in yeast (Figure 8D, 10A). However, *in vitro*, hnRNPA1 1-195 did not aggregate, whereas constructs bearing the PrLD aggregated rapidly (Figure 11B, C). Indeed, deletion of RRM1 in the presence of the D262V missense mutation (construct hnRNPA1^{D262V} 105-320) created a protein that aggregated more rapidly than hnRNPA1^{D262V}, which in turn aggregated more rapidly than hnRNPA1 (Figure 11B). Electron microscopy revealed that hnRNPA1, hnRNPA1^{D262V}, and hnRNPA1^{D262V} 105-320 formed fibrils, whereas the isolated hnRNPA1 RRMs did not (Figure 11C). These findings suggest that the RRM1 and RRM2 protein, 1-195, is not intrinsically aggregation prone in contrast to the PrLD-containing hnRNPA1 proteins. Thus, the formation of

hnRNPA1 1-195 aggregates in yeast (Figure 8D, 10A) likely reflects a more complex process such as incorporation into RNP granules, which we do not recreate *in vitro*.

2.2.5 RRM1, RRM2, and PrLD determinants enable maximal hnRNPA2 toxicity

Do hnRNPA2 and hnRNPA1 have similar domain requirements for toxicity, mislocalization, and aggregation? To answer this question, we created a set of GFP-tagged protein constructs corresponding to those designed for hnRNPA1 (Figure 8A, 12A-C). All of these constructs were robustly expressed (Figure 12C). Thus, variations in the toxicity of hnRNPA2^{D290V} constructs are not due to altered expression. The domain structure of hnRNPA2 closely resembles that of hnRNPA1, containing two RRMs and a C-terminal glycine-rich PrLD spanning residues 190-337, which also includes a smaller core PrLD (residues 266-303), a RGG box (residues 191-218), and a PY-NLS (residues 296-319; Figure 12A) [31,39,40,130,269]. As with hnRNPA1, the yeast nuclear import machinery does not recognize the hnRNPA2 PY-NLS [262]. Thus, WT hnRNPA2 is mislocalized to the cytoplasm as in MSP cases caused by mutations in hnRNPA1 or VCP [134]. Indeed, both hnRNPA2^{D290V} and hnRNPA2 are highly toxic in yeast (Figure 12A, B) [48,134].

As with hnRNPA1, deletion of the hnRNPA2 steric zipper motif (residues 287-292) created by the D290V mutation did not lessen this toxic phenotype, nor did deletion of the core PrLD (residues 266-303) (Figure 12A, B, constructs Δ 287-292 and Δ 266-303). It was surprising that these very aggregation-prone segments were not required for toxicity. Hence, we tested whether the hnRNPA2 PrLD was required for toxicity. Deletion of the entire hnRNPA2 PrLD spanning residues 184-341, preserving only the RRMs eliminated toxicity (Figure 12A, B, construct 1-185), demonstrating that the PrLD is

critical for toxicity. Likewise, RRM1 alone was not toxic (Figure 8A, B, construct 1-92). These findings distinguish hnRNPA2 from hnRNPA1, as deletion of the hnRNPA1 PrLD does not eliminate toxicity (Figure 8A, B, construct 1-195). Thus, the domain requirements for hnRNPA1 and hnRNPA2 toxicity in yeast are subtly different.

Next, we added back progressively larger portions of the hnRNPA2 PrLD (Figure 12A, B, constructs 1-266, 1-303, and 1-319) in an effort to restore maximal toxicity. Here too, hnRNPA2 differed from hnRNPA1 as addition of a short N-terminal portion of the PrLD containing the RGG box (residues 186-266) was not sufficient to restore maximal toxicity (Figure 12A, B, construct 1-266) as it did for hnRNPA1 (Figure 8A, B, construct 1-233). Indeed, larger portions of the PrLD were required to restore maximal hnRNPA2 toxicity (Figure 12A, B, constructs 1-303 and 1-319).

In further contrast to hnRNPA1^{D262V}, hnRNPA2^{D290V} was much less toxic upon deletion of RRM1 (Figure 12A, B, construct 100-341), whereas the equivalent hnRNPA1^{D262V} construct exhibited maximal toxicity (Figure 8A, B, construct 105-320). Moreover, deletion of RRM2 alone completely suppressed hnRNPA2^{D290V} toxicity (Figure 12A, B, construct Δ 100-179), but only partially reduced hnRNPA1^{D262V} toxicity (Figure 8A, B, construct Δ 105-184). Thus, maximal hnRNPA2^{D290V} toxicity is more dependent upon both RRMs, with a larger contribution from RRM2, and also requires a larger portion of the PrLD in comparison to hnRNPA1^{D262V}.

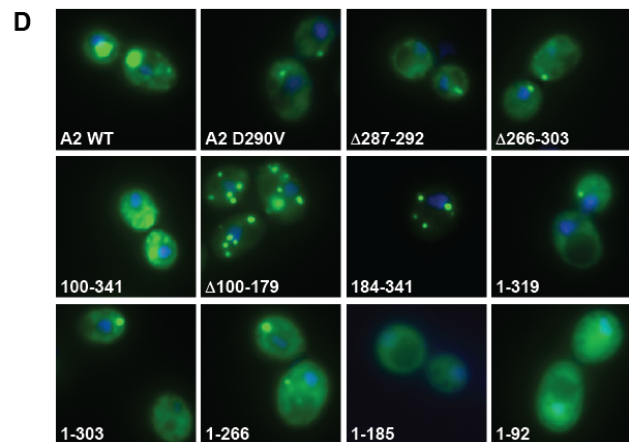
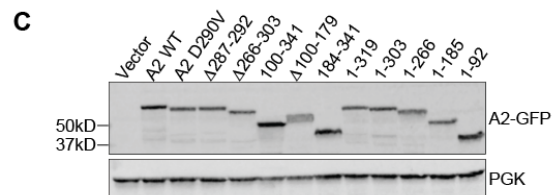
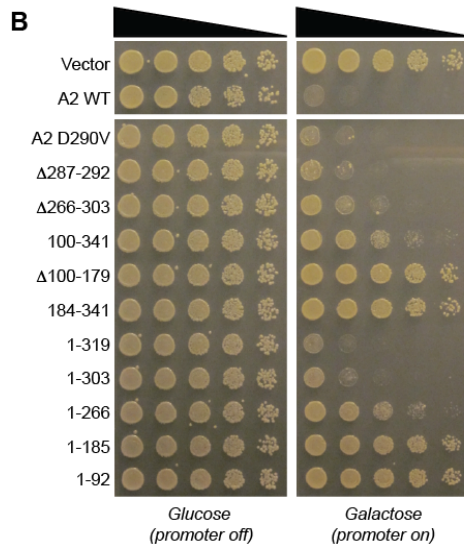
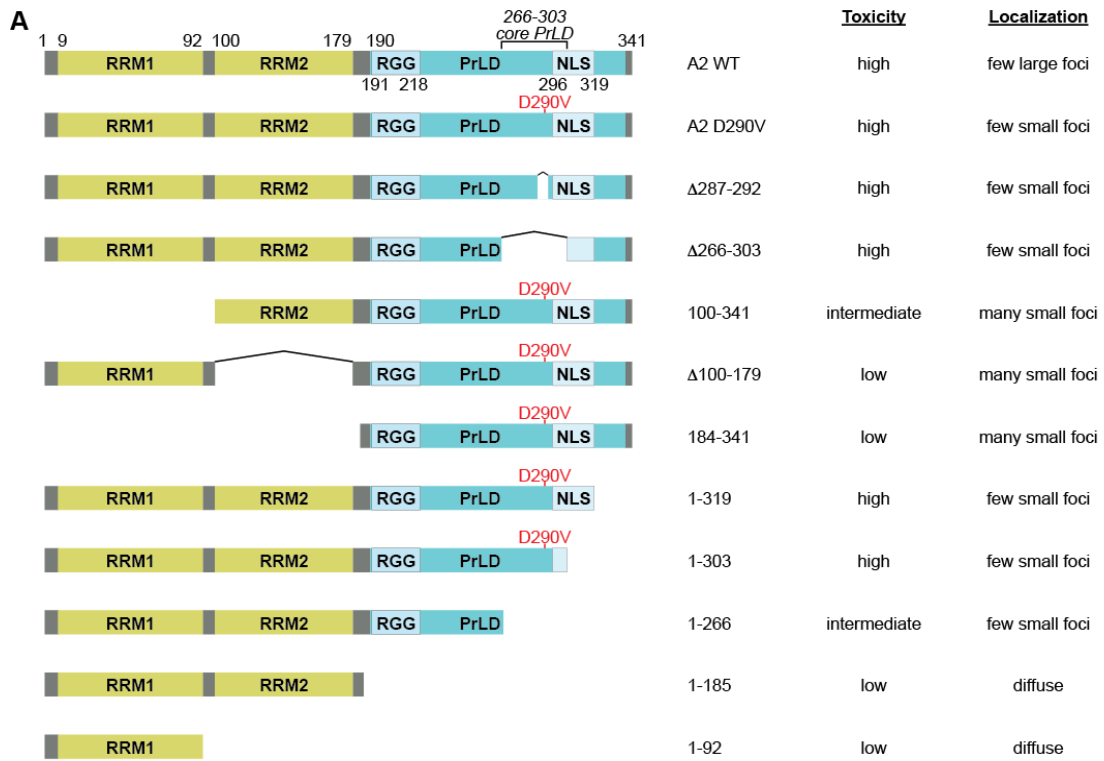


Figure 12: Mapping the domain requirements for hnRNPA2^{D290V} aggregation and toxicity in *S. cerevisiae*.

(A) The domain structure of hnRNPA2 is highly similar to that of hnRNPA1 (depicted in Figures 5 and 8). A series of hnRNPA2^{D290V} deletion and truncation constructs were expressed in *S. cerevisiae* and assayed for toxicity and cellular localization. **(B)** A spotting assay (five-fold serial yeast dilutions) was performed to compare toxicities of hnRNPA2 constructs. hnRNPA2 and hnRNPA2^{D290V} were highly toxic when expressed in yeast, and both RRMs were required for maximal toxicity (constructs 100-341 and Δ 100-179). Part of the C-terminal PrLD was also essential (construct 1-185). hnRNPA2 expression is repressed on glucose media and induced on galactose media. **(C)** Immunoblot confirmed robust expression of all hnRNPA2 protein constructs. **(D)** Fluorescence microscopy illustrates the cellular localization of GFP-tagged hnRNPA2 constructs. The WT protein and all mutants were found in the cytoplasm. All proteins containing a portion of the PrLD formed foci, while the isolated RRM domains were diffuse throughout the cytoplasm (constructs 1-185 and 1-92). Deletion of one or both RRMs resulted in an increase in the number of foci formed (constructs 100-341, Δ 100-179, and 184-341). WT, wild type; RRM, RNA-recognition motif; PrLD, prion-like domain; NLS, nuclear localization signal.

2.2.6 PrLD determinants are critical for hnRNPA2 aggregation in yeast

hnRNPA2 and hnRNPA2^{D290V} formed cytoplasmic foci in yeast (Figure 12D), although those formed by hnRNPA2^{D290V} were smaller and less common than those formed by hnRNPA1 (Figure 12D). Deletion of the steric zipper hexapeptide (residues 287-292) maintained this pattern of diffuse staining with few small foci, as did elimination of the core hnRNPA2 PrLD (Figure 12D, constructs Δ 287-292 and Δ 266-303). C-terminal deletions in the PrLD also did not affect this localization (Figure 12A, D, constructs 1-319, 1-303 and 1-266). As with hnRNPA1^{D262V} (Figure 8D), deletion of one or both RRMs of hnRNPA2^{D290V} resulted in an increase in the number of cytoplasmic puncta (Figure 12D, constructs 100-341, Δ 100-179 and 184-341). Interestingly, deletion of both RRMs appeared to decrease the amount of diffuse cytoplasmic hnRNPA2 and yield intense hnRNPA2 foci (Figure 12D, construct 184-341). In the absence of the PrLD, hnRNPA2 constructs yielded predominantly diffuse cytoplasmic staining (Figure 12D, constructs 1-

185, 1-92). Thus, in contrast to hnRNPA1, the hnRNPA2 RRM1 and RRM2 construct, 1-185, does not readily form cytoplasmic foci.

Next, we asked whether the cytoplasmic foci formed by various hnRNPA2 and hnRNPA2^{D290V} constructs represent bona fide aggregates via sedimentation analysis of yeast lysates [79,235]. Significant fractions of hnRNPA2 and hnRNPA2^{D290V} were partitioned to the insoluble fraction (Figure 13A). However, hnRNPA2 and hnRNPA2^{D290V} were also found in the soluble fraction (Figure 13A). Indeed, hnRNPA2 was more soluble in comparison to hnRNPA1 (Figure 10A, 13A). By contrast, the hnRNPA2^{D290V} PrLD was primarily insoluble (Figure 13A, construct 184-341). The RRMs were found in primarily the soluble fraction with a small proportion of protein in the insoluble fraction (Figure 13A, construct 1-185). hnRNPA2 1-92 did not aggregate and was detected only in the soluble fraction (Figure 13A, construct 1-92). Thus, the hnRNPA2 PrLD primarily drives hnRNPA2 aggregation in yeast, whereas RRM1 and RRM2 also contribute in hnRNPA1 (Figure 13A).

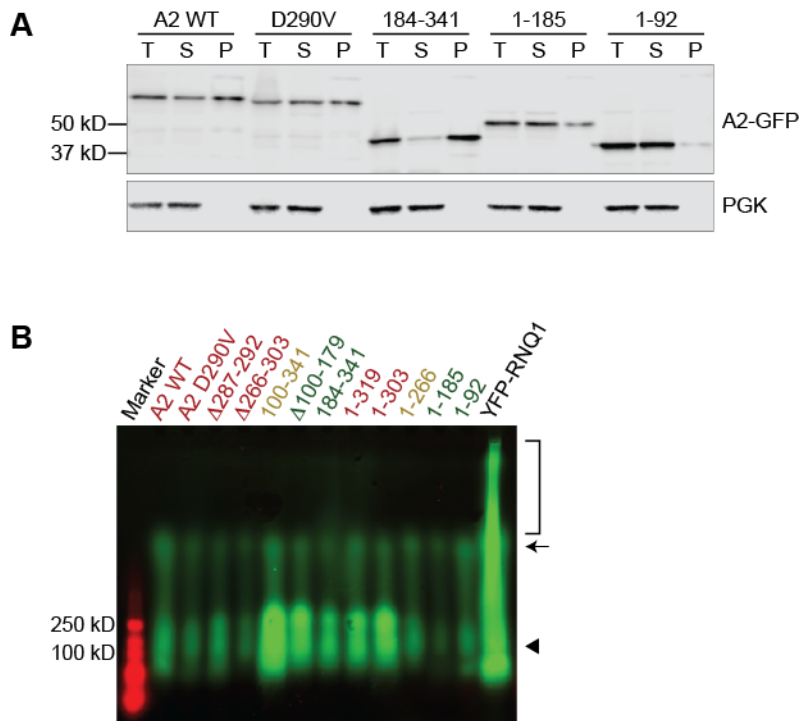


Figure 13: The PrLD of hnRNPA2 is crucial for the aggregation of the full-length protein.

(A) Overexpressed hnRNPA2, hnRNPA2^{D290V}, and construct 184-341 aggregated and entered the pellet fraction when clarified yeast cell lysates were subjected to ultracentrifugation. The RRMs (construct 1-185) formed both aggregated and soluble species, while RRM1 alone (construct 1-92) segregated predominantly to the soluble lysate fraction. For all constructs, 10% of each of the total and soluble fractions was run alongside 20% of the pelleted protein fraction. **(B)** hnRNPA2 and all hnRNPA2^{D290V} constructs were subject to SDD-AGE with YFP-tagged Rnq1 serving as a positive, amyloid-forming control. None formed the high molecular weight smear that is characteristic of Rnq1 prion species (bracket). All hnRNPA2 proteins did form a secondary high molecular weight species (arrow). Red-, yellow-, and green-labeled constructs have high, intermediate, and low toxicity, respectively. SDD-AGE was performed in collaboration with Michael Y. Soo.

SDD-AGE revealed that none of the hnRNPA2 constructs formed very high molecular weight species similar to Rnq1-YFP prions (Figure 13B). Thus, in contrast to the hnRNPA1^{D262V} PrLD, the hnRNPA2^{D290V} PrLD does not form a higher order amyloid

species akin to Rnq1-YFP prions (Figure 10B, 13B). Rather, all the hnRNPA2 constructs formed two distinct SDS-resistant species, one from ~75-250kDa and another greater than 250kDa (Figure 13B, arrow). These high molecular weight forms likely represent SDS-resistant oligomeric structures or stable RNP particles. However, no pattern emerged for formation of these species by toxic or non-toxic constructs. Indeed, the toxic full-length hnRNPA2 constructs and non-toxic RRM constructs (1-185 and 1-92) both partitioned to these two species (Figure 13B). Interestingly, these two discrete higher order hnRNPA2 structures were smaller than those formed by hnRNPA1 (Figure 10B, 13B), indicating that the two hnRNPs assemble into particles of different sizes.

2.2.7 The hnRNPA2 PrLD is critical for fibrillization *in vitro*

Next, we tested the *in vitro* determinants of hnRNPA2 fibrillization. hnRNPA2^{D290V} assembles into fibrils more rapidly than hnRNPA2 [134]. However, in contrast to hnRNPA1, hnRNPA2 and hnRNPA2^{D290V} form ThT-negative fibrils *in vitro* (Figure 14A and 14C). The hnRNPA2 PrLD is required for aggregation, as the isolated RRMs (construct 1-185) did not aggregate (Figure 14B). Deletion of RRM1 from hnRNPA2^{D290V} did not affect the accelerated lag time of the assembly of the mutant protein (Figure 14B). hnRNPA2, hnRNPA2^{D290V}, and hnRNPA2 100-341 all formed abundant fibrils, whereas RRM1 and RRM2 in the absence of the PrLD were unable to do so (Figure 14C). Thus, the hnRNPA2 PrLD is critical for fibrillization.

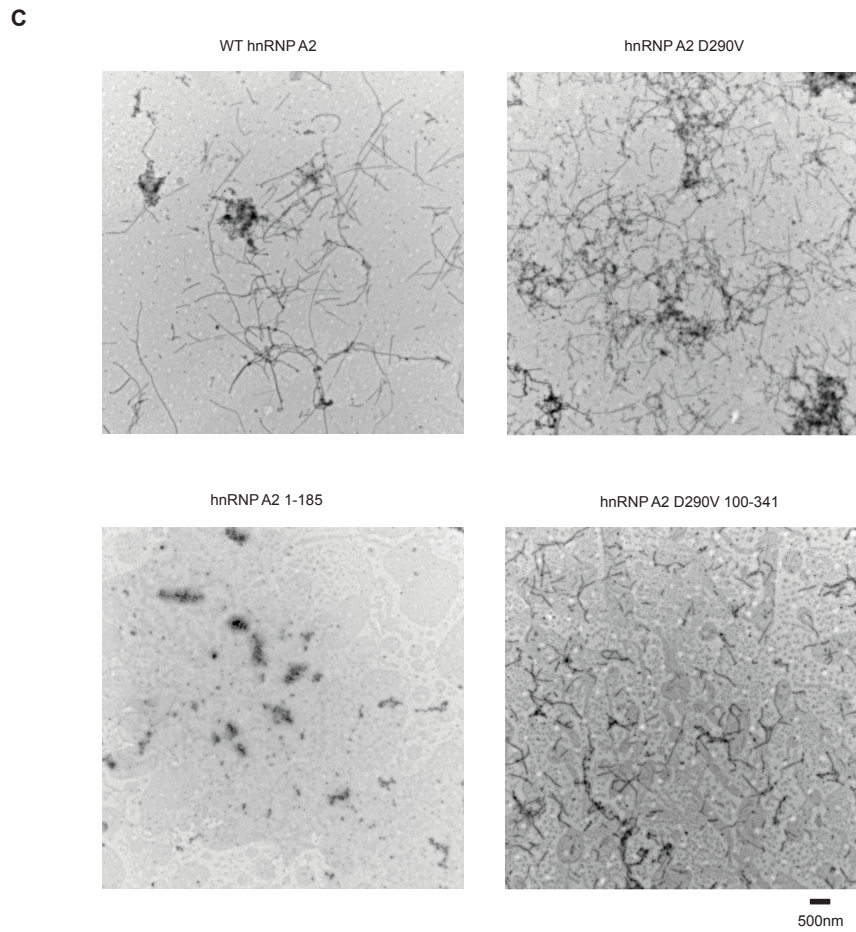
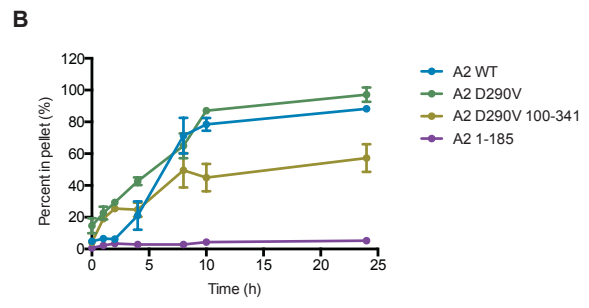
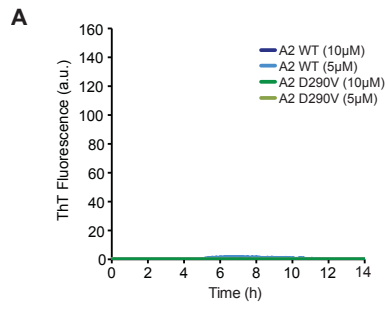


Figure 14: hnRNPA2^{D290V} forms THT negative fibrils and requires the C-terminal prion-like domain to fibrillize *in vitro*.

(A) Fluorescence spectroscopy was used to show that, in contrast to hnRNPA1, purified hnRNPA2 and hnRNPA2^{D290V} did not form ThT-positive aggregates. (B) Purified hnRNPA2, hnRNPA2^{D290V}, and construct 1-185 were agitated at 25°C for 24 hours. hnRNPA2^{D290V} 100-341 was agitated at 37°C. Protein aggregation was monitored by sedimentation. Values represent means ± s.e.m. (n=3). Deletion of the PrLD (construct 1-185) eliminated aggregation. (C) Transmission electron microscopy images taken at 24 hours show that hnRNPA2 formed fibrillar structures, but a construct lacking the PrLD (construct 1-185) did not. ThT assays were conducted by Zamia Diaz and Emily Scarborough. Sedimentation and EM were performed by Lin Guo.

2.2.8 Disruption of RRM-RNA interactions suppressed hnRNPA1^{D262V}, hnRNPA2^{D290V}, and TDP-43 toxicity

Mutation of conserved phenylalanine residues to aspartic acid in the RRM interferes with the RNA-binding ability of hnRNPA1 and hnRNPA2 [179,260]. Thus, we introduced these missense mutations into RRM1, RRM2, or both RRMs of hnRNPA1^{D262V} and hnRNPA2^{D290V} and assessed toxicity (Figure 15A, B). All constructs were expressed at similar levels (Figure 15C). Mutation of F57 and F59 in RRM1 of hnRNPA1^{D262V} strongly suppressed toxicity (Figure 15B), whereas mutation of F148 and F150 in RRM2 of hnRNPA1^{D262V} suppressed toxicity to a lesser extent (Figure 15B). When both RRMs of hnRNPA1^{D262V} were mutated toxicity was suppressed to a similar extent as when only RRM1 was disrupted (Figure 15B). The strong suppression of toxicity by the F57D:F59D mutation of RRM1 of hnRNPA1^{D262V} was not anticipated as deletion of RRM1 from hnRNPA1^{D262V} had minimal effect on toxicity (Figure 8A, construct 105-320). However, a crystal structure of the hnRNPA1 RRM1 and RRM2 isolated and bound to a trinucleotide RNA target suggests that while the unbound RRMs are tightly packed with limited space for RNA interaction with RRM2, binding of RNA to

RRM1 causes a conformational change that shifts the two RRM's away from one another [270]. We suggest that deletion of RRM1 does not affect hnRNPA1 toxicity because RRM2-RNA interactions are uninhibited. In the case of RRM1 missense mutations, the tight packing of the RRM's is maintained in the absence of RNA binding to RRM1, effectively diminishing RNA interactions with both RRM's, thereby significantly reducing protein toxicity.

Interestingly, when we mutated corresponding phenylalanine residues in hnRNPA2^{D290V} (F52 and F54 in RRM1 and F143 and F145 in RRM2) to aspartic acid, we observed complete suppression of toxicity whether RRM1, RRM2, or both RRM's were mutated (Figure 15B). These findings suggest that RNA binding to both RRM's of hnRNPA2^{D290V} is critical for toxicity. By contrast, in the context of *full-length* hnRNPA1^{D262V}, RNA binding to RRM1 is more critical for toxicity than RNA binding to RRM2, perhaps because RNA binding to RRM2 is at least partially contingent upon RNA binding to RRM1 [270].

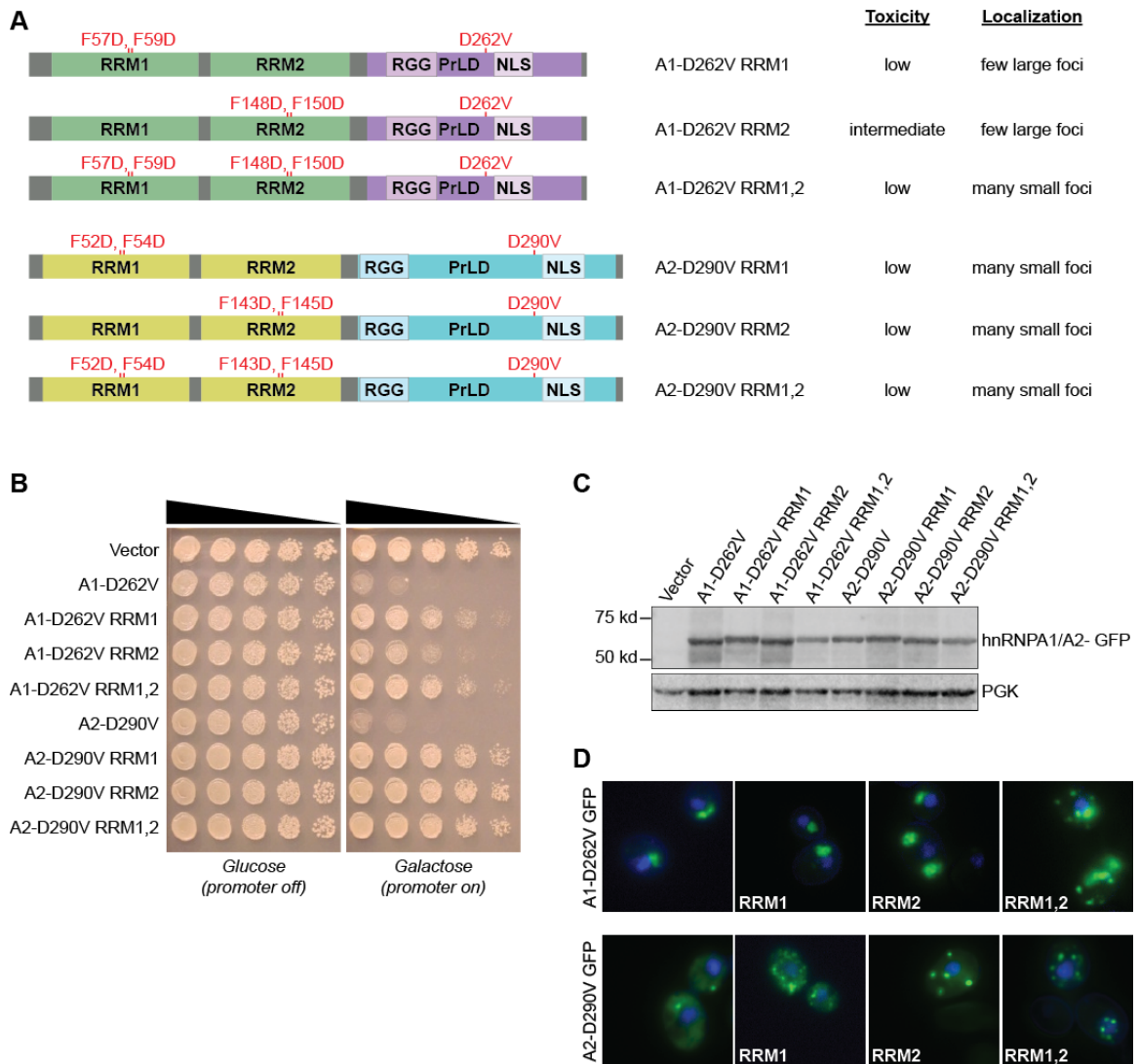


Figure 15: Disruption of RRM-mediated RNA binding reduces the toxicity of hnRNPA1^{D262V} and hnRNPA2^{D290V} and alters cytoplasmic aggregation patterns. (A) Missense mutations were introduced at the indicated locations in RRM1 and 2 of hnRNPA1^{D262V} and hnRNPA2^{D290V} to disrupt RNA binding. (B) Yeast were spotted in five-fold dilution series, and mutation of one or both RRMs of hnRNPA1^{D262V} or hnRNPA2^{D290V} suppressed toxicity. (C) Western blotting confirmed robust expression of RNA-binding deficient proteins. (D) Fluorescence microscopy revealed that missense mutations in both RRMs of hnRNPA1^{D262V} resulted in the formation of smaller and more numerous cytoplasmic foci (RRM1,2). This pattern was also observed when either or both RRMs of hnRNPA2^{D290V} are perturbed (RRM1, RRM2, RRM1,2). RRM, RNA-recognition motif; PrLD, prion-like domain; NLS, nuclear localization signal.

Next, we asked whether RRM:RNA interactions influence the aggregation pattern of hnRNPA1^{D262V} and hnRNPA2^{D290V}. hnRNPA1^{D262V} formed large cytoplasmic foci after mutation of RRM1 or RRM2 (Figure 15D). However, mutation of RRM1 and RRM2 caused hnRNPA1^{D262V} to form smaller, more scattered foci throughout the cytoplasm (Figure 15D). By contrast, mutation of RRM1, RRM2, or both RRMs alter the distribution of hnRNPA2^{D290V} from few large foci to many small foci (Figure 15D).

Next, we compared these requirements for RRM-RNA binding to hnRNPA1^{D262V} and hnRNPA2^{D290V} for toxicity to those of TDP-43 (Figure 16A-C). Thus, we mutated each of five crucial phenylalanine residues to leucine to ask whether RRM:RNA binding is critical for the toxicity of TDP-43 (Figure 16A) [60,271]. Mutation of F147 or F149 in RRM1 had no effect on TDP-43 toxicity (Figure 16C), and mutation of these two residues simultaneously only partially suppressed protein toxicity (Figure 16C). Mutation of F194, F229, or F231 in RRM2 provided stronger toxicity suppression (Figure 16C). The toxicity mitigating effect of mutating any two of these together was comparable to mutating each alone (Figure 16C). The strongest toxicity suppression was evident after mutation of all three RRM2 phenylalanines or all five described residues together (Figure 16C). Thus, RNA binding to RRM2 of TDP-43 is more critical for toxicity than RNA binding to RRM1. Mutation of one or more phenylalanines in either RRM1 or RRM2 had no effect on the formation of cytoplasmic TDP-43 foci (Figure 16B). However, mutation of all five phenylalanine residues restored nuclear TDP-43 localization (Figure 16B). Taken together, these data suggest that the toxic effects of TDP-43, hnRNPA1^{D262V}, and hnRNPA2^{D290V} all require RNA binding by RRMs.

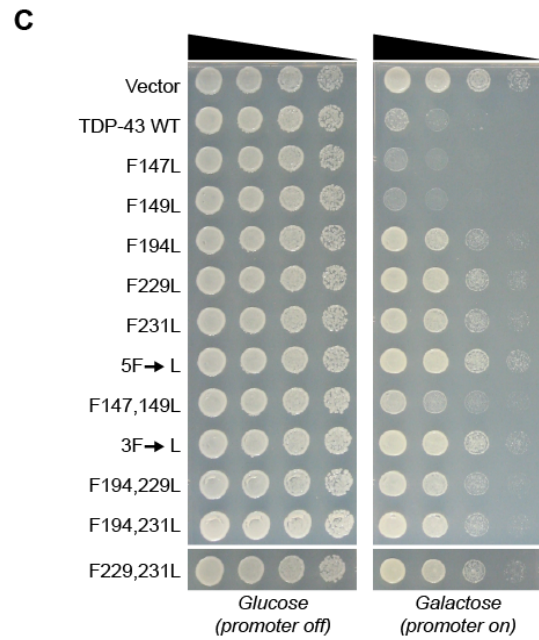
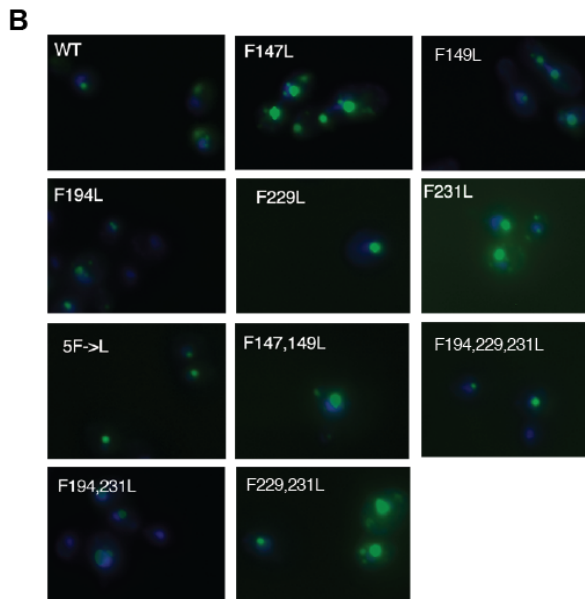
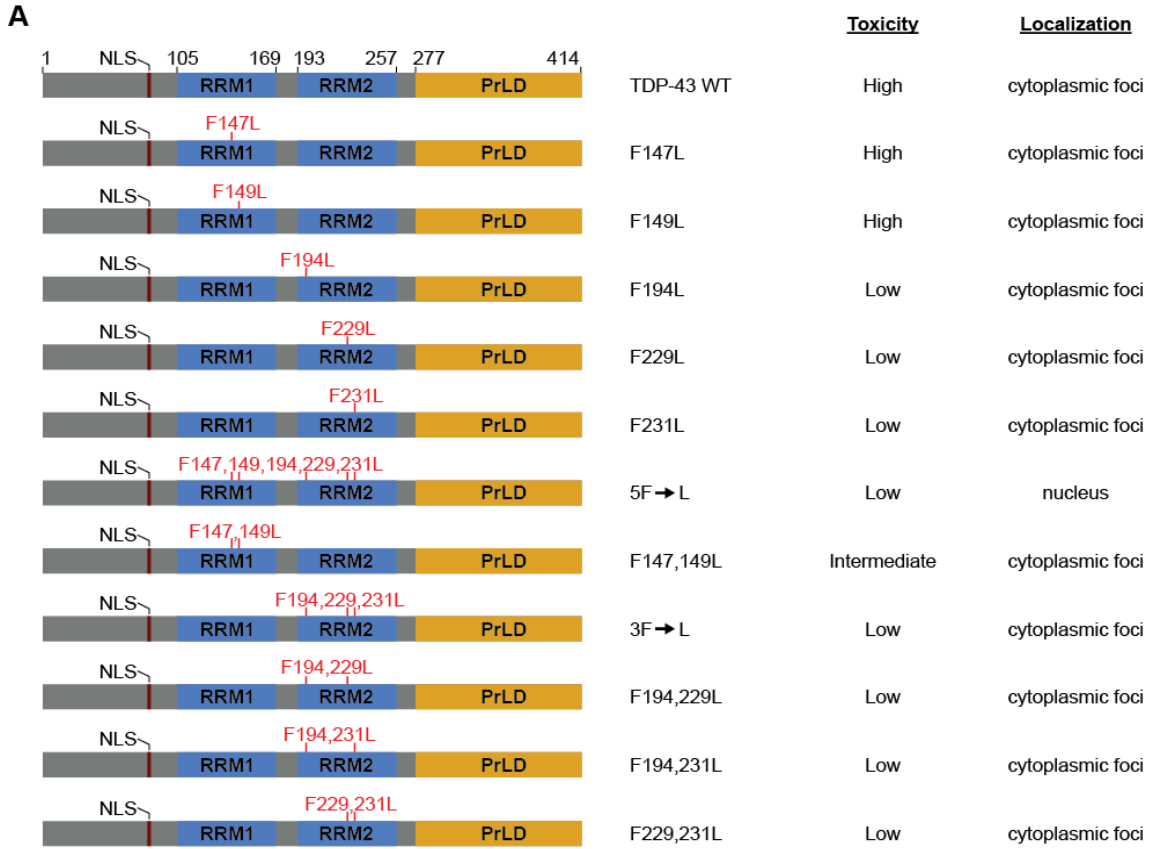


Figure 16: Disruption of RRM-mediated RNA binding reduces the toxicity of TDP-43 and can restore nuclear localization.

(A) The domain structure of TDP-43 is illustrated. The indicated RRM-mutants were expressed in *S. cerevisiae*. (B) Fluorescence microscopy was used to assess the cellular localization of RNA-binding deficient TDP-43 mutants. The 5F->L protein is nuclear, while all other mutants form cytoplasmic aggregates, similar to TDP-43. (C) Spotting onto inducing galactose media demonstrated that missense mutations in RRM2 were more effective than those in RRM1 at suppressing the toxic effect of TDP-43. RRM, RNA-recognition motif; PrLD, prion-like domain; NLS, nuclear localization signal. Experiments in the figure were performed by Maria Armakola.

2.2.9 Potentiated Hsp104 variants suppress hnRNPA1^{D262V} and hnRNPA2^{D290V} toxicity

Hsp104 is a AAA+ protein (ATPase Associated with diverse Activities) and a yeast protein disaggregase that is found in all eukaryotes except metazoa [8,231,232]. Hsp104 disassembles both amyloid and amorphous aggregates, and promotes survival in yeast by renaturing misfolded proteins after environmental stress [231,238]. Expression of Hsp104 in a rat model of PD reduced assembly of α -synuclein inclusions and degeneration of dopaminergic neurons [8]. Potentiated Hsp104 variants, including Hsp104^{A503S}, Hsp104^{V426L} and Hsp104^{A437W}, reduce aggregation and toxicity of TDP-43, FUS, and α -synuclein in yeast [234,235]. These three missense mutations fall in the coiled-coil middle domain (MD) of Hsp104, and increase ATPase and unfoldase activity [235]. It is hypothesized that specific mutations in the MD enhance activity by disruption of autoinhibitory interactions or by mimicking allosteric activation events, perhaps including the binding of Hsp70 to the MD [235,242,243]. Thus, we tested whether potentiated Hsp104 variants could mitigate the toxicity of hnRNPA1, hnRNPA2 and the disease-associated mutants in $\Delta hsp104$ yeast (Figure 17A).

When yeast were plated onto inducing galactose media and allowed to grow for 2 days at 30°C, we observed that potentiated variants had no effect on the toxicity of hnRNPA1, hnRNPA1^{D262V}, or hnRNPA2, but were able to weakly suppress the toxicity of hnRNPA2^{D290V} and FUS (Figure 17A). The toxicity suppression of FUS and hnRNPA2^{D290V} was more robust after 3 days of growth at 30°C (Figure 17C). We lowered the expression levels of all toxic proteins and potentiated Hsp104 variants by plating on a combination of galactose and sucrose, which reduced the toxicity of hnRNPA1, hnRNPA1^{D262V}, hnRNPA2, and hnRNPA2^{D290V}. hnRNPA1, hnRNPA1^{D262V}, hnRNPA2, and hnRNPA2^{D290V} toxicity was mitigated by Hsp104^{A503S}, Hsp104^{V426L} and Hsp104^{A437W}, but not by Hsp104 (Figure 17A). Thus, hnRNPA1^{D262V} and hnRNPA2^{D290V} toxicity can be alleviated by enhanced protein disaggregases based on Hsp104. Overexpression of enhanced Hsp104 variants slightly decreased the expression of hnRNPA1, hnRNPA2, and MSP-associated variants (Figure 17B). Hsp104^{A503S}, Hsp104^{V426L} and Hsp104^{A437W} had similar effects on FUS expression levels (Figure 17B). Thus, the reductions in hnRNPA1 and hnRNPA2 toxicity may be due to destabilization or increased degradation of these proteins. Interestingly, hnRNPA2^{D290V} expression appears to be reduced the most by potentiated Hsp104 variants (Figure 17B). This may explain why hnRNPA2^{D290V} toxicity could be suppressed by Hsp104 variants on pure galactose media but hnRNPA1, hnRNPA1^{D262V}, and hnRNPA2 toxicity could not.

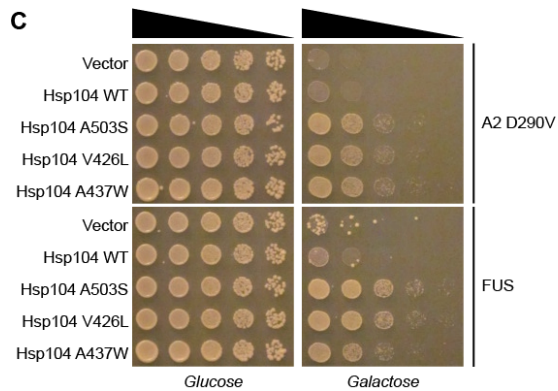
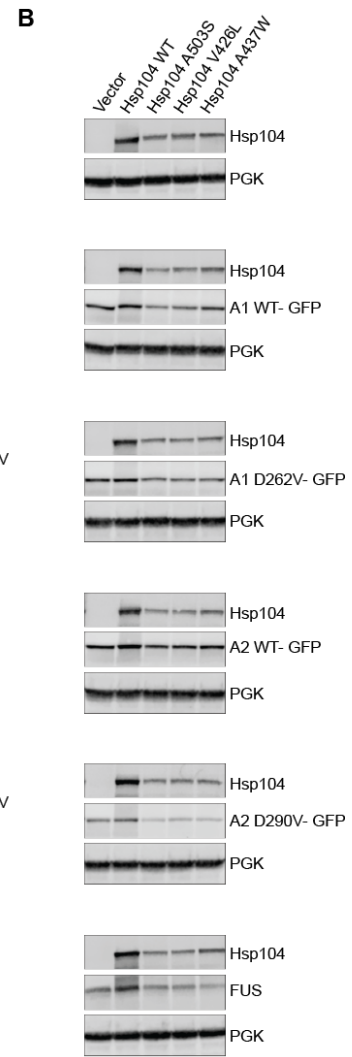
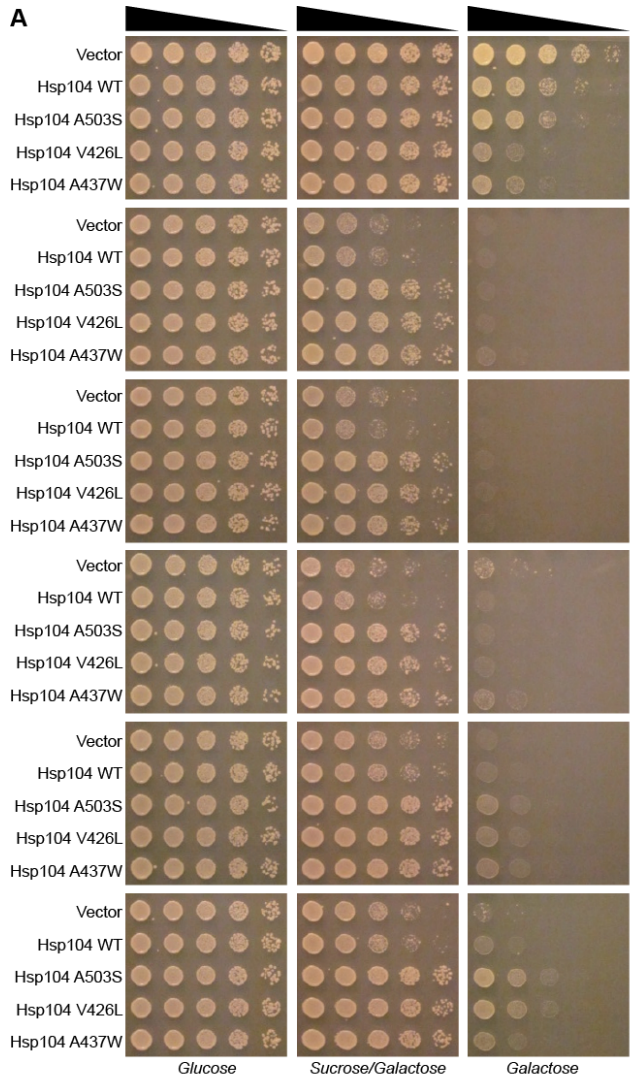


Figure 17: Potentiated forms of Hsp104 can suppress the toxicity of hnRNPA1, hnRNPA1^{D262V}, hnRNPA2, and hnRNPA2^{D290V}.

(A) Yeast coexpressing toxic disease proteins with Hsp104 or potentiated Hsp104 variants were spotted onto inducing galactose media or a mixture of sucrose and galactose that causes a reduction in expression driven by the galactose promoter. Hsp104 variants A503S, V426L and A437W, but not the WT disaggregase, effectively suppressed the toxicity of hnRNPA1, hnRNPA1^{D262V}, hnRNPA2 and hnRNPA2^{D290V} on growth media containing a 1:1 mixture of sucrose and galactose. Hsp104 and disease proteins were both under the regulation of the GAL1 promoter. FUS was used as positive control for toxicity suppression. Spotting assays are shown after 2 days of growth at 30°C. (B) Western blotting confirmed expression of Hsp104 and toxic, disease-associated proteins after growth in media supplemented with both sucrose and galactose. (C) hnRNPA2^{D290V} and FUS expressing strains from (A) shown after 3 days of growth at 30°C on glucose- and galactose-containing media. Hsp104^{A503S}, Hsp104^{V426L}, and Hsp104^{A437W} robustly suppressed the toxicity of hnRNPA2^{D290V} at high expression levels.

2.2.10 hnRNPA1 and hnRNPA2 colocalize with a stress granule marker

RNP granules including stress granules and P bodies play an important role in RNA metabolism and homeostasis, serving as sites of stalled translation initiation and mRNA degradation, respectively [50]. We asked whether association with stress granules plays a role in the toxicity of hnRNPA1 and hnRNPA2. We coexpressed GFP-tagged hnRNPA1 or hnRNPA2 with mCherry tagged Pab1, a yeast stress granule protein [196]. Pab1 is a cytoplasmic poly(A)-binding protein consisting of four RRM domains that mediate RNA binding and protein-protein interactions [272]. Pab1 regulates mRNA deadenylation, increases mRNA stability by opposing decapping, and facilitates mRNA translation [273-276]. Pab1 contributes to, but is not required for, the formation of stress granules in yeast [196]. It has also been suggested that Pab1 promotes the removal of mRNAs from P bodies [196,277].

Pab1 was localized diffusely throughout the cytoplasm of cells when expressed in control cells (Figure 18A). However, expression of hnRNPA1 or hnRNPA1^{D262V} caused Pab1 to form foci that co-localized with hnRNPA1 or hnRNPA1^{D262V} (Figure 18A). hnRNPA1^{D262V} lacking RRM1 or RRM2 also colocalized with Pab1 foci (Figure 18A, constructs 105-320 and Δ 105-184). Expression of the hnRNPA1 RRMs alone (1-195) was also accompanied by formation of Pab1 foci, which colocalized with hnRNPA1 1-195 (Figure 18A, construct 1-195). 70-90% of cells harboring inclusions formed by RRM-containing hnRNPA1 constructs also demonstrated Pab1 inclusion formation (Figure 18B). By contrast, Pab1 remained diffuse upon expression of the non-toxic hnRNPA1^{D262V} PrLD construct (Figure 18A, construct 195-320), with only 5% of cells that contained hnRNPA1^{D262V} inclusions also exhibiting Pab1 foci (Figure 18B, construct 195-320). Thus, hnRNPA1 induces the formation of Pab1 foci, in a manner that depends on the hnRNPA1 RRMs. Importantly, only toxic hnRNPA1 constructs induced formation of Pab1 foci, indicating that inappropriate Pab1 localization or altered stress granule assembly may contribute to hnRNPA1 toxicity. While we observed that the hnRNPA1 PrLD did not induce the formation of Pab1 foci or Pab1-containing stress granules, the PrLD is efficiently recruited to stress granules in HeLa cells exposed to sodium arsenite stress [222]. Taken together, these observations suggest that the hnRNPA1 PrLD may be capable of interaction with stress granule components, but, in yeast, is not sufficient to drive their assembly.

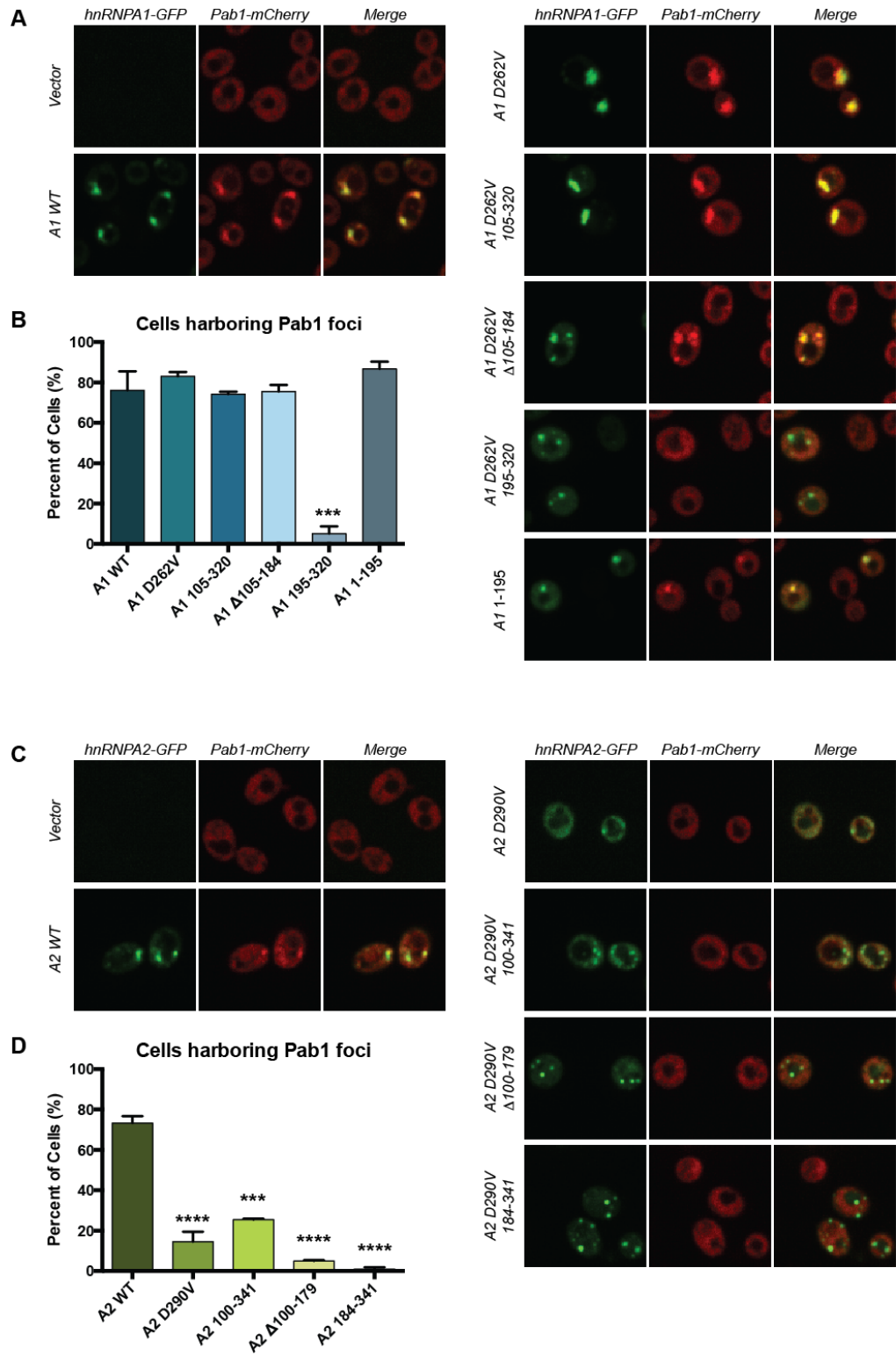


Figure 18: A stress granule marker, Pab1, forms foci that colocalize with aggregated hnRNPA1 and hnRNPA1^{D262V}, and hnRNPA2, but remains diffuse throughout the cytoplasm when coexpressed with hnRNPA2^{D290V}.

(A) Fluorescence microscopy was used to compare the localization of GFP-tagged hnRNPA1 constructs and mCherry-tagged Pab1. Yeast expressing mCherry-tagged Pab1 were a gift from Frank Luca. Pab1 formed foci in the presence of hnRNPA1 constructs containing an RRM, but not when coexpressed with the isolated hnRNPA1^{D262V} PrLD. When present, Pab1 foci colocalized with hnRNPA1. **(B)** Quantification of (A). Values represent means \pm s.e.m.; n=2 (**p \leq 0.001; one-way ANOVA comparing each construct to the WT protein using a Dunnett correction for multiple comparisons). **(C)** Fluorescence microscopy showed that, when coexpressed with hnRNPA2, Pab1 formed foci that colocalize with hnRNPA2, but Pab1 did not form foci when coexpressed with hnRNPA2^{D290V}. **(D)** Quantification of (C). Values represent means \pm s.e.m.; n=2 (**p \leq 0.001, ****p \leq 0.0001; one-way ANOVA comparing each construct to the WT protein using a Dunnett correction for multiple comparisons).

Pab1 also formed foci when coexpressed with hnRNPA2, and hnRNPA2 colocalized with Pab1 foci (Figure 18C). Roughly 70% of cells harboring hnRNPA2 foci also demonstrated Pab1 assemblies (Figure 18D). Surprisingly, however, expression of hnRNPA2^{D290V} was not accompanied by the formation of Pab1 foci, and only ~14% of cells with hnRNPA2^{D290V} inclusions also exhibited Pab1 focus formation (Figure 18C,D). In this minority of cells, Pab1 foci colocalized with hnRNPA2^{D290V} foci. When overexpressed with hnRNPA2^{D290V}, Pab1 was primarily localized diffusely throughout the cytoplasm (Figure 18C). Pab1 was similarly diffuse throughout cells expressing hnRNPA2^{D290V} lacking either or both RRMs (Figure 18C, constructs 100-341, Δ 100-179 and 184-341). Fewer than 6% of cells expressing hnRNPA2^{D290V} constructs lacking RRM2 that formed foci also contained Pab1 inclusions (Figure 18D). Expression of hnRNPA2^{D290V} lacking RRM1 was accompanied by Pab1 focus formation in ~25% of cells (Figure 18D). Of cells that did form Pab1 assemblies, we observed that, on average, ~30% contained at least one Pab1 focus that did not colocalize with co-

occurring hnRNPA2^{D290V} 100-341 foci, which we did not observe upon expression of full-length hnRNPA2 or hnRNPA2^{D290V}. We confirmed that the expression of mCherry-tagged Pab1 from the endogenous promoter did not affect the toxicity of any hnRNPA1 or hnRNPA2 protein constructs (compare Figures 19A and 19B with 8B and 12B). Our results suggest that the introduction of the D290V mutation into the hnRNPA2 PrLD disrupts the robust formation of Pab1 foci induced by hnRNPA2, and RNA binding via RRM is important for the colocalization of hnRNPA2 with Pab1. Moreover, unlike hnRNPA1 and hnRNPA1^{D262V}, hnRNPA2^{D290V} toxicity is not accompanied by Pab1 inclusion formation. Thus, the formation of Pab1 foci is not a general requirement of hnRNPA1 and hnRNPA2 toxicity in yeast. Aberrant aggregation of Pab1 may contribute to the toxicity of hnRNPA1, hnRNPA1^{D262V}, and hnRNPA2, but is likely a single element of multiple perturbations caused by hnRNPA1 or hnRNPA2 expression. hnRNPA2^{D290V} does not typically induce Pab1 foci but is very toxic, suggesting that, in yeast, an interaction between Pab1 and hnRNPA2^{D290V} is not essential for toxicity.

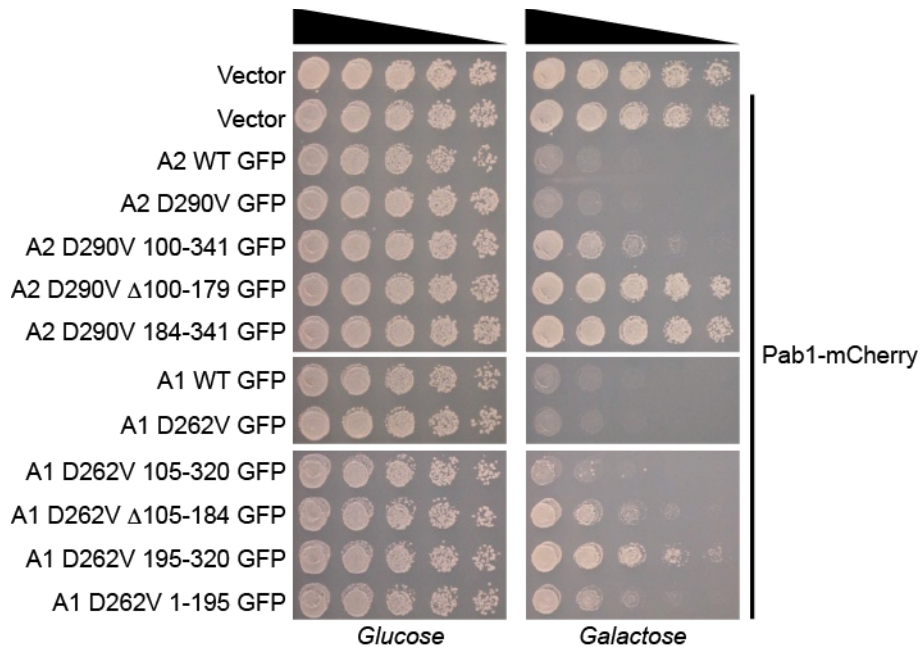


Figure 19: Expression of mCherry-tagged Pab1 does not affect toxicity of hnRNPA1, hnRNPA2, or deletion constructs.

Yeast expressing Pab1-mCherry from the endogenous Pab1 promoter and hnRNPA1 or hnRNPA1^{D262V} constructs from the Gal1 promoter were spotted in five-fold dilution series onto inducing galactose media. The toxicity of hnRNPA1 constructs is unchanged by the expression of mCherry-tagged Pab1. When Pab1-mCherry was similarly coexpressed with hnRNPA2 constructs and spotted onto galactose media, it had no effect on the toxicity of hnRNPA1, hnRNPA2^{D290V}, or hnRNPA2^{D290V} deletion constructs.

2.2.11 Overexpression of Tif2, but not Pab1, reduces hnRNP toxicity

If the mislocalization of Pab1 to aberrant cytoplasmic foci plays a role in the toxicity phenotype caused by hnRNPA1 and hnRNPA1^{D262V} expression, we hypothesized that overexpression of Pab1 might compensate for this sequestration and reduce the toxicity of hnRNPA1 and hnRNPA1^{D262V}. Pab1 overexpression is known to reduce the toxicity of FUS when overexpressed [110], as is overexpression of another stress-granule marker, Tif2 [110,278]. Tif2 is an RNA-helicase that is homologous to the

mammalian translation initiation factor eIF4A [279]. Tif2 facilitates protein synthesis by unwinding mRNA secondary structures to allow ribosomal binding to the mRNA [279,280]. In mammalian cells, inhibition or alteration of eIF4A activity is sufficient to induce stress granule formation [281]. We observed no effect on the toxicity of hnRNPA1, hnRNPA1^{D262V}, hnRNPA2, or hnRNPA2^{D290V} when Pab1 was simultaneously overexpressed (Figure 20A). Pab1 overexpression did not suppress toxicity on either galactose or sucrose/galactose media. By contrast, overexpression of Tif2 weakly reduced the toxicity of hnRNPA1, hnRNPA2, and both disease-linked hnRNPs, but only when Tif2 was expressed from a high copy number 2-micron plasmid (Figure 20B). Moreover, Tif2-mediated suppression of hnRNPA1 and hnRNPA2 toxicity was only evident when cells were grown on sucrose/galactose media. At higher expression levels induced by galactose media, Tif2 overexpression did not affect hnRNPA1 or hnRNPA2 toxicity. The effect of Tif2 on hnRNPA1 and hnRNPA2 toxicity could not be attributed to a reduction in hnRNP expression levels (Figure 20C). It is possible that increased protein translation induced by Tif2 overexpression negatively regulates assembly of stress-granule components, preventing the formation of pathologic assemblies mediated by hnRNPA1 and hnRNPA2.

These data suggest that RNP-granule components can mitigate the toxic effect of RBPs in neurodegenerative pathology. Moreover, different RNP-granule components suppress FUS toxicity compared to hnRNPA1 and hnRNPA2 toxicity, indicating possible mechanistic differences in how these RBPs confer toxicity. Tif2 facilitates translation initiation [279], and its overexpression suppresses hnRNPA1, hnRNPA2, and FUS toxicity, suggesting that increased translation may decrease the toxicity of each of these

RBPs in yeast. Though Pab1 also facilitates translation initiation directly by binding to eIF4G and indirectly by stabilizing mRNA [272,275], its overexpression suppresses the toxicity of FUS but not of hnRNPA1 or hnRNPA2. These findings may indicate that the helicase activity of Tif2 is a rate-limiting step in translation initiation, preventing significant increases in translation as a result of increased expression of only Pab1. If this is true, Pab1 suppression of FUS toxicity must occur via a mechanism other than increased protein translation. If, for example, Pab1 interacts directly with FUS but not hnRNPA1 or hnRNPA2, increased binding of overexpressed Pab1 to FUS could prevent aberrant FUS binding to other essential proteins and RNAs. This would explain the specific ability of Pab1 overexpression to suppress FUS toxicity but not that of hnRNPA1 or hnRNPA2.

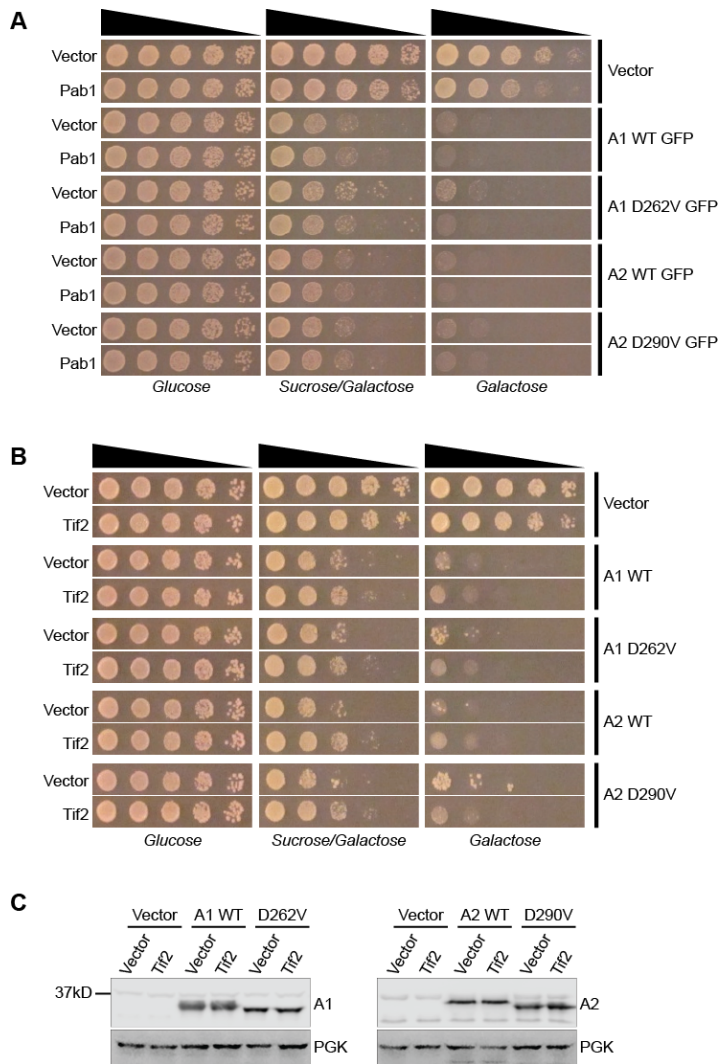


Figure 20: Overexpression of Tif2, but not Pab1, reduces the toxicity of hnRNPA1, hnRNPA1^{D262V}, hnRNPA2, and hnRNPA2^{D290V}.

(A) A spotting assay demonstrates that overexpression of the stress granule marker Pab1 did not affect the toxicity of hnRNPA1, hnRNPA1^{D262V}, hnRNPA2 or hnRNPA2^{D290V}. **(B)** Overexpression of the stress-granule marker Tif2 weakly reduced the toxicity of hnRNPA1, hnRNPA1^{D262V}, hnRNPA2 and hnRNPA2^{D290V}. **(C)** Overexpression of Tif2 did not affect hnRNPA1, hnRNPA1^{D262V}, hnRNPA2 or hnRNPA2^{D290V} expression levels after 5-7 hours of induction in liquid media containing sucrose and galactose. Galactose-supplemented media was used for maximal expression of overexpressed proteins from the galactose-inducible promoter. Sucrose was added to the media to reduce expression from the galactose promoter. Overexpression modifier studies were performed in collaboration with Olivia Zhou.

2.2.12 hnRNPA1 and hnRNPA2 colocalize with a P-body marker

Next, we coexpressed hnRNPA1 constructs with RFP-tagged Dcp2, a yeast P-body protein [282]. Dcp2 is a decapping enzyme that represents a crucial element of the mRNA decapping and decay machinery that accumulates in cytoplasmic P bodies [177]. With Dcp1, Dcp2 removes the 5' cap from mRNA transcripts that have been deadenylated, preparing them for 5' to 3' degradation by the exonuclease Xrn1 [176,177]. Dcp2 is required for recruitment of Dcp1 to P bodies [282]. Dcp2 is not required for P-body assembly, but loss of Dcp2 activity leads to a reduction in P-body size [282].

When expressed with an empty vector, Dcp2 displayed diffuse fluorescence plus discrete punctae (Figure 21A, vector). hnRNPA1 and hnRNPA1^{D262V} foci overlapped with Dcp2 foci (Figure 21A). hnRNPA1^{D262V} lacking RRM1 or RRM2 also colocalized with large Dcp2 foci (Figure 21A, constructs 105-320 and Δ 105-184). Greater than 80% of cells containing Dcp2 inclusions and aggregated hnRNPA1, hnRNPA1^{D262V}, hnRNPA1^{D262V} 105-320 or hnRNPA1^{D262V} Δ 105-184 demonstrated colocalization of Dcp2 and hnRNPA1 construct foci (Figure 21B). The isolated hnRNPA1 RRM1, too, consistently colocalized with Dcp2 foci (Figure 21A, construct 1-195). By contrast, the PrLD construct showed reduced colocalization with Dcp2 (Figure 21A, construct 195-320), with only ~50% of cells demonstrating overlap between hnRNPA1^{D262V} 105-320 and Dcp2 foci (Figure 21B). This hnRNPA1 PrLD construct is characterized by small, scattered protein punctae, and while there was frequent colocalization with Dcp2 (Figure 21A, construct 195-320, top), we also observed many cells in which the hnRNPA1 PrLD

punctae were spatially distinct from Dcp2 punctae (Figure 21A, construct 195-320, bottom). Thus, toxic hnRNPA1 constructs typically form foci that colocalize with stress-granule (Pab1) and P-body (Dcp2) markers, while the PrLD is recruited to P bodies with reduced efficiency. Yeast P bodies are liquid-like assemblies that form via LLPS, and the hnRNPA1 PrLD readily undergoes LLPS *in vitro* [217,222]. Taken with our data, this suggests that, in yeast, although the hnRNPA1 PrLD likely undergoes LLPS it does not necessarily do so in the setting of P-body formation. Thus, LLPS may be insufficient for maximal hnRNPA1 recruitment to P bodies in the absence of RNA binding by RRM.

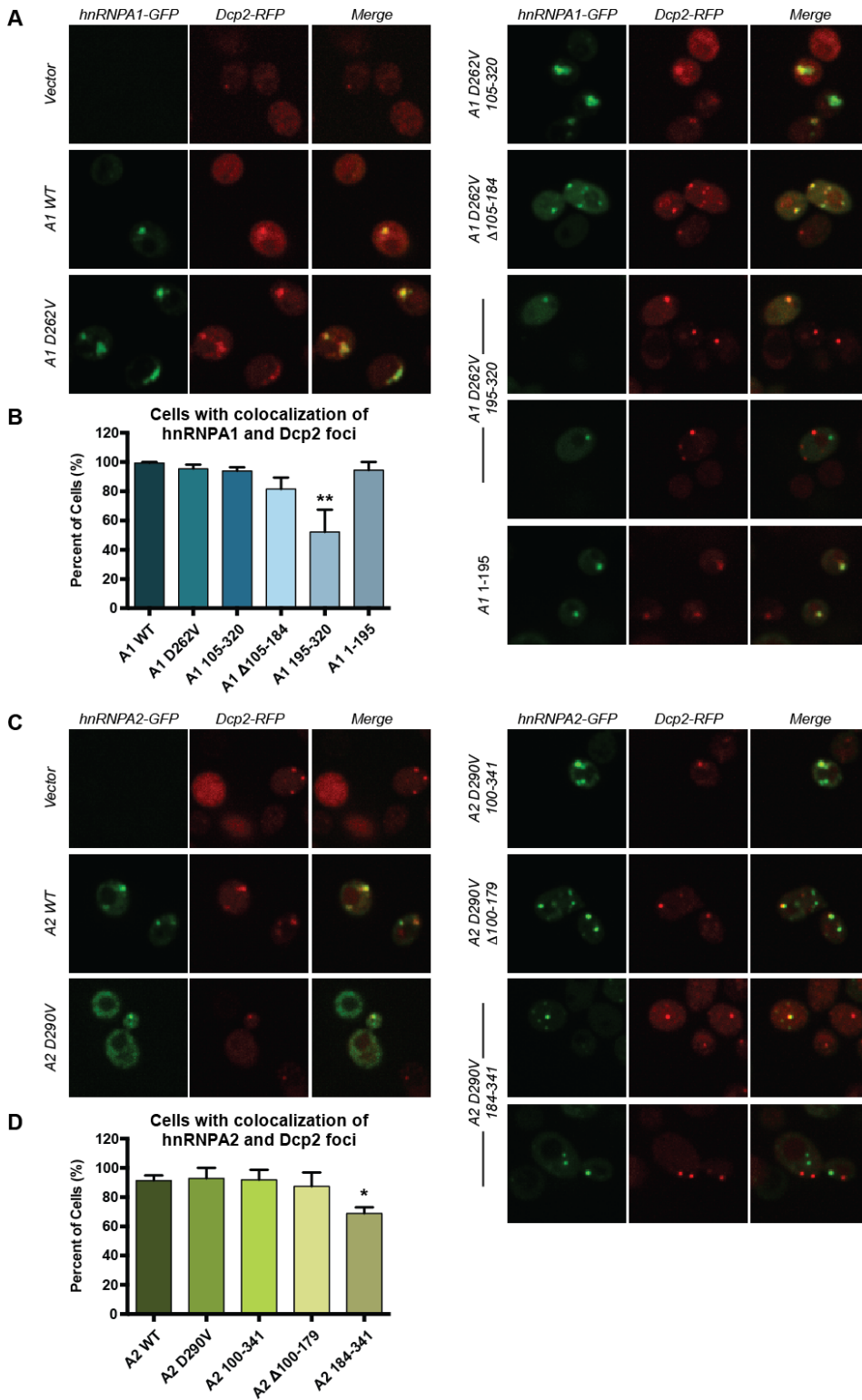


Figure 21: Deletion of both RRMs disrupts the colocalization of hnRNPA1^{D262V} and hnRNPA2^{D290V} with the P-body protein Dcp2.

(A) Fluorescence microscopy was used to compare the localization of GFP-tagged hnRNPA1 constructs and RFP-tagged Dcp2. Dcp2 formed punctae in the absence and presence of hnRNPA1 expression. These punctae colocalize with hnRNPA1 and hnRNPA1^{D262V}, but colocalization was reduced when hnRNPA1^{D262V} lacked both RRMs (construct 195-320). An example of colocalization and an instance of non-colocalization are shown for yeast expressing this construct. **(B)** Quantification of (A). Values represent means \pm s.e.m.; n=2-3 (**p \leq 0.01; one-way ANOVA comparing each construct to the WT protein using a Dunnett correction for multiple comparisons). **(C)** Fluorescence microscopy showed that Dcp2 formed punctae that colocalize with hnRNPA2 and hnRNPA2^{D290V}. There was decreased colocalization when hnRNPA2^{D290V} lacked both RRM domains (construct 184-341). An example of colocalization and an instance of non-colocalization are shown for yeast expressing this construct. **(D)** Quantification of (C). Values represent means \pm s.e.m.; n=2-4 (*p \leq 0.05; one-way ANOVA comparing each construct to the WT protein using a Dunnett correction for multiple comparisons).

We observed very similar results when we followed Dcp2-RFP localization upon expression of hnRNPA2 or hnRNPA2^{D290V} (Figure 21C). Thus, we observed colocalization of hnRNPA2 and hnRNPA2^{D290V} with the P-body protein in ~90% of cells containing both Dcp2 foci and hnRNPA2 foci (Figure 21C,D). Deletion of RRM1 or RRM2 maintained colocalization of hnRNPA2^{D290V} with Dcp2 foci (Figure 21C,D constructs 100-341 and Δ 100-179). Deletion of both RRMs reduced colocalization with Dcp2 foci (Figure 21C, 184-341), and ~30% of cells demonstrated no overlap between Dcp2 foci and hnRNPA2^{D290V} 184-341 inclusions. Our findings suggest that toxic hnRNPA2^{D290V} constructs aggregate and colocalize with P-body markers, but not stress-granule markers. By contrast, toxic hnRNPA1^{D262V} constructs aggregate and colocalize with both P-body and stress-granule markers. Thus, the effects of hnRNPA1^{D262V} and hnRNPA2^{D290V} on RNP-granule markers in yeast are distinct. It is also important to note that P-body colocalization is not sufficient to drive hnRNPA2^{D290V} toxicity, as hnRNPA2^{D290V} Δ 100-179 was not toxic but colocalized with Dcp2.

We performed a spotting assay to confirm that expression of RFP-tagged Dcp2 from the endogenous Dcp2 promoter did not alter the viability of cells expressing hnRNPA1, hnRNPA2, MSP-associated mutants, or deletion constructs (Figure 22). The toxicity of each hnRNP construct was comparable in cells with and without Dcp2-RFP expression (Compare figures 8B, 12B, and 22).

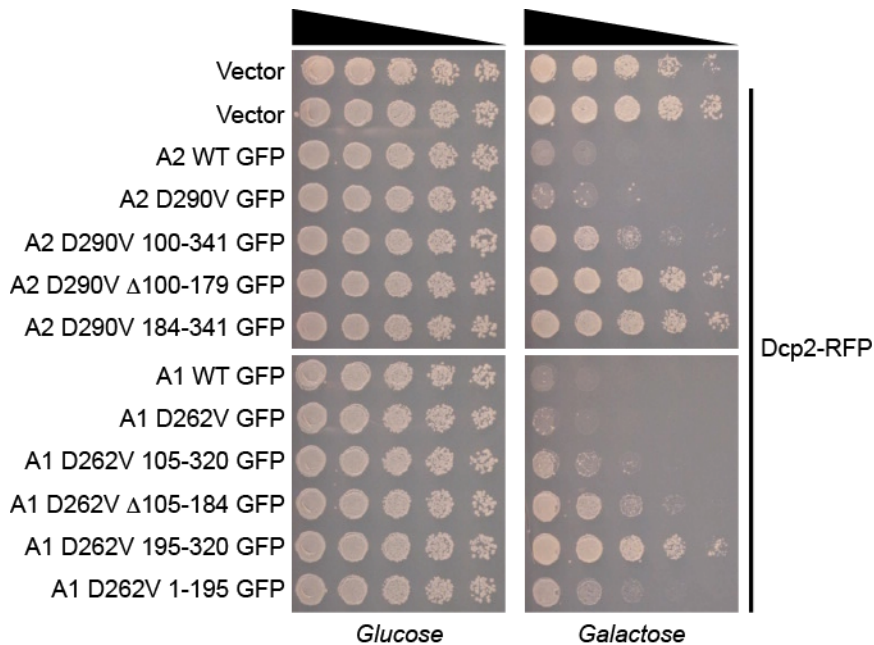


Figure 22: Expression of RFP-tagged Dcp2 does not alter the toxicity of hnRNPA1, hnRNPA2, or deletion constructs.

A spotting assay was used to compare cell viability of yeast strains expressing hnRNPA1, hnRNPA2, MSP-associated mutants, or deletion constructs with and without concurrent expression of RFP-tagged Dcp2. hnRNP construct toxicity was unaffected by expression of Dcp2-RFP from the endogenous Dcp2 promoter.

2.2.13 Deletion of *Lsm7*, but not *Pub1* or *Pbp1*, is protective against *hnRNPA1* and *hnRNPA2* toxicity.

We wished to identify genetic deletion suppressors of *hnRNPA1*^{D262V} and *hnRNPA2*^{D290V} toxicity, which could have important therapeutic implications for MSP patients. Previous screens have uncovered genetic modifiers that suppress the toxicity of TDP-43 and FUS in yeast models [110,251], and we explored the possibility that these approaches could be used to combat the toxic phenotype of *hnRNPA1* and *hnRNPA2* overexpression. We first employed a candidate gene strategy to identify putative modifiers of *hnRNPA1* and *hnRNPA2* toxicity. We honed in on *Lsm7*, a P-body protein that was identified as a deletion suppressor of FUS toxicity [110,282], *Pbp1*, a stress granule marker that suppresses the toxicity of TDP-43 when deleted [196,251,278], and *Pub1*, a stress granule protein that reduces FUS toxicity when deleted [110,196,278]. *Lsm7* is a component of the nuclear *Lsm2-8* complex and the cytoplasmic *Lsm1-7* heptamer [202,207]. In the nucleus, *Lsm2-8* stabilizes newly synthesized U6 snRNA, enabling efficient pre-mRNA splicing [202,205]. In the cytoplasm, *Lsm1-7* localizes to P bodies and serves as an activator of decapping during mRNA degradation [203]. *Lsm1-7* also, in concert with another decapping activator, *Pat1*, protects mRNA transcripts from 3' to 5' end trimming [204]. *Pbp1* is the yeast homologue of human ataxin 2 [81]. Both *Pbp1* and ataxin 2 are crucial for stress granule formation [208,210]. *Pbp1* interacts with the C-terminal end of *Pab1* and regulates mRNA polyadenylation [283]. The interactome of *Pbp1* suggests that it may also contribute to RNA editing, pre-mRNA splicing, nuclear export of mRNA, and mRNA degradation [283]. *Pub1* is a polyadenylated-RNA-binding protein found in both the nucleus and cytoplasm [284]. The human homologue of *Pub1*, *TIA1* is essential for

stress granule formation, and depletion of Pub1 impairs stress granule assembly in yeast [208,209]. Pub1 also functions in the regulation of mRNA decay by stabilizing specific mRNA transcripts and may play a role in the regulation of translation [285].

We expressed hnRNPA1, hnRNPA2 and their disease-associated mutants in LSM7-, PBP1-, and PUB1-deletion strains and plated cultures on galactose for high hnRNP expression and a sucrose/galactose mix for lower hnRNP expression. In the $\Delta sm7$ background there was no evidence of toxicity suppression on galactose media, but on sucrose/galactose hnRNPA1, hnRNPA1^{D262V}, hnRNPA2 and hnRNPA2^{D290V} were less toxic in yeast lacking the gene encoding Lsm7 (Figure 23A). Deletion of LSM7 suppressed toxicity but did not reduce toxic protein expression levels (Figure 23B). Deletion of PBP1 or PUB1 did not reduce the toxicity of hnRNPA1, hnRNPA1^{D262V}, hnRNPA2 or hnRNPA2^{D290V} at high or low expression levels (Figure 23C). In contrast to TDP-43 and FUS, hnRNPA1 and hnRNPA2 remain toxic in the absence of these stress granule components.

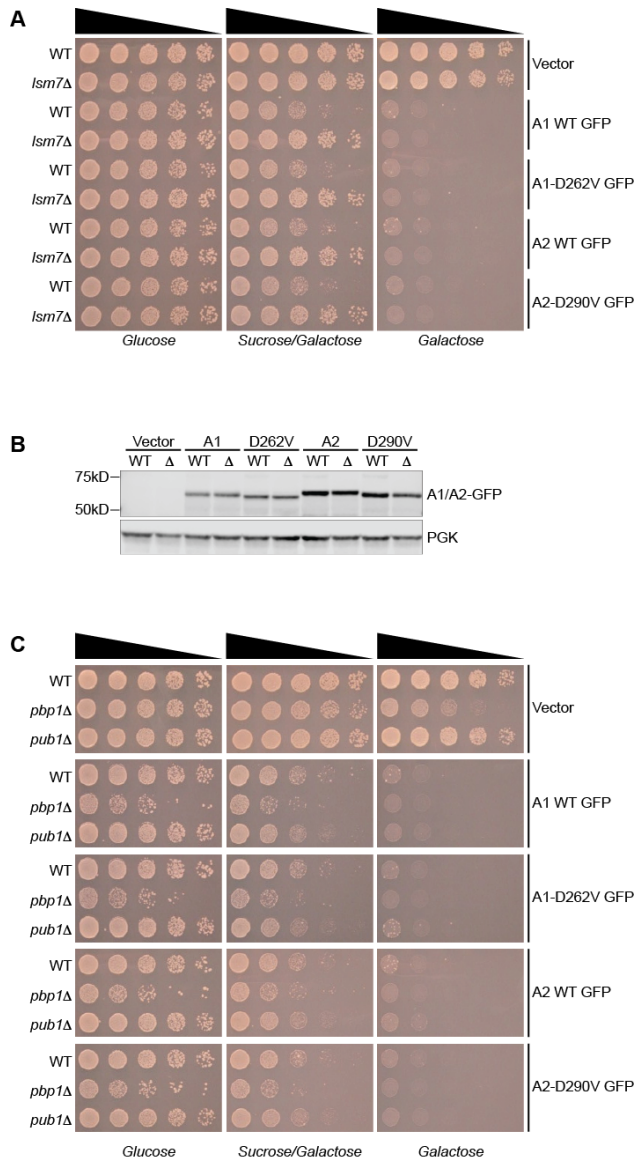


Figure 23: Deletion of LSM7, but not PBP1 or PUB1, reduces the toxicity of hnRNPA1, hnRNPA1^{D262V}, hnRNPA2, or hnRNPA2^{D290V} in *S. cerevisiae*.

(A) Spotting of serial yeast dilutions to compare hnRNP toxicity in WT yeast and yeast lacking the LSM7 gene. Deletion of LSM7 reduced the toxicity of hnRNPA1, hnRNPA1^{D262V}, hnRNPA2, and hnRNPA2^{D290V} on sucrose/galactose but not galactose.

(B) Immunoblotting confirmed that deletion of LSM7 did not alter the expression of hnRNPA1, hnRNPA2, or disease associated mutants.

(C) A spotting assay demonstrated that deletion of the stress-granule genes PBP1 and PUB1 did not affect the toxicity of hnRNPA1, hnRNPA1^{D262V}, hnRNPA2, or hnRNPA2^{D290V} at high or low expression levels.

2.2.14 Overexpression of U6 snRNA does not suppress hnRNPA1 or hnRNPA2 toxicity.

Our data indicate that a function of Lsm7 is crucial to the pathogenic mechanism underlying the toxicity conferred by hnRNPA1, hnRNPA2, and FUS. Lsm7 plays a role in two distinct cellular pathways: it is an element of the cytoplasmic Lsm1-7 complex that localizes to P bodies and functions in mRNA degradation, and it is a component of the nuclear Lsm2-8 heteroheptamer that stabilizes the U6 snRNA during pre-mRNA splicing [203,205]. One of the consequences of LSM7 deletion is the cytoplasmic accumulation of U6 snRNA, which is normally confined to the nucleus [286]. We wondered whether this RNA mislocalization could mitigate hnRNPA1 and hnRNPA2 toxicity by creating a binding decoy for these toxic RBPs, thereby preventing them from sequestering essential RNAs and proteins. To investigate this possibility, we overexpressed U6 snRNA in WT yeast expressing hnRNPA1, hnRNPA1^{D262V}, hnRNPA2, or hnRNPA2^{D290V} to recapitulate the cytoplasmic increase in U6 snRNA (Kristen Lynch, personal communication). Overexpression of U6 did not reduce the toxicity of hnRNPA1, hnRNPA2, or either MSP-associated variant (Figure 24). Thus, overexpression of U6 snRNA does not phenocopy LSM7 deletion (Figure 24). It remains to be determined whether the nuclear or cytoplasmic functions of Lsm7 are crucial to disrupt hnRNPA1 or hnRNPA2 toxicity.

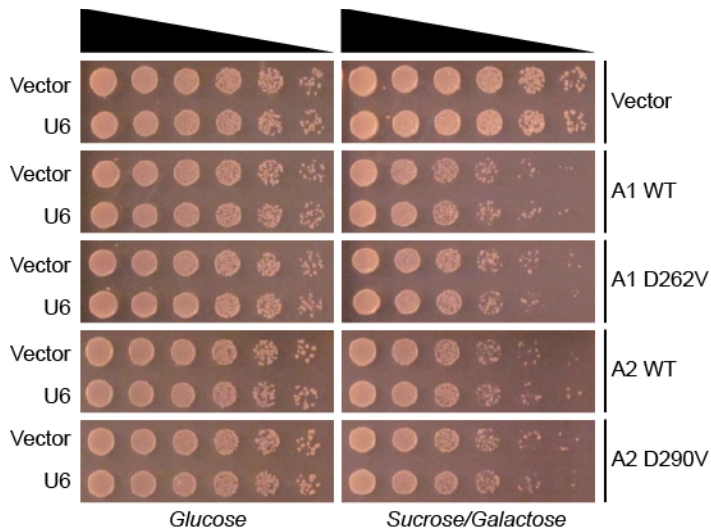


Figure 24: Overexpression of U6 snRNA does not reduce hnRNPA1, hnRNPA2, or MSP-linked variant toxicity.

Yeast were transformed to overexpress U6 snRNA concurrently with hnRNPA1, hnRNPA2, hnRNPA1^{D262V}, or hnRNPA2^{D290V}. A spotting assay demonstrated that U6 snRNA did not reduce the toxicity of these RBPs.

2.2.15 Deletion of DBR1 does not protect against hnRNPA1 or hnRNPA2 toxicity.

Another candidate toxicity modifier to emerge from screens against TDP-43 and FUS was deletion of DBR1, which suppresses toxicity of both TDP-43 and FUS in yeast [251]. DBR1 encodes a lariat-debranching enzyme, which cleaves intronic lariats that are released during pre-mRNA splicing, thereby initiating the degradation of these noncoding RNAs [251,287]. Loss of Dbr1 enzymatic activity results in the accumulation of cytoplasmic lariats, which reduces TDP-43 and FUS toxicity, perhaps by acting as a binding “decoy” and preventing their association with essential endogenous RNAs and RBPs [251]. In humans, roughly three quarters of all genomic hnRNPA1 and hnRNPA2 binding sites are intronic, with over half found in distal introns [148]. Thus, we tested whether deletion of DBR1 mitigated hnRNPA1 and hnRNPA2 toxicity. Deletion of DBR1

mitigated FUS toxicity without affecting FUS expression (Figure 25A, B). By contrast, deletion of DBR1 did not affect WT or MSP-linked hnRNPA1 or hnRNPA2 toxicity or expression (Figure 25A, B). Thus, strategies to inhibit Dbr1 are unlikely to be effective against MSP-linked hnRNPA1 or hnRNPA2 toxicity. These data further reinforce the idea that reducing the toxicity of RBPs with PrLDs may need to be tailored to the specific RBP in question.

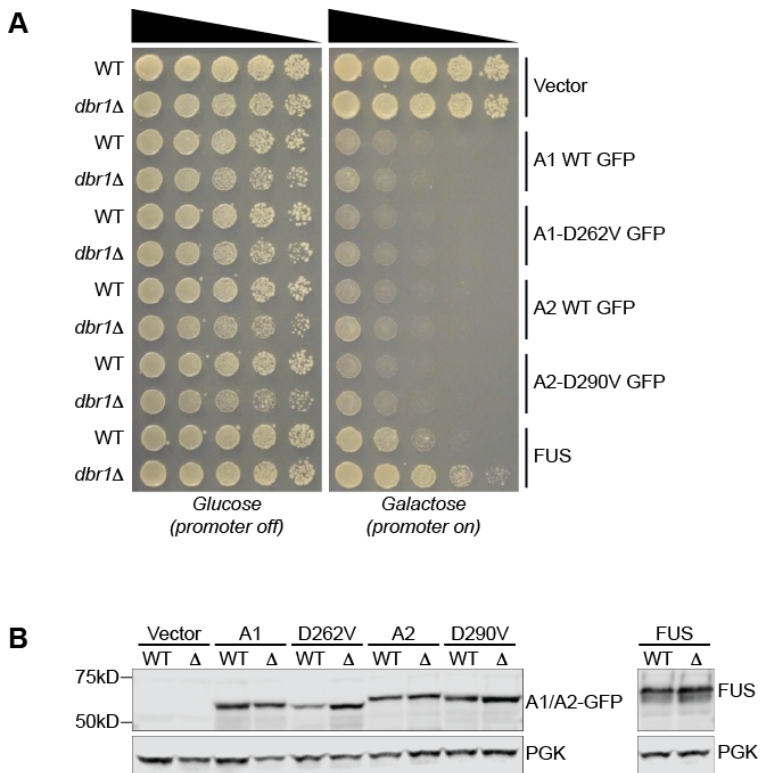


Figure 25: Loss of the lariat-debranching enzyme, Dbr1, does not suppress the toxicity of hnRNPA1, hnRNPA1^{D262V}, hnRNPA2, or hnRNPA2^{D290V}.

(A) A spotting assay demonstrates that deletion of the gene encoding the lariat-debranching enzyme, DBR1, had no effect on the toxicity of hnRNPA1, hnRNPA2, or disease-associated mutants. FUS was used as a positive control for toxicity suppression. (B) Western blotting confirmed expression of toxic proteins in WT and *dbr1*Δ strains.

2.2.16 A deletion screen reveals novel suppressors of hnRNPA1 and hnRNPA2 toxicity.

To identify genetic modifiers of hnRNPA1 that do not overlap with those previously isolated for TDP-43 and FUS, we performed a deletion screen of the ~4850 non-essential yeast genes [110]. We expressed hnRNPA1 or hnRNPA2 in yeast strains lacking each non-essential gene and compared growth on a sucrose and galactose mixture to the growth of WT yeast expressing hnRNPA1 or hnRNPA2. Due to the strong toxicity phenotype associated with these proteins, we did not identify any enhancers of protein toxicity. We did, however, identify forty gene deletions that suppressed the toxicity of both hnRNPA1 and hnRNPA2 (Table 1, Figures 26 and 27). All of these also suppressed the toxicity of the MSP-associated variants hnRNPA1^{D262V} and hnRNPA2^{D290V}. Importantly, we did not observe any deletions that affected the toxicity of only hnRNPA1 or hnRNPA2. Thus, despite subtle differences in the domains that drive hnRNPA1 and hnRNPA2 toxicity (Figures 8 and 12) and differences in how they colocalize with RNP granules (Figure 18), these results indicate that their toxicities can be overcome via similar mechanisms.

We identified two deletion suppressors that had previously been identified as deletion suppressors of FUS toxicity: *LSM7* and *SSE1* (Figure 26) [110]. We did not uncover any genetic deletions that suppress the toxicity of TDP-43 in addition to hnRNPA1 and hnRNPA2 (Figure 26) [251]. Two proteins that suppressed hnRNPA1 and hnRNPA2 toxicity when deleted, *Sbp1* and *Sko1*, are known to reduce the toxicity of FUS when overexpressed [99,110]. A single protein, *Rtt103*, was found to suppress

hnRNPA1 and hnRNPA2 toxicity when deleted, and also suppresses FUS toxicity when overexpressed [110].

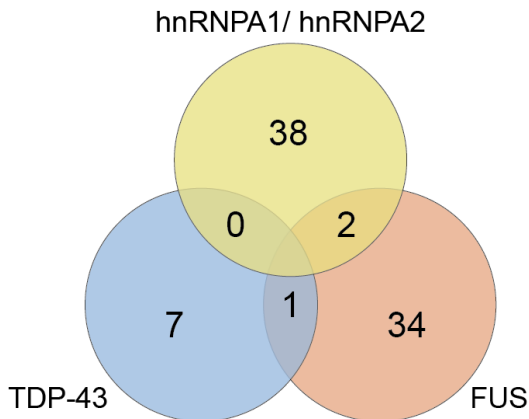


Figure 26: Deletion suppressors of hnRNPA1 and hnRNPA2 toxicity have little overlap with those uncovered as suppressors of TDP-43 and FUS toxicity.

The number of gene deletions that are known to suppress the toxicity of various RBPs is shown. Deletion suppressors have been identified by screening each of the non-essential genes in the yeast genome [110,251]. Yeast deletion screens uncovered genetic deletion suppressors of TDP-43 and FUS toxicity, and only one gene deletion was found to suppress both TDP-43 and FUS toxicity [110,251]. We performed a deletion screen using the same yeast library and uncovered 40 suppressors of hnRNPA1 and hnRNPA2 toxicity, only two of which are known to suppress FUS toxicity and none of which were identified in the screen for TDP-43 toxicity suppressors [110,251].

We can infer mechanistic dissimilarity between the toxic effects of FUS and those of hnRNPA1 and hnRNPA2 based on the fact that genetic screens have indicated a lack of overlap between suppressors of FUS toxicity and suppressors of hnRNPA1 and hnRNPA2 toxicity (Figure 26) [110]. Moreover, the functional pathways that include genetic suppressors of FUS toxicity are distinct from those that involve genes that

suppress the toxicity of hnRNPA1 and hnRNPA2 [110,288]. GO term analysis of a functional network of deletion suppressors of hnRNPA1 and hnRNPA2 toxicity and twenty related genes demonstrated enrichment for genes encoding proteins with roles in RNA splicing, proteasome assembly, protein folding, and protein acetylation (Table 1) [288]. We also noted three P body-associated proteins: Lsm7, Sbp1 and Lsm6 [200,203,205]. Sbp1 is also found in stress granules [200]. Sbp1 is involved in, but not required for, mRNA decapping and facilitates translational repression and P-body formation [200,201]. Lsm6 and Lsm7 function in P-bodies as part of a complex containing Lsm proteins 1-7 that serves to promote mRNA decapping [203,205,289,290]. They also, however, are found in the heteroheptameric Lsm2-8 ring, which prevents the degradation of newly synthesized U6 snRNA, allowing efficient mRNA splicing to proceed [205,206].

Function	FDR	Genes in network	Genes in genome
protein refolding	3.66082E-05	6	17
protein folding	0.004331147	8	89
proteasome assembly	0.010457544	5	28
mRNA splicing, via spliceosome	0.066845626	7	108
RNA splicing, via transesterification reactions with bulged adenosine as nucleophile	0.066845626	7	109
ATPase regulator activity	0.066845626	4	24
RNA splicing, via transesterification reactions	0.090527236	7	118
'de novo' protein folding	0.096157976	3	11
protein acetylation	0.111055477	5	56
small nuclear ribonucleoprotein complex	0.128240701	5	59

Table 1: Functional enrichment of an interaction network incorporating deletion suppressors of hnRNPA1 and hnRNPA2 toxicity and related proteins.

An interaction network incorporating the forty deletion suppressors of hnRNPA1 and hnRNPA2 toxicity uncovered in our unbiased screen and twenty related proteins is functionally enriched for proteins involved in protein folding and refolding, splicing, proteasome assembly, and protein acetylation. Interaction network and functional data from the GeneMANIA prediction server [288].

Interestingly, components of the U2 and U5 snRNPs, Bud31 [291] and Prp18 [292], respectively, were also identified in our screen as suppressors of hnRNPA1 and hnRNPA2 toxicity, suggesting the importance of the regulation of splicing to RBP-mediated toxicity. Bud31 is a highly conserved element of the *S. cerevisiae* splicing machinery that facilitates entry into the first catalytic step of pre-mRNA splicing and, at elevated temperatures, is required for the second catalytic step [293,294]. It is required for splicing of certain RNA transcripts, including several that are involved in budding, yet dispensable in the processing of others [295]. Prp18 functions in exon ligation during splicing, serving to stabilize the interaction of exon ends with the spliceosome to facilitate the joining of exons [292,296].

We were also interested to observe four members of the yeast chaperone network emerge as toxicity suppressors: Hsc82 (an Hsp90 chaperone [297]), Sti1 (an Hsp90 co-chaperone [298]), Sse1 (an Hsp110 chaperone [299]), and Ydj1 (an Hsp40 chaperone [300]). Hsc82 is the constitutively expressed Hsp90 homologue in yeast [301]. It is expressed at high levels and induced further upon heat shock [302]. Hsp90 proteins function with co-chaperones to mediate late-stage folding of client proteins, either upon de novo protein synthesis or during reactivation of denatured proteins following stress [303,304]. Hsp90 proteins can stabilize signaling proteins in conformations that allow activation [297]. They are involved in the assembly and disassembly of protein complexes including the proteasome, transcriptional complexes, and the kinetochore complex [297,301]. Hsp90 proteins have also been implicated in telomere length regulation [305] and determination of prion variants in yeast [306]. The

Hsp90 co-chaperone Sti1 facilitates maturation of Hsp90 client proteins by mediating the transfer of substrate to Hsp90 from Hsp70, which functions in early folding of nascent or denatured substrates [297,304,307]. Sti1 modulates ATPase activity, serving to activate the ATPase activity of Hsp70 and inhibit the ATPase activity of Hsp90 [307-309]. Sti1, with Hsp70 and Hsp90, has also been implicated in mitochondrial function and loss of yeast [*PSI⁺*] prions due to overexpression of Hsp104 [310-312]. Sse1 is an Hsp110 chaperone that acts as a nucleotide exchange factor for Ssa1 and Ssb1, cytoplasmic yeast Hsp70s [313]. *In vitro*, Sse1 binds, but does not refold, denatured substrates [314]. Sse1 is essential for the maturation of several Hsp90 clients and for Hsp90-mediated repression of Hsf1, a yeast transcription factor that activates the heat shock response [299,304,314]. Sse1 also plays a role in prion formation and propagation [315,316]. Ydj1 is an Hsp40 in yeast that serves as an Hsp70 co-chaperone [317]. Ydj1 stimulates Hsp70 ATPase activity and contributes to a number of Hsp70 functions including protection and folding of nascent or denatured polypeptides [300,318,319], protein translocation across the membranes of the endoplasmic reticulum and mitochondria [320,321], and ubiquitin-mediated proteasomal protein degradation [300,319,322]. Ydj1 is a cofactor for the remodeling factor Hsp104 [323], and overexpression of Ydj1 cures select yeast prions [317,324]. Interestingly, Ydj1 is essential for yeast P-body formation in stress conditions [325]. It also is thought to promote dissolution of stress granules and reinitiation of translation following stress, as deletion of Ydj1 leads to increased vacuolar degradation of stress granules and impaired translational recovery after stress [326].

It is not unexpected that the proteostasis network would play an integral role in neurodegenerative diseases linked to aberrations in protein homeostasis, though it is

intriguing that this set of proteins has not emerged as a means of suppressing TDP-43 or FUS toxicity [110,251] and thus seems to have some specificity for hnRNPA1 and hnRNPA2. Future studies should seek to identify the mechanistic role these chaperone proteins play in conferring hnRNPA1 and hnRNPA2 toxicity. Both Sti1 and Sse1 collaborate with both Hsp70 and Hsp90 [297,299,313], suggesting that disruption of the functional interface between Hsp70 and Hsp90 could be key to limiting the toxicity of hnRNPA1 and hnRNPA2.

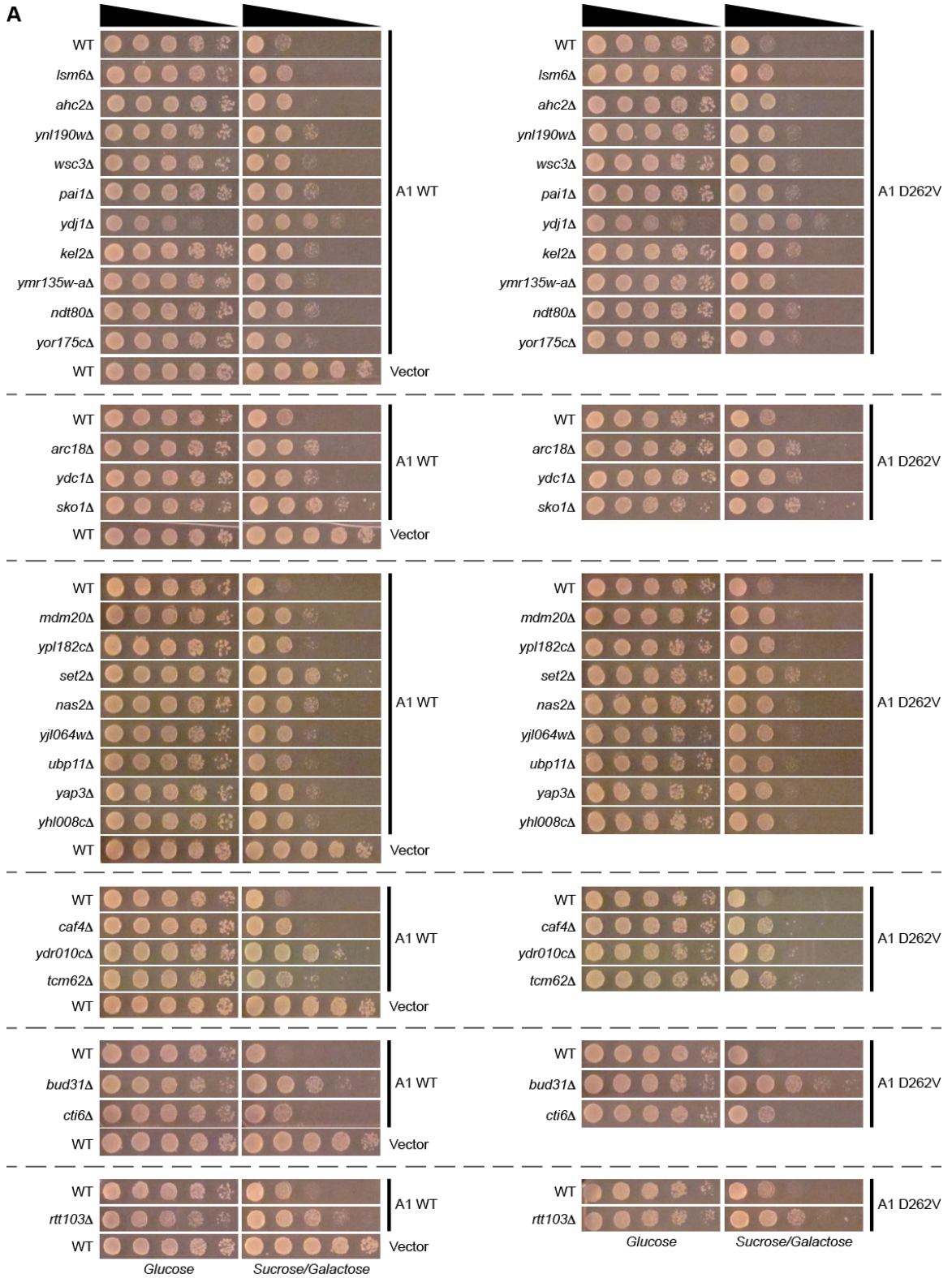
We uncovered several dubious open reading frames that suppressed hnRNPA1 and hnRNPA2 toxicity when deleted (Table 2, Figures 27 and 28). These may represent functional non-coding RNAs that facilitate hnRNPA1 and hnRNPA2 toxicity. Non-coding RNAs in yeast and humans can regulate transcription and thereby affect gene expression [327,328], which may contribute to RBP-mediated toxicity.

YEAST GENE	HUMAN HOMOLOGUE	YEAST LOCALIZATION	FUNCTION IN YEAST
<i>AHC2</i>	-	cytoplasm, nucleus	Component of ADA histone acetyltransferase complex
<i>ALE1</i>	<i>MBOAT2</i> , <i>MBOAT1</i> , <i>MBOAT5</i> , <i>MBOAT7*</i>	endoplasmic reticulum	Lysophospholipid acyltransferase
<i>ARC18</i>	<i>ARPC3</i>	actin colocalization	Subunit of ARP2/3 complex, which is required for cortical actin patch motility and integrity
<i>BUD31</i>	<i>BUD31</i>	nucleus	Component of U2 snRNP; functions in mRNA splicing and bud site selection
<i>CAF4</i>	-	mitochondrion	WD40 repeat-containing protein associated with the CCR4-NOT complex; involved in mitochondrial fission
<i>CT16</i>	-	nucleus	Component of Rpd3L histone deacetylase complex; relieves transcriptional repression
<i>DUR3</i>	-	-	Plasma membrane transporter for urea and polyamines
<i>HSC82</i>	<i>HSP90AA1</i> , <i>HSP90AB1</i>	cytoplasm	Hsp90 chaperone; involved in determination of prion variants
<i>KEL2</i>	-	bud	Negative regulator of mitotic exit; involved in regulation of actin cable assembly, cytokinesis and polarized growth
<i>LSM6</i>	<i>LSM6</i>	cytoplasm, nucleus [205]	Component of cytoplasmic Lsm1-7 complex involved in mRNA decay and nuclear Lsm2-8 complex that comprises part of the U6 snRNP; P-body protein
<i>LSM7</i>	<i>LSM7</i>	cytoplasm, nucleus [205]	Component of cytoplasmic Lsm1-7 complex involved in mRNA decay and nuclear Lsm2-8 complex that comprises part of the U6 snRNP; P-body protein
<i>MDM20</i>	<i>NAA25</i>	cytoplasm	Non-catalytic subunit of NatB acetyltransferase; involved in mitochondrial inheritance and actin assembly
<i>MEC3</i>	<i>HUS1</i> [329]	-	DNA damage and meiotic checkpoint protein
<i>NAS2</i>	<i>PSMD9</i>	cytoplasm	Proteasome-interacting protein; involved in assembly of 19S proteasomal regulatory particle
<i>NDT80</i>	<i>C11orf9</i> [330]	-	Meiosis specific transcription factor
<i>PAI3</i>	-	cytoplasm, nucleus	Cytoplasmic proteinase A inhibitor
<i>POC4</i>	<i>PAC4</i> [331]	cytoplasm	Component of Poc4p-Irc25p chaperone complex; involved in proteasome formation
<i>PRP18</i>	<i>PRPF18</i> [332]	-	Component of snRNP U5; functions in 3' splice site positioning during mRNA splicing
<i>PSY2</i>	<i>PPP4R3A</i> , <i>PPP4R3B</i>	nucleus	Subunit of protein phosphatase PP4 complex; regulates recovery from DNA damage and non-homologous end-joining

<i>PUN1</i>	-	cytoplasm, cell periphery, bud	Plasma membrane protein; involved in cell wall integrity and thermotolerance
<i>RTT103</i>	<i>Kub5-Hera</i> [333]	nucleus	Involved in transcription termination by RNA polymerase II; regulates Ty1 transposition
<i>SBP1</i>	<i>RBM14</i> [99]	cytoplasm	P-body protein; involved in repression of translation
<i>SEM1</i>	<i>DSS1</i> [334]	nucleus	Lid component of 26S proteasome regulatory subunit; functions in nuclear mRNA export
<i>SET2</i>	<i>SETD2</i> [335]	nucleus	Histone methyltransferase; plays a role in transcriptional elongation
<i>SKO1</i>	-	cytoplasm, nucleus	Basic leucine zipper transcription factor; activates and represses transcription; involved in osmotic and oxidative stress responses
<i>SPT3</i>	<i>SUPT3H</i>	nucleus	Transcriptional regulator
<i>SSE1</i>	<i>HSPH1</i>	cytoplasm	Hsp110 chaperone; involved in prion propagation and determining prion variants
<i>STI1</i>	<i>STIP1</i>	cytoplasm	Hsp90 and Hsp70 cochaperone; regulates spatial organization of cytosolic amyloid-like proteins
<i>TCM62</i>	-	-	Putative mitochondrial chaperone; involved in assembly of succinate dehydrogenase complex
<i>UBP11</i>	-	-	Ubiquitin protease
<i>WSC3</i>	-	cell periphery	Sensor-transducer of stress-activated signaling pathway; involved in cell wall maintenance and in response to heat shock and other stress
<i>YAP3</i>	-	cytoplasm, nucleus	Basic leucine zipper (bZIP) transcription factor
<i>YDC1</i>	<i>ACER3</i>	vacuole	Alkaline dehydroceramidase; involved in sphingolipid metabolism
<i>YDJ1</i>	<i>DNAJA1, DNAJA2, DNAJA4</i>	cytoplasm, nucleus	Hsp40 cochaperone; involved in regulation of Hsp90 and Hsp70 function
<i>YDR010C</i>	-	-	Dubious open reading frame
<i>YHL008C</i>	-	vacuole	Putative protein of unknown function
<i>YJL064W</i>	-	-	Dubious open reading frame; overlaps with DLS1 gene
<i>YMR135W-A</i>	-	-	Dubious open reading frame
<i>YNL190W</i>	-	endoplasmic reticulum, cell periphery	Hydrophilin protein; essential in desiccation-rehydration process; cell wall protein
<i>YPL182C</i>	-	-	Dubious open reading frame; overlaps with CTI6 gene

Table 2: A genome-wide deletion screen uncovers suppressors of both hnRNPA1 and hnRNPA2 toxicity.

Listed are genetic deletions that emerged as suppressors of hnRNPA1^{D262V} or hnRNPA2^{D290V} toxicity from a screen of all non-essential yeast genes. Human orthologues are noted. Functional descriptions were adapted from the Saccharomyces Genome Database [336]. Cellular localization information is from the Yeast GFP Fusion Localization Database unless otherwise noted [337]. The genetic deletion screen was done in collaboration with Julien Couthouis and Olivia Zhou.



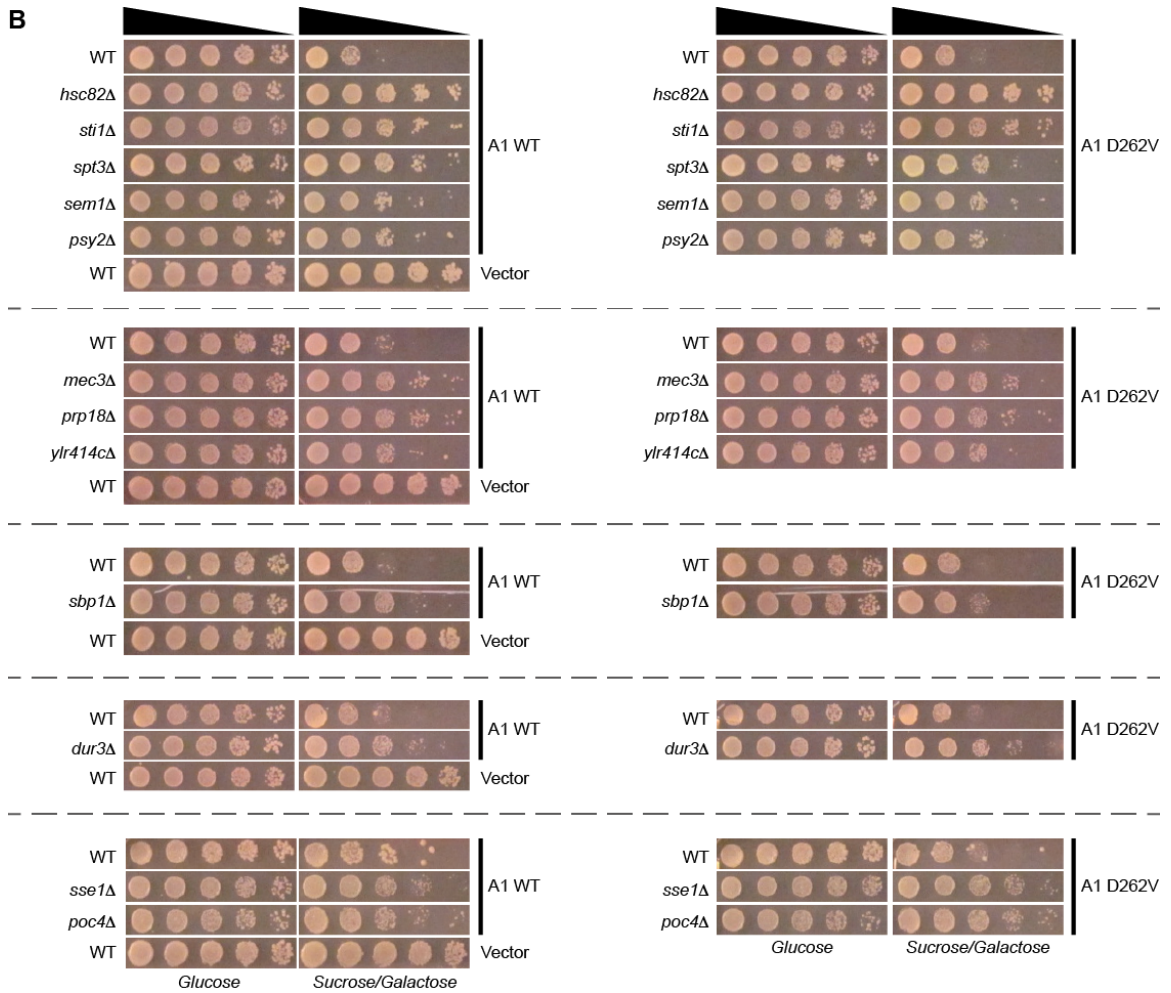
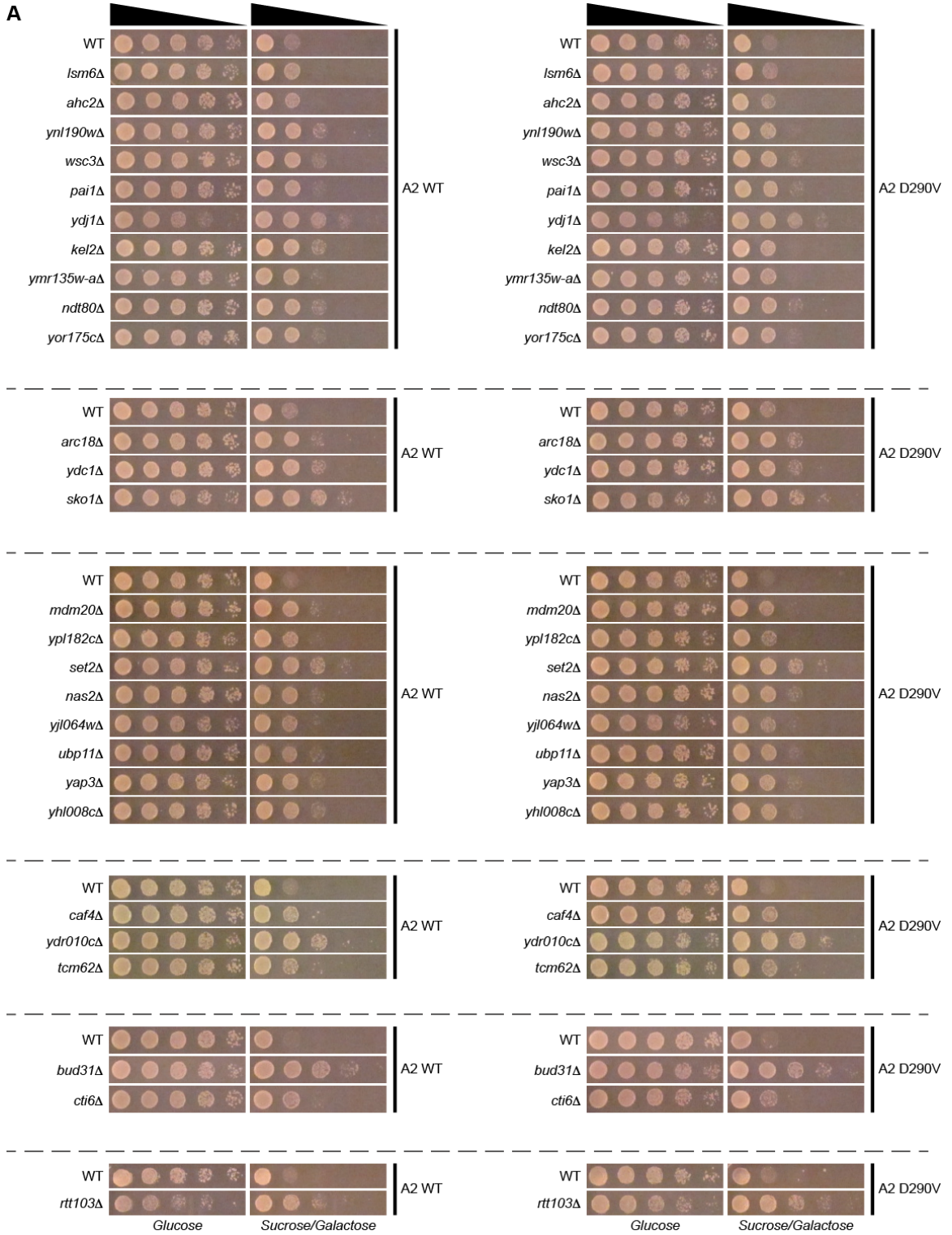


Figure 27: Gene deletions suppress toxicity of hnRNPA1 and hnRNPA1^{D262V}. Representative spotting assays are shown for 40 gene deletions that suppressed the toxicity of hnRNPA1 and hnRNPA1^{D262V}. Yeast strains harboring gene deletions were transformed to express hnRNPA1 or hnRNPA1^{D262V}, spotted in five-fold dilution series onto sucrose/galactose media to induce protein expression, and allowed to grow for 2 (A) or 3 (B) days at 30°C. Experiments are separated by dashed lines. Spotting assays to validate hits from gene deletion screen were done in collaboration with Julien Couthouis and Olivia Zhou.



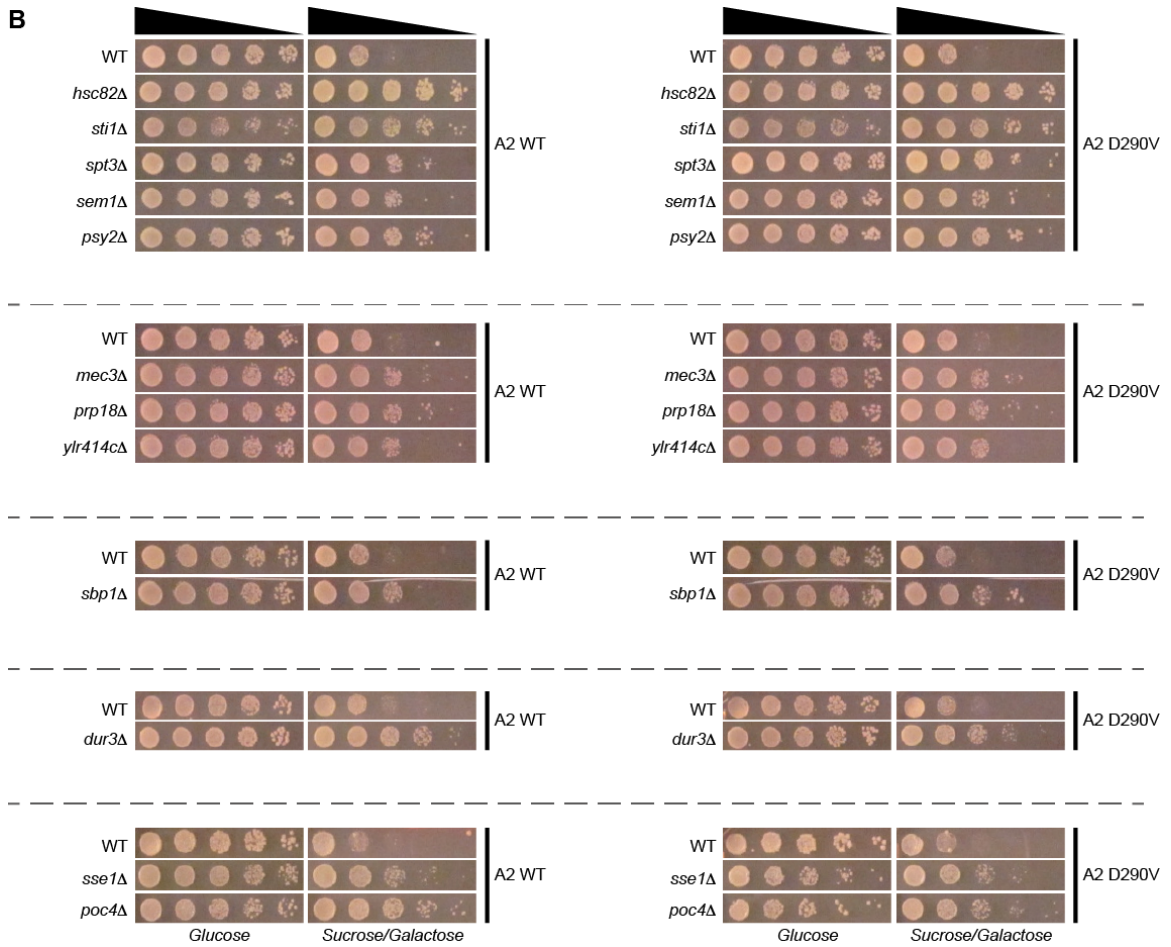


Figure 28: Gene deletions that suppress hnRNPA1 toxicity also suppress toxicity of hnRNPA2 and hnRNPA2^{D290V}.

Spotting assays are shown for gene deletions shown in Figure 27 that suppressed the toxicity of hnRNPA1 and hnRNPA1^{D262V}. Yeast deletion strains were transformed to express hnRNPA2 or hnRNPA2^{D290V}, spotted in five-fold dilution series onto sucrose/galactose media to induce protein expression, and allowed to grow for 2 (A) or 3 (B) days at 30°C. All forty strains also exhibited suppression of hnRNPA2 and hnRNPA2^{D290V} toxicity. Experiments are separated by dashed lines. Spotting assays to validate hits from gene deletion screen were done in collaboration with Julien Couthouis and Olivia Zhou.

2.2.17 Overexpression of Hsp82 does not suppress hnRNPA1 or hnRNPA2 toxicity.

The constitutively expressed Hsp90 chaperone in yeast, Hsc82 [302,338], which emerged from our deletion screen as one of the strongest deletion suppressors of both hnRNPA1 and hnRNPA2 toxicity, is one of two closely related heat shock proteins in yeast [302]. The other is Hsp82 [302]. Under homeostatic conditions, Hsc82 is abundantly expressed, while Hsp82 is expressed at significantly lower levels [302]. Upon heat stress, expression of both proteins is induced, but Hsp82 is induced more robustly [302]. Deletion of HSC82 results in a compensatory increase in HSP82 mRNA levels [338], and so we wondered whether increased Hsp82 expression, rather than a loss of Hsc82, was the cause of the strong reduction in hnRNPA1 and hnRNPA2 toxicity. To answer this question, we overexpressed Hsp82 from a high-copy 2-micron plasmid in yeast also overexpressing hnRNPA1, hnRNPA1^{D262V}, hnRNPA2, or hnRNPA2^{D290V}. Overexpression of Hsp82 had no effect on the toxicity of these proteins (Figure 29). This finding might suggest that loss of Hsc82 function directly disrupts the toxic effects of hnRNPA1 and hnRNPA2. However, genes other than HSP82 that get overexpressed upon HSC82 deletion may also be important to suppress hnRNPA1 and hnRNPA2 toxicity in yeast.

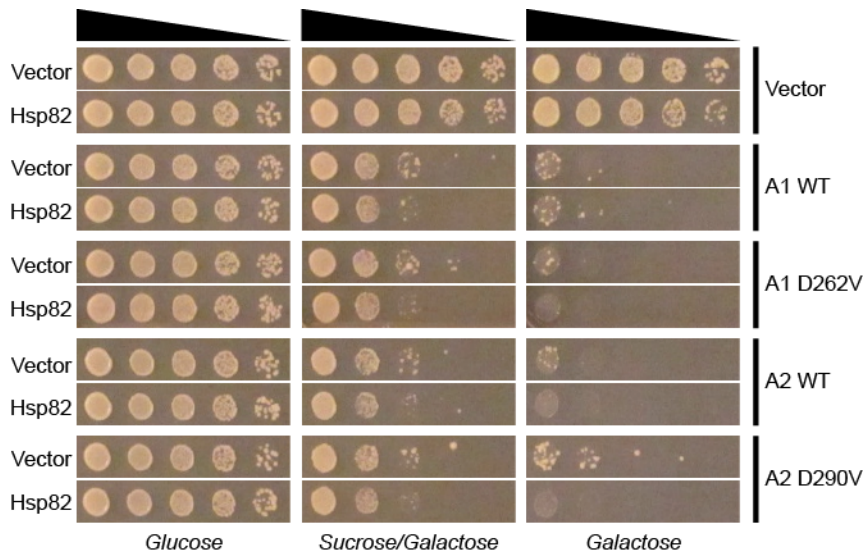


Figure 29: Overexpression of Hsp82 does not affect hnRNPA1 or hnRNPA2 toxicity.

Yeast were transformed to overexpress hnRNPA1, hnRNPA1^{D262V}, hnRNPA2, or hnRNPA2^{D290V} with high levels of Hsp82. Yeast strains were spotted onto inducing media. Hsp82 did not decrease the toxic phenotype of hnRNPA1, hnRNPA1^{D262V}, hnRNPA2, or hnRNPA2^{D290V}. Hsp82 experiments were done in collaboration with Olivia Zhou.

2.3 Discussion

We have demonstrated important mechanistic similarities and differences among the toxic effects caused by various RBPs that are inextricably linked to neurodegenerative disease, including hnRNPA1 and hnRNPA2, which cause MSP and ALS, and FUS and TDP-43, which are causally linked to ALS and FTD [29,65,72,134,258]. We have shown that hnRNPA1 and hnRNPA2 require at least a single RRM and a portion of the PrLD to confer significant toxicity in a yeast model. This observation suggests that the pathogenicity of these hnRNPs is mechanistically two-fold, involving both RNA binding and protein aggregation. This finding, in turn, is consistent

with the model that has emerged from studies of TDP-43 and FUS, which both also require the presence of an intact RRM and a portion of the PrLD for maximal toxicity [78,110]. This similarity is important in that it provides two potential mechanisms of action for possible therapeutics that could be of broad utility in neurodegenerative diseases caused by RBPs: 1) inhibition of RNA binding or 2) disruption of protein aggregation. We have identified enhanced Hsp104 variants that show promise in combating a large repertoire of toxic proteins [235], and other agents that interfere with either RNA binding or protein aggregation may be similarly efficacious.

Interestingly, though we know that both hnRNPA1 and hnRNPA2 form fibrillar structures *in vitro*, constructs lacking a critical hexapeptide that are incapable of forming fibers *in vitro* still confer toxicity *in vivo* and form protein foci. It has been shown that the hnRNPA1 hexapeptide deletion construct still assembles into liquid-like droplets *in vitro* [222,339], leading us to wonder if liquid assemblies built on transient PrLD interactions rather than stable fibrous aggregates are mediators of hnRNPA1 and hnRNPA2 toxicity. Indeed, it was recently shown that liquid-liquid demixing causes dosage sensitivity of Mip6, an RBP with two LCDs that are not predicted to be prion-like, in yeast [39,340]. Upon overexpression, Mip6 forms toxic cytoplasmic liquid-like compartments that incorporate mRNA and proteins including transcription factors from the cytosol [340]. We propose that hnRNPA1 and hnRNPA2 may act via a similar mechanism, sequestering essential proteins and RNA transcripts. It is important to note that protein aggregation was not sufficient to confer toxicity in the absence of RNA-binding mediated by RRMs. Indeed, the isolated PrLDs of hnRNPA1^{D262V} and hnRNPA2^{D290V} formed cytoplasmic

aggregates in our yeast model, including an SDS-resistant amyloid species formed by the hnRNPA1 PrLD, but did not affect the viability of cells.

Like other RBPs with LCDs, hnRNPA1 and hnRNPA2 are recruited to stress granules, and disease-associated mutations alter the dynamics of incorporation [50,134]. In our model, too, hnRNPA1 and hnRNPA2 associated with RNP granule components, though it was not clear whether the resultant protein foci represented bona fide stress granules or p-bodies. The emergence, however, of RNP granule components (Lsm6, Lsm7 and Sbp1) as modifiers of protein toxicity suggested that the interaction of hnRNPA1 and hnRNPA2 with elements of these cellular compartments may play a central role in toxicity. It is especially notable that different RNP granule components are effective in the suppression of TDP-43 and FUS as compared to each other and hnRNPA1 and hnRNPA2, with very limited overlap.

There is significant evidence to suggest that increased protein translation may be sufficient to overcome the toxicity of FUS in yeast. Theoretically increased translation could compensate for sequestration of proteins and RNA to pathologic RNP granules and increased mRNA degradation. FUS toxicity is suppressed by overexpression of Pab1 or deletion of Pub1 [110]. Both Pab1 and Pub1 are poly(A)-binding proteins involved in stress granule formation [208,272,284], but Pab1 is thought to facilitate translation while Pub1 may negatively regulate translation via interaction with AREs [276,285]. FUS toxicity is also suppressed by overexpression of the stress granule-associated translation initiation factors Tif2 and Tif3 [110]. Both Tif2 and Tif3 have helicase activity, and Tif3 promotes the interaction of Tif2 with eiF4G [279,341,342]. LSM7 deletion suppresses FUS toxicity, and could also do so via increased translation

due to increased mRNA transcript availability in the setting of reduced Lsm1-7-mediated decapping [203].

Two other P-body proteins, Sbp1 and Edc3, suppress FUS toxicity when overexpressed [110]. However, both Sbp1 and Edc3 promote P-body formation and mRNA decapping and would be predicted to decrease translation when overexpressed [177,201,208], suggesting that their effects on protein translation do not explain their suppression of FUS toxicity. These proteins may directly interact with FUS, serving as a buffer against the sequestration of essential RNA and proteins. It is also possible that FUS expression in yeast causes the formation of non-functional P body-like structures, and that overexpression of P-body components that promote assembly can facilitate additional formation of functional structures.

Lastly, overexpression of the P-body protein Tis11, also known as Cth2 [343], which promotes decay of specific mRNAs during iron deprivation in yeast, suppresses FUS toxicity [110,344]. Tis11 is an RNA-binding protein that is upregulated during iron depletion and facilitates downregulation of iron-consuming cellular processes, including respiration and the tricarboxylic acids cycle, via enhanced degradation of crucial mRNA targets [345]. It is also thought to similarly mediate an adaptive response in yeast during oxidative stress [345]. This finding suggests that specific proteins that are downregulated in the setting of iron deficiency may directly contribute to FUS toxicity in yeast. Tis11 overexpression also suppresses the toxicity of TDP-43 [195], suggesting the possibility that investigation of the genes that are downregulated during iron starvation in yeast might yield insight into mechanistic overlap between TDP-43 and FUS toxicity.

Overexpression of the P-body protein Vts1, another facilitator of mRNA decay, also suppresses the toxicity of TDP-43 in yeast [195,346]. Vts1 facilitates mRNA degradation by the recruitment of a deadenylase complex [346]. Overexpression of the stress-granule protein Hrp1, which is involved in 3' cleavage and polyadenylation of mRNA to produce stable transcripts [347], enhances TDP-43 toxicity [195]. The stress-granule protein Pbp1 is also important for the addition of the 3' poly(A) tail that is important for transcript stability, nuclear mRNA export, and mRNA translation [283,347]. Loss of Pbp1, which leads to impaired polyadenylation [283], suppresses TDP-43 toxicity [251]. Taken together, these observations suggest that decreased transcript availability, and perhaps decreased translation of specific protein products, mitigates TDP-43 toxicity. Thus, specific TDP-43 protein interactions may confer toxic gain-of-function in the yeast cytoplasm. Finally, overexpression of the 5'-3' exonuclease Xrn1 enhances TDP-43 toxicity [195,208]. Xrn1 is an effector of mRNA degradation but also promotes transcription initiation and elongation [348]. Thus, it is possible that Xrn1 overexpression enhances TDP-43 toxicity by increasing mRNA transcript levels and, consequently, protein translation.

The three RNP granule components that suppress hnRNPA1 and hnRNPA2 toxicity when depleted are Sbp1, Lsm6, and Lsm7 (Table 2). All three are P-body proteins that enhance decapping, and their loss would be predicted to increase translation [201,203]. This finding suggests that the mechanism underpinning hnRNPA1 and hnRNPA2 toxicity is more similar to the mechanism of FUS toxicity than that of TDP-43 toxicity. This idea is also supported by the fact that we have identified deletion suppressors of hnRNPA1 and hnRNPA2 toxicity that also suppress FUS toxicity [110]

but none that also suppress TDP-43 toxicity [251] (Figure 26). However, SBP1 overexpression suppresses FUS toxicity [110], while SBP1 deletion suppresses hnRNPA1 and hnRNPA2 toxicity (Table 2, Figure 28). It is, therefore, possible that FUS, hnRNPA1, and hnRNPA2 do not cause toxicity in mechanistically similar ways, and that genetic modifications that suppress the toxicity of all three do so via distinct pathways. For example, deletion of Lsm6 and Lsm7 could cause increased translation that suppresses FUS toxicity and splicing alterations that suppress hnRNPA1 and hnRNPA2 toxicity. Sbp1 could directly interact with FUS, competitively buffering FUS toxicity caused by aberrant RNA and protein binding when overexpressed. Sbp1 could also compete with hnRNPA1 and hnRNPA2 for binding to certain non-essential proteins in the cytoplasm. Deletion of Sbp1 might then reduce hnRNPA1 and hnRNPA2 toxicity by increasing the availability of these cytoplasmic proteins to bind hnRNPA1 or hnRNPA2 and prevent sequestration of essential mRNA.

It is likely that FUS and TDP-43 cause toxicity by affecting distinct processes within the RNA-metabolism machinery or differentially affecting specific subsets of RNAs when compared to hnRNPA1 and hnRNPA2. TDP-43, FUS, hnRNPA1, and hnRNPA2 participate in the regulation of multiple steps of RNA metabolism, including transcription, splicing, and translation [57,143-146,150,151,155-157]. Thus it is possible that these RBPs could activate or perturb any of these processes in yeast. Furthermore, it is likely that their RNA targets would differ, as FUS and TDP-43 do not share binding targets with each other or with hnRNPA1 and hnRNPA2 in mammalian cells [57,59,62,143,147,148]. The preferred binding motifs of hnRNPA1 and hnRNPA2 are

similar, which is in accord with the fact that their shared modifiers suggest that they affect the same pathways [143,147,148].

Additional deletion modifiers identified by our screens against hnRNPA1 and hnRNPA2 were largely non-overlapping with known modifiers of TDP-43 and FUS toxicity from similarly executed screens, indicating that despite the structural and functional similarities among these RBPs, there are mechanistic differences underlying the pathologies caused by each (Figure 26). Two intriguing functional protein classes emerged as being linked to hnRNPA1 and hnRNPA2 toxicity: members of the yeast proteostasis network and snRNP complex proteins. One advantage of using yeast as a model system for human disease is the strong homology between the yeast and human genomes, which allows us to draw inferences about the cellular processes perturbed in disease based on genetic toxicity modifiers in yeast [1,7]. Indeed, the spliceosome machinery is highly conserved between yeast and humans, and Lsm6, Lsm7, Bud31, and Prp18 all have human homologues. Thus, inhibition of specific splicing factors may represent a therapeutic strategy for diseases of hnRNPA1 and hnRNPA2 misfolding. One hypothesis to explain the suppression of hnRNPA1 and hnRNPA2 toxicity by splicing perturbations would be that increased intronic inclusion causes cytoplasmic accumulation of transcripts targeted for nonsense-mediated decay (NMD) rather than translation [349]. If hnRNPA1 and hnRNPA2 aberrantly sequester essential mRNAs in RNP granules, causing their inappropriate degradation, nonfunctional intron-containing transcripts might compete for the degradation machinery (Figure 30A). Alternatively, hnRNPA1 and hnRNPA2 could cause detrimental splicing alterations that are eliminated by the disruption of the splicing machinery (Figure 30B). Finally, the genes encoding one

or more proteins that interact with hnRNPA1 and hnRNPA2 to functionally confer toxicity could contain introns. Reductions in the activity of the splicing machinery would render these transcripts nonfunctional, and translation would be diminished, leading to reduced toxicity (Figure 30C).

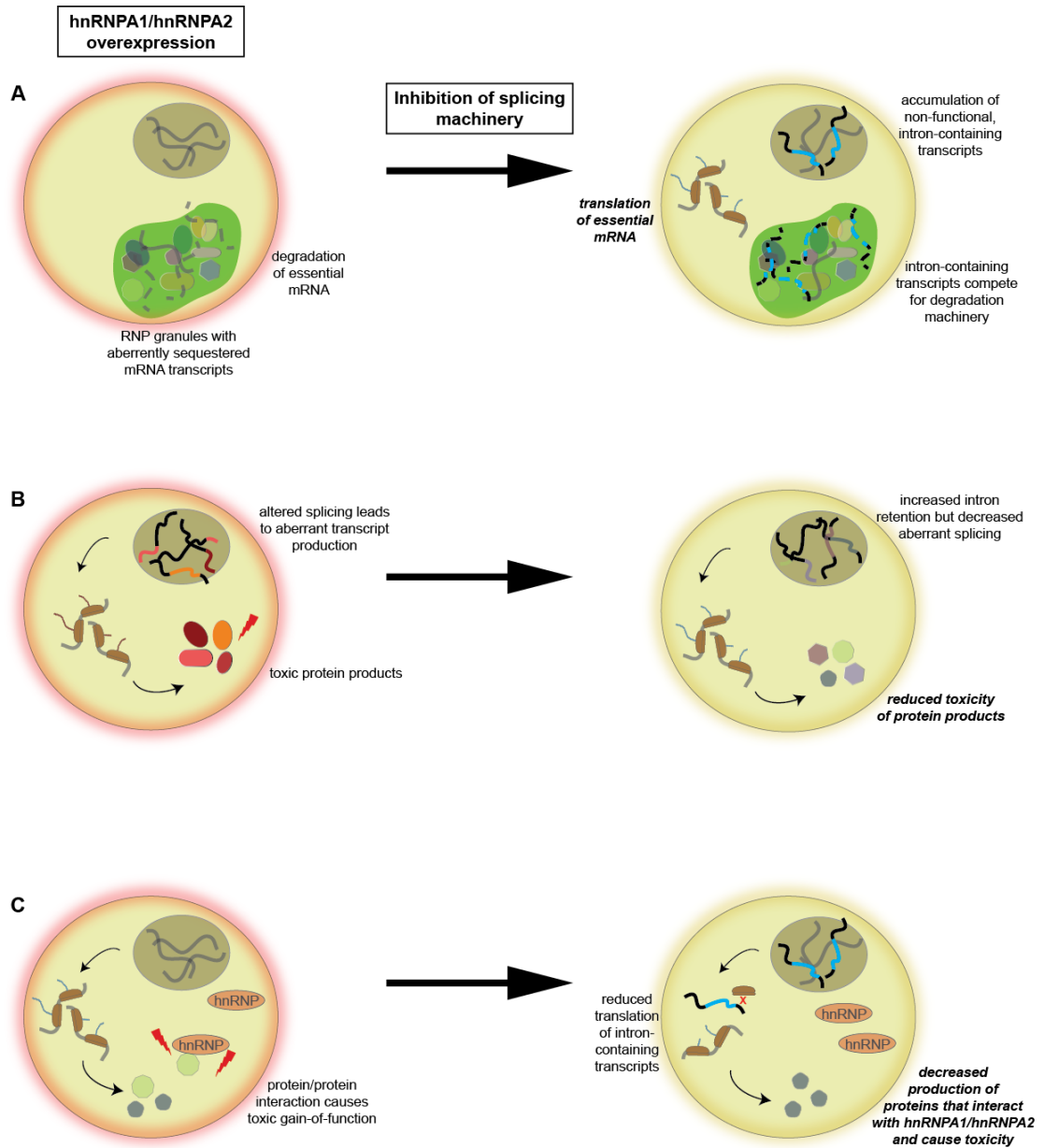


Figure 30: Proposed mechanisms to explain the suppression of hnRNPA1 and hnRNPA2 toxicity by perturbation of the splicing machinery in yeast. (A) It is possible that hnRNPA1 and hnRNPA2 sequester essential mRNAs to RNP granules preventing their translation and leading instead to their degradation. Disruption of the splicing machinery could lead to the accumulation of intron-containing transcripts that compete for the mRNA degradation machinery, making essential transcripts once again available for translation. (B) Alterations in splicing caused by hnRNPA1 and hnRNPA2 might lead to production of proteins with gain-of-function toxicity, and disruption of the splicing machinery could eliminate production of the improperly spliced

transcripts encoding these toxic proteins. **(C)** The toxic effects of hnRNPA1 and hnRNPA2 could be dependent upon their interactions with one or more cellular proteins. If the mRNA transcripts encoding these interacting proteins contain introns, the disruption of the splicing machinery could diminish their translation and reduce the availability of these proteins for toxic protein-protein interactions.

Our screen has also implicated the human protein quality control machinery, as homologs of several chaperones and cochaperones reduce hnRNPA1 and hnRNPA2 toxicity when deleted in yeast. Moreover, the human homologue of Hsc82, Hsp90AA1, and the human homolog of Ydj1, DnaJA1, have known clients that cause neurodegeneration. Overexpression of DnaJA1 was found to reduce the accumulation of tau, one of the pathologically aggregated proteins in AD and other 'tauopathies,' in cultured cells, and DNAJA1 levels were observed to be lower in the brains of patients with AD [350]. Hsp90AA1 has an inhibitory effect on the amyloidogenesis of A β [351], which points to a model in which Hsc82 may be acting to prevent the formation of fibrillar hnRNPA1 and hnRNPA2 structures, and its deletion mitigates toxicity by shifting the equilibrium away from toxic oligomer or droplet formation and towards non-toxic fibrous aggregate accumulation. In a yeast model of Huntingtin (Htt) toxicity, Htt harboring an expanded polyglutamine tract (Htt103Q) can form tight, amyloid-like assemblies that are benign or detergent soluble aggregates that are more amorphous and can be toxic [352,353]. In this model, Sti1 reduces Htt103Q toxicity by incorporating Htt103Q into large amyloid-like inclusions [353]. It is possible that Sti1 similarly facilitates the assembly of large hnRNPA1 and hnRNPA2 inclusions that represent a toxic species, while STI1 deletion causes an increased proportion of benign, amorphous species.

Yeast chaperones also affect RNP granule dynamics, providing possible insight into their role in hnRNPA1 and hnRNPA2 toxicity [217,325,326]. Loss of Sse1 alters yeast stress granule assembly dynamics and delays stress granule dissolution [217]. Ydj1 has an LC domain and is required for the formation of P bodies [325]. Moreover, loss of Ydj1 causes increased targeting of stress granules to the vacuole for degradation and prevents the restoration of protein translation during recovery from stress [326]. Another cytoplasmic yeast Hsp40, Sis1, promotes stress granule clearance via autophagy rather than dissolution and returning of mRNAs to translation [326]. These findings suggest that stress-granule clearance via autophagy via the Sis1 pathway may be beneficial in the setting of overexpression of hnRNPA1 or hnRNPA2 in yeast.

Members of the Hsp90 family are a particularly appealing therapeutic target, as inhibitors are currently in clinical trials as anti-cancer agents [354] and have shown promise in models of neurodegeneration, specifically a mouse model of spinal and bulbar muscular atrophy and a *Drosophila* model of Parkinson's disease [355,356]. Our data suggest that Hsp90 inhibitors might be similarly efficacious in MSP patients. Future studies should focus on testing the modifiers of hnRNPA1 and hnRNPA2 toxicity that we have uncovered in metazoan model systems, including *C. elegans*, *Drosophila*, and mammalian neuronal cell culture to establish their relevance in the nervous system.

A lingering question in the field of RBP pathology as it relates to neurodegeneration is whether therapeutic strategies targeting specific RBPs will be preferable to, or more attainable than, a broadly efficacious anti-disease agent. We have demonstrated potential avenues for both approaches. All genetic overexpression and deletion suppressors discussed appear to be specifically efficacious against one or more

RBPs, but there is not a known alteration of gene expression that suppresses the toxicity of hnRNPA1 and hnRNPA2 in addition to both TDP-43 and FUS. This presents the opportunity for tailored therapeutic strategies designed to approach specific mutations and protein pathologies. We have, however, identified engineered Hsp104 variants that antagonize the toxic effects of all four RBPs. Hsp104 variants including A503S, V426L, and A437W, therefore, may ultimately be of utility in patients with ALS and FTD of various etiologies in addition to IBM, PFD, and MSP. Future work will include a focus on identifying small-molecule modifiers of hnRNPA1 and hnRNPA2 toxicity and exploring the specificity of these modifiers to expand our repertoire of therapeutic candidates and to gain additional mechanistic insight into the RBP-misfolding disorders.

2.4 Materials and Methods

2.4.1 Yeast strains, plasmids, and media

All experiments were performed using BY4741 yeast (MATa, his3 Δ 1, leu2 Δ 0, met15 Δ 0, ura3 Δ 0). Deletion strains harbor the KanMX cassette in place of the deleted gene of interest. BY4741 *pbp1* Δ and BY4741 *pub1* Δ were obtained from F. Bradley Johnson. BY4741 *ism7* Δ and BY4741 *dbr1* Δ [251] were obtained from Aaron Gitler. The construction of centromeric pAG416Gal-hnRNPA1-GFP and pAG416Gal-hnRNPA2-GFP plasmids for yeast expression was previously described [134], as was the construction of pAG416Gal-FUS [110] and pAG416Gal-TDP-43 [78]. All missense mutations and deletions were generated using QuikChange Lightning site-directed mutagenesis (Agilent) and confirmed by DNA sequencing. pAG413Gal-Hsp104, pAG413Gal-Pab1, pAG413Gal-Dcp2, pAG423Gal-Tif2, and pAG423Gal-Hsp82 were used for coexpression studies. Frank Luca provided a plasmid for the expression of

RFP-tagged Dcp2 driven by the endogenous promoter and a yeast strain expressing integrated mCherry-tagged Pab1, also under the control of the endogenous promoter. The pSNR6 plasmid for overexpression of U6 snRNA was provided by Roy Parker. Yeast were grown in rich media (YPD) or selective synthetic media lacking the appropriate amino acids and supplemented with 2% glucose, raffinose, or galactose, or a combination of sucrose and galactose totaling 2% of the final volume.

2.4.2 Yeast transformation and spotting assay

Yeast were transformed with plasmid DNA using polyethylene glycol and lithium acetate according to standard protocols [357]. Transformed yeast were grown at 30°C on non-inducing, selective glucose media. They were then passaged overnight in raffinose-containing media to mid/late log-phase, and normalized for OD₆₀₀. A five-fold dilution series was spotted in parallel on solid non-inducing, glucose containing media and solid media containing either galactose or a combination of sucrose and galactose to induce protein expression. Plates were incubated for 2-3 days at 30°C.

2.4.3 Immunoblotting

Yeast cells from overnight liquid raffinose cultures were spun down, resuspended in galactose- or sucrose/galactose-containing media and grown >5 hours at 30°C to induce protein expression. Cells were harvested and treated with 0.1M NaOH for five minutes at room temperature. After centrifugation, pelleted cells were resuspended in 1x SDS sample buffer and boiled for five minutes. Total protein concentration was normalized based on the OD₆₀₀ of the induced cultures, and lysates were resolved via SDS-PAGE (4%-20% gradient, BioRad) followed by transfer to a PVDF membrane. Membranes were blocked overnight at 4°C in Odyssey® Blocking Buffer (LI-COR

Biosciences) and probed using rabbit anti-GFP polyclonal antibody (Sigma-Aldrich), mouse anti-PGK monoclonal antibody (Novex), rabbit anti-FUS polyclonal antibody (Bethyl Laboratories), rabbit anti-Hsp104 polyclonal antibody (Enzo Life Sciences), 680RD goat anti-rabbit secondary antibody (LI-COR), and 800CW goat anti-mouse secondary antibody (LI-COR). Blots were visualized using an Odyssey® Fc imager and Image Studio software.

2.4.4 Sedimentation analysis of yeast lysates

Yeast cells were grown overnight in raffinose-containing media at 30°C, then grown for 5-6 hours in galactose-containing media before harvesting for sedimentation. OD₆₀₀ was normalized to 1.2 and 200mL cells were spun down and resuspended in 12mL lysis buffer (30mM HEPES pH 7.4, 150mM NaCl, 1% glycerol, 0.5% Triton X-100, 5mM EDTA, 1mM DTT, 1mM PMSF, 1% fungal protease inhibitor cocktail (Sigma)). The suspension was then passed three times through a French press (Emulsiflex C-3) to lyse the cells. Lysates were cleared by centrifugation (6000g for 5 minutes) and a 200ul fraction was taken to represent the total cellular protein content and boiled for five minutes in 3x SDS sample buffer. Another 200ul aliquot was separated into soluble and pelleted fractions by centrifugation at 100,000g for 15 minutes. The soluble fraction was boiled for five minutes in 3x SDS sample buffer and the pellet was dissolved and boiled for 10 minutes in 1x SDS sample buffer. 10% of the total and soluble protein fractions and 20% of the pelleted protein fraction were separated via SDS-PAGE and immunoblotted as described above.

2.4.5 Fluorescence Microscopy

Yeast cultures grown overnight in raffinose media were diluted to early/mid log-phase in galactose media and grown for >5 hours at 30°C to induce hnRNP expression. Live, untreated cells were visualized at 100x magnification on a Leica-DMIRBE microscope. To visualize nuclear material, cells were incubated for 15-30 minutes at room temperature with Hoechst 33342 stain (167µg/mL). All images were analyzed and processed using ImageJ software.

2.4.6 SDD-AGE

Yeast cells were grown overnight in raffinose-containing media, then harvested by centrifugation and resuspended in galactose-containing media to induce protein expression. Following 6-hour induction, yeast were pelleted by centrifugation, washed in water and then resuspended in spheroplasting solution (1.2 M D-sorbitol, 0.5 mM MgCl₂, 220 mM Tris, pH 7.5, 50 mM β-mercaptoethanol and 0.5 mg/ml Zymolyase 100T) and incubated for 1 hour at 30°C. Spheroplasts were collected by centrifugation (500 rcf for 5 minutes) and resuspended in lysis buffer (100 mM Tris (pH 7.5), 50 mM NaCl, and 2x Sigma Protease Inhibitor cocktail—P8215). The suspensions were vortexed at high speed for 1 minute at 4°C and then snap-frozen in dry ice and ethanol. Samples were thawed on wet ice and protein concentrations were determined by BCA Protein Assay. 4X sample buffer (2X TAE, 20% glycerol, 2 or 8% SDS, 10% β-mercaptoethanol, and bromophenol blue) was added and lysates were incubated for 5 minutes at room temperature. Samples of the same total protein concentration were loaded on a 1.5% Agarose gel with 1X TAE and 0.1% SDS, cast in a horizontal slab electrophoresis apparatus tray. Samples were run at 5 V/cm gel length in a cold room until dye front was

1.5 cm from the end of the gel. The samples were then transferred overnight to a nitrocellulose membrane as previously described [358]. The membrane was processed for Western Blot analysis with α -GFP (Roche Cat. No. 11814460001) primary and α -Mouse (Rockland Anti-MOUSE IgG (H&L) IRDye800) secondary antibodies and proteins were detected using a Li-Cor Odyssey Model 9120.

2.4.7 Confocal microscopy

Yeast coexpressing GFP-tagged hnRNP constructs and mCherry- or RFP-tagged stress granule and P-body proteins were grown overnight at 30°C in non-inducing raffinose media lacking uracil and leucine. Cultures were spun down and cell pellets were resuspended in galactose media to induce hnRNP expression. After 5-6 hours of induction at 30°C, cells were harvested for microscopy. Live, unstained cells were imaged using a spinning disk confocal microscope equipped with a Yokogawa CSU X1 scan head combined with an Olympus IX 81 microscope. Acquisition and hardware were controlled by MetaMorph, version 7.7 (Molecular Devices, Downingtown PA). An Andor iXon3 897 EMCCD camera (Andor Technology, South Windsor CT) was used for image capture. Solid-state lasers for excitation (488 nm for GFP, 561 nm for RFP/mCherry) were housed in a launch constructed by Spectral Applied Research (Richmond Hill, Ontario, Canada). All images were analyzed and processed using ImageJ software.

2.4.8 Protein Purification

WT and mutant hnRNPA1 and hnRNPA2 were expressed and purified from *E. coli* as GST-tagged proteins. Expression constructs were generated in pDuet to contain a TEV-cleavable site, resulting in a GST-TEV-hnRNP construct. GST-TEV-hnRNP was

overexpressed in *E. coli* BL21-CodonPlus(DE3)-RIL cells (Agilent) and purified under native conditions using a glutathione-sepharose column (GE) according to the manufacturer's instructions. Proteins were eluted from the glutathione sepharose with assembly buffer (hnRNPA1 D262V 105-320: 50 mM Tris-HCl, pH 8, 200 mM trehalose, and 20 mM glutathione; all other constructs: 40mM HEPES-NaOH, 150mM KCl, 5% glycerol, 20mM glutathione, pH 7.4). Protein was centrifuged for 10 min at 16,100g, and supernatant was separated from pellet to remove any protein aggregates. Protein concentration was determined by Bradford assay (Bio-Rad) in comparison to BSA standards.

2.4.9 Sedimentation analysis of hnRNPA1 fibrillization

To follow the reaction kinetics by sedimentation analysis, at different time points, samples were centrifuged at 16,100 g for 10 min at 4°C. Supernatant and pellet fractions were then resolved by SDS-PAGE and stained with Coomassie Brilliant Blue. The amount of protein in either fraction was determined by densitometry in comparison to known quantities of hnRNPA1/hnRNPA2.

2.4.10 Transmission electron microscopy

Samples (10 µl) were adsorbed onto glow-discharged 300-mesh Formvar/carboncoated copper grid (Electron Microscopy Sciences) and stained with 2% (w/v) aqueous uranyl acetate. Excess liquid was removed, and grids were allowed to air dry. Samples were viewed by a JEOL 1010 transmission electron microscope.

2.4.11 ThT fluorescence

ThT fluorescence was used to assess fibrillization as previously described [359].

2.4.12 Genetic deletion screen for toxicity modifiers

We used the synthetic genetic array (SGA) technique to screen the collection of non-essential only yeast knockout strains. Screens were performed as described [360-362] with some modifications [363], using a Singer RoToR HDA (Singer Instruments, Somerset, UK). The galactose-inducible expression constructs (pAG416Gal-hnRNPA1 and pAG416Gal-hnRNPA2B1) were introduced into MAT α strain Y7092 to generate the query strains. Query strains were mated to the yeast haploid deletion collection of non-essential genes (MAT α , each gene deleted with KanMX cassette). Diploids were selected for by plating yeast onto glucose media lacking uracil with G418 added. Diploids were then grown on 2% YPD prior to sporulation. Yeast were induced to undergo sporulation by plating on media containing 1.5% potassium acetate, 0.1% glucose, 0.25% yeast extract, 0.01% amino-acids supplement mixture (2 g histidine, 10 g leucine, 2 g lysine, 2 g uracil), and 50 mg/L G418. Glucose media lacking histidine, arginine, lysine, and uracil and supplemented with canavanine and thialysine was used to select for MAT α haploids. G418 was then used to select for MAT α haploids harboring the KanMX cassette and yeast were grown in the presence of glucose (hnRNPA1 or hnRNPA2 expression “off”) or a 1:1 mixture of sucrose and galactose (hnRNPA1 or hnRNPA2 expression “on”). After growth at 30°C for 2 days for glucose plates and 4 days for sucrose/galactose plates, plates were photographed and colony sizes measured by ImageJ image analysis software, based on Collins et al. 2006 [364]. The screen was repeated twice and hits were selected and validated by repeat transformations and spotting on 1:1 or 3:1 sucrose:galactose.

CHAPTER 3: CONCLUSIONS AND FUTURE DIRECTIONS

Using *Saccharomyces cerevisiae* as a model system, we have mapped the determinants of protein toxicity for two RBPs with PrLDs that are known to cause MSP, a degenerative syndrome encompassing features of ALS, FTD, IBM, and PDB. We have established that both hnRNPA1 and hnRNPA2 require an intact RRM and a portion of the PrLD, and thus propose a mechanism of toxicity that requires both RNA-binding and the formation of protein assemblies. It is unknown whether the toxic species in yeast is a solid fibrous state, a liquid droplet-like assembly, a soluble oligomer or a combination of these. We have highlighted the importance of the splicing machinery, the yeast protein quality control machinery, and RNP-granule components to the toxicity of both hnRNPA1 and hnRNPA2 through a genetic deletion screen to identify modifiers of toxicity. Identifying cellular pathways that affect RBP-mediated toxicity can give us insight into the mechanisms underlying cell death. Importantly, all suppressors of hnRNPA1 also suppressed hnRNPA2 toxicity, and vice versa, suggesting a shared molecular pathway underlying the pathogenesis of disease caused by these proteins. It was also notable that there was very little overlap between modifiers of hnRNPA1 and hnRNPA2 toxicity and modifiers of other toxic, disease causing RBPs, specifically TDP-43 and FUS. Our data suggest mechanistic differences underpinning toxicity among these structurally and functionally similar proteins.

We have also expanded the repertoire of disease substrates rescued by engineered variants of the protein disaggregase Hsp104 (A503S, V426L, and A437W). These potentiated disaggregases with elevated ATPase activity robustly suppress the

toxicity of TDP-43, FUS, and α -synuclein in yeast, whereas Hsp104 has no effect [234,235]. We have shown that these Hsp104 mutants, and likely many others, given the wide genetic landscape that supports rescue of cell viability in the setting of TDP-43 and FUS expression [234,235], are also able to suppress hnRNPA1 and hnRNPA2 toxicity. Ultimately, adaptation of Hsp104 for use in patients with neurodegenerative diseases could represent a broadly applicable therapeutic strategy that does not require the use of genotyping or biopsy to identify patient-specific protein pathology.

These studies will provide a framework for extending the study of MSP to mammalian and other higher order systems, and future work will use the insights gleaned from these experiments to explore candidate therapeutic agents in *Drosophila*, mouse models, or primary neuronal cultures. There remain, however, unanswered questions and further yeast studies that could potentially add to our knowledge base and generate additional leads for exploration in other models. A genetic overexpression screen to complement our deletion screen would be a natural first step, and a high-throughput small molecule screen could tease out additional information about specific pathways affected by hnRNPA1 and hnRNPA2. The results from our deletion screen provide an arsenal of genes and pathways that can be targeted in a host of disease models using short interfering RNAs (siRNAs), antisense oligonucleotides (ASOs), or CRISPR/Cas9 technology [365-367]. They also raise a number of mechanistic questions that could begin to be answered in yeast.

It was particularly curious to us that deletion of DBR1, which encodes the lariat-debranching enzyme, did not suppress the toxic effects of hnRNPA1 and hnRNPA2, as it does for TDP-43 and FUS. Loss of Dbr1 causes the cytoplasmic accumulation of

intronic RNA lariats as they are excised from mRNA transcripts during splicing and cannot be degraded in the absence of the initial debranching step [251,368]. It is proposed that in the absence of lariat debranching, the undegraded RNA lariats bind to FUS and TDP-43, acting as 'decoy' interactors and preventing these toxic proteins from sequestering essential RNA and proteins [251]. We hypothesized that this mechanism would be widely applicable across toxic RBPs, however the observation that hnRNPA1 and hnRNPA2 toxicity was unaffected by DBR1 deletion led us to consider the possibility that the nucleotide content of the yeast intronic genome is preferentially bound by TDP-43 and FUS, but not hnRNPA1 or hnRNPA2. We propose that noncoding RNAs tailored to the preferred binding motifs of hnRNPA1 or hnRNPA2 and expressed at high levels in the cytoplasm could functionally replace RNA lariats and buffer protein toxicity as non-essential binding partners. One approach to achieving this goal would be to design long, repetitive RNA sequences that could be expressed as circular RNA. Circular RNA is, in general, protected from cytoplasmic degradation, likely because, without linear ends, it is not recognized by the RNA-decay machinery [369]. Delivery of exogenous RNAs, though not without difficulties, is currently being explored in various forms, including siRNAs and ASOs, for a range of disorders including hepatitis B, cardio-metabolic disorders, and rare genetic disorders [367]. Three ASO therapeutics have been approved for use by the FDA [367]. Though these therapies are aimed at silencing endogenous RNA, the same principles of delivery could be applied to introduce a circular non-coding RNA species to buffer the toxicity of neurodegeneration-causing RBPs.

We are especially intrigued by the ability of either LSM6 or LSM7 deletion to suppress the toxicity of hnRNPA1 and hnRNPA2, because the encoded proteins both participate in two disparate aspects of RNA metabolism: splicing and degradation [40]. It would be of great utility to discern which of these processes, when perturbed, disrupts the toxicity of hnRNPA1 and hnRNPA2. Lsm6 and Lsm7 assemble into two distinct heteroheptameric complexes; Lsm1-7 is localized to P bodies in the cytoplasm, sites of mRNA degradation, and Lsm2-8 is a component of the spliceosomal U6 snRNP [202,203]. Of the eight proteins present in these two complexes, three are non-essential (Lsm1, Lsm6, and Lsm7) [202], and, therefore, candidate toxicity suppressors within the parameters of our deletion screen. Lsm1-7 play a role in promoting decapping in the mRNA degradation pathway, as does another deletion suppressor that emerged from our screen, Sbp1 [200,201,203]. Our evidence suggests that it is less likely that the decapping role of Lsm6 and Lsm7 is crucial to the toxicity of hnRNPA1 and hnRNPA2 for a number of reasons. First, the third non-essential gene in the Lsm1-7 complex was not found to be a suppressor of hnRNPA1 or hnRNPA2. Additionally, we did not find deletion of other elements of the decapping machinery, including Pat1 and Dhh1 [177], to have any effect on hnRNPA1- or hnRNPA2-mediated toxicity. Moreover, Sbp1 is also found in stress granules, suggesting that its role in hnRNPA1 and hnRNPA2 toxicity may be related to a process other than RNA decapping and decay [200].

An alternative hypothesis is that splicing perturbations from the disruption of the Lsm2-8 complex inhibit the toxic effects of hnRNPA1 and hnRNPA2. This hypothesis could be confirmed by treating cells with a small molecule inhibitor of splicing concurrent with overexpression of hnRNPA1 or hnRNPA2. If, in fact, the inhibition of splicing

suppresses the toxicity of these RBPs, it could be due to the effective depletion of spliced yeast genes. In yeast, intron-retaining transcripts are degraded either by the nuclear exosome or by NMD and do not get translated [349]. Experimentally determining whether the depletion of specific essential proteins through reduced splicing efficiency reduces hnRNPA1 and hnRNPA2 toxicity could yield insight into additional toxicity-modifying biologic pathways that were not revealed by scanning the non-essential genome. Just under 5% of the yeast genome (283 genes) contains introns [370]. After filtering this list to exclude non-essential genes (which were explored in our deletion screen), each remaining yeast gene with an intronic sequence could be tested for modifying effects on hnRNPA1 and hnRNPA2 toxicity. This could be done in two ways. Knowing that we expect decreased gene expression to suppress toxicity, we could overexpress each gene and look for those that enhance toxicity in the setting of hnRNPA1 or hnRNPA2 overexpression. This approach could prove difficult because hnRNPA1 and hnRNPA2 both confer a high level of toxicity at baseline. An alternative approach would include generating temperature-sensitive, conditional mutant strains for each intron-containing gene. Temperature-sensitive strains typically allow for the manipulation of gene expression levels within a range of growth temperatures [371]. Altering growth conditions to reduce expression of individual essential genes could reveal genetic interactions that modify RBP toxicity. This approach could be expanded to include inhibition of all untested essential yeast genes, but the information from our deletion screen suggests that intron-containing genes may be a fruitful starting point.

An important question that has not been resolved is: what species represents the toxic conformation of hnRNPA1 and hnRNPA2 in *S. cerevisiae*? A portion of the PrLD is

required for maximal toxicity, suggesting that the formation of protein assemblies is crucial for toxicity. Whether these toxic assemblies are liquid droplets, fibrillar aggregates, or perhaps prefibrillar oligomers remains unclear. Several pieces of evidence suggest that, in yeast, more stable fibrillar hnRNPA1 or hnRNPA2 aggregates may be protective, just as more stable aggregates are the benign species in a yeast model of Htt toxicity [353]. First, hnRNPA1 lacking a crucial steric zipper motif does not readily fibrillize *in vitro*, but does form liquid droplets [134,222]. This construct is highly toxic in yeast (Figure 8). Moreover, the PrLD of hnRNPA1^{D262V} forms stable aggregates that are detergent-insoluble in yeast, and this construct is benign (Figures 8 and 10). Finally, the human homologue of Hsc82 negatively regulates amyloidogenesis [351]. Deletion of Hsc82, which suppresses hnRNPA1 and hnRNPA2 toxicity in yeast, may shift the relative abundance of protein conformers away from oligomers and droplets and towards stable cross- β structures. It would be useful to examine whether toxic hnRNPA1 and hnRNPA2 form liquid droplets in yeast, and whether the elimination of these species can reduce toxicity.

Aliphatic alcohols, including 1,6-hexanediol, 2,5-hexanediol, 1,5-pentanediol, or 1,4-butanediol, can disrupt the weak interactions between LCDs that mediate LLPS, and they have been proposed as a method of elucidating whether cellular structures form via LLPS [217,229,230]. New evidence suggests, however, that 1,6-hexanediol can also disrupt elements of cytoskeletal organization and reduce cellular viability [372]. It would, therefore, not be straightforward to examine which, if any, hnRNPA1 and hnRNPA2 constructs form liquid-like assemblies simply by exposing cells to aliphatic alcohols and

assessing for alterations in hnRNPA1 or hnRNPA2 localization or dissolution of hnRNPA1 or hnRNPA2 foci using fluorescence microscopy.

Finally, the contribution of hnRNPA1 and hnRNPA2 mutations to the overall landscape of neurodegeneration is currently unknown in that we do not yet know how frequently these mutations occur or how penetrant they are. The discovery of hnRNPA1 and hnRNPA2 mutations in MSP was rapidly followed by the identification of additional hnRNPA1 and hnRNPA2 mutations in patients with sporadic and familial ALS [94,134], and we expect the number of patients suffering from neurodegenerative phenotypes with identified mutations in hnRNPA1 or hnRNPA2 to grow as our knowledge of disease increases. Moreover, mutations in the PrLD of *hnRNPD*, leading to D378N or D378H substitutions, have now been linked to limb-girdle muscular dystrophy type 1G [373]. We anticipate that over time additional RBPs with PrLDs will continue to emerge in connection with degenerative diseases [31,41].

BIBLIOGRAPHY

1. Khurana V, Lindquist S (2010) Modelling neurodegeneration in *Saccharomyces cerevisiae*: why cook with baker's yeast? *Nat Rev Neurosci* 11: 436-449.
2. Lepesant J-A (2015) The promises of neurodegenerative disease modeling. *Comptes Rendus Biologies* 338: 584-592.
3. Swinnen B, Robberecht W (2014) The phenotypic variability of amyotrophic lateral sclerosis. *Nat Rev Neurol* 10: 661-670.
4. Li YQ, Tan MS, Yu JT, Tan L (2016) Frontotemporal lobar degeneration: mechanisms and therapeutic strategies. *Mol Neurobiol* 53: 6091-6105.
5. Ferrari R, Kapogiannis D, Huey ED, Momeni P (2011) FTD and ALS: a tale of two diseases. *Curr Alzheimer Res* 8: 273-294.
6. Bunner KD, Rebec GV (2016) Corticostriatal dysfunction in Huntington's disease: the basics. *Front Hum Neurosci* 10: 317.
7. Gitler AD (2008) Beer and bread to brains and beyond: can yeast cells teach us about neurodegenerative disease? *Neurosignals* 16: 52-62.
8. Lo Bianco C, Shorter J, Regulier E, Lashuel H, Iwatsubo T, et al. (2008) Hsp104 antagonizes alpha-synuclein aggregation and reduces dopaminergic degeneration in a rat model of Parkinson disease. *J Clin Invest* 118: 3087-3097.
9. Skovronsky DM, Lee VM, Trojanowski JQ (2006) Neurodegenerative diseases: new concepts of pathogenesis and their therapeutic implications. *Annu Rev Pathol Mech Dis* 1: 151-170.
10. Liscic RM, Grinberg LT, Zidar J, Gitcho MA, Cairns NJ (2008) ALS and FTL: two faces of TDP-43 proteinopathy. *Eur J Neurol* 15: 772-780.
11. Mathis S, Couratier P, Julian A, Vallat J-M, Corcia P, et al. (2016) Management and therapeutic perspectives in amyotrophic lateral sclerosis. *Expert Review of Neurotherapeutics*: 1-14.
12. Cummings J, Aisen PS, DuBois B, Frölich L, Jack CR, et al. (2016) Drug development in Alzheimer's disease: the path to 2025. *Alzheimer's Research & Therapy* 8: 39.
13. Farzanehfar P (2016) Towards a better treatment option for Parkinson's disease: a review of adult neurogenesis. *Neurochem Res* 41: 3161-3170.
14. Bose S, Cho J (2016) Targeting chaperones, heat shock factor-1, and unfolded protein response: Promising therapeutic approaches for neurodegenerative disorders. *Ageing Res Rev*.
15. Da Cruz S, Cleveland DW (2011) Understanding the role of TDP-43 and FUS/TLS in ALS and beyond. *Curr Opin Neurobiol* 21: 904-919.
16. Forman MS, Trojanowski JQ, Lee VM (2004) Neurodegenerative diseases: a decade of discoveries paves the way for therapeutic breakthroughs. *Nat Med* 10: 1055-1063.
17. Braak H, Del Tredici K, Rub U, de Vos RA, Jansen Steur EN, et al. (2003) Staging of brain pathology related to sporadic Parkinson's disease. *Neurobiol Aging* 24: 197-211.

18. Cushman M, Johnson BS, King OD, Gitler AD, Shorter J (2010) Prion-like disorders: blurring the divide between transmissibility and infectivity. *J Cell Sci* 123: 1191-1201.
19. Giasson BI, Lee VM, Trojanowski JQ (2003) Interactions of amyloidogenic proteins. *NeuroMolecular Med* 4: 49-58.
20. Ash PE, Bieniek KF, Gendron TF, Caulfield T, Lin WL, et al. (2013) Unconventional translation of C9ORF72 GGGGCC expansion generates insoluble polypeptides specific to c9FTD/ALS. *Neuron* 77: 639-646.
21. Banez-Coronel M, Ayhan F, Tarabochia AD, Zu T, Perez BA, et al. (2015) RAN translation in Huntington disease. *Neuron* 88: 667-677.
22. Todd PK, Oh SY, Krans A, He F, Sellier C, et al. (2013) CGG repeat-associated translation mediates neurodegeneration in fragile X tremor ataxia syndrome. *Neuron* 78: 440-455.
23. Zu T, Gibbens B, Doty NS, Gomes-Pereira M, Huguet A, et al. (2011) Non-ATG-initiated translation directed by microsatellite expansions. *Proc Natl Acad Sci USA* 108: 260-265.
24. Robberecht W, Philips T (2013) The changing scene of amyotrophic lateral sclerosis. *Nat Rev Neurosci* 14: 248-264.
25. Belzil VV, Katzman RB, Petrucelli L (2016) ALS and FTD: an epigenetic perspective. *Acta Neuropathol* 132: 487-502.
26. Rippon GA, Scarmeas N, Gordon PH, Murphy PL, Albert SM, et al. (2006) An observational study of cognitive impairment in amyotrophic lateral sclerosis. *Arch Neurol* 63: 345-352.
27. Lillo P, Hodges JR (2009) Frontotemporal dementia and motor neurone disease: overlapping clinic-pathological disorders. *J Clin Neurosci* 16: 1131-1135.
28. Strong MJ, Yang W (2011) The frontotemporal syndromes of ALS. Clinicopathological correlates. *J Mol Neurosci* 45: 648-655.
29. Chen-Plotkin AS, Lee VM, Trojanowski JQ (2010) TAR DNA-binding protein 43 in neurodegenerative disease. *Nat Rev Neurol* 6: 211-220.
30. Mackenzie IR, Rademakers R, Neumann M (2010) TDP-43 and FUS in amyotrophic lateral sclerosis and frontotemporal dementia. *Lancet Neurol* 9: 995-1007.
31. King OD, Gitler AD, Shorter J (2012) The tip of the iceberg: RNA-binding proteins with prion-like domains in neurodegenerative disease. *Brain Res* 1462: 61-80.
32. Halfmann R, Alberti S, Lindquist S (2010) Prions, protein homeostasis, and phenotypic diversity. *Trends Cell Biol* 20: 125-133.
33. Halfmann R, Lindquist S (2010) Epigenetics in the extreme: prions and the inheritance of environmentally acquired traits. *Science* 330: 629-632.
34. Prusiner SB (1998) Prions. *Proc Natl Acad Sci USA* 95: 13363-13383.
35. Shorter J (2010) Emergence and natural selection of drug-resistant prions. *Mol Biosyst* 6: 1115-1130.
36. True HL, Lindquist SL (2000) A yeast prion provides a mechanism for genetic variation and phenotypic diversity. *Nature* 407: 477-483.
37. Shorter J, Lindquist S (2005) Prions as adaptive conduits of memory and inheritance. *Nat Rev Genet* 6: 435-450.
38. Wiltzius JJ, Landau M, Nelson R, Sawaya MR, Apostol MI, et al. (2009) Molecular mechanisms for protein-encoded inheritance. *Nat Struct Mol Biol* 16: 973-978.

39. Alberti S, Halfmann R, King O, Kapila A, Lindquist S (2009) A systematic survey identifies prions and illuminates sequence features of prionogenic proteins. *Cell* 137: 146-158.
40. Toombs JA, McCarty BR, Ross ED (2010) Compositional determinants of prion formation in yeast. *Mol Cell Biol* 30: 319-332.
41. March ZM, King OD, Shorter J (2016) Prion-like domains as epigenetic regulators, scaffolds for subcellular organization, and drivers of neurodegenerative disease. *Brain Res* 1647: 9-18.
42. Masison DC, Maddelein M, Wickner RB (1997) The prion model for [URE3] of yeast: Spontaneous generation and requirements for propagation. *Proc Natl Acad Sci USA* 94: 12503-12508.
43. Li L, Lindquist S (2000) Creating a protein-based element of inheritance. *Science* 287: 661-664.
44. Osherovich LZ, Weissman JS (2001) Multiple Gln/Asn-rich prion domains confer susceptibility to induction of the yeast [PSI⁺] prion. *Cell* 106: 183-194.
45. Tyedmers J, Treusch S, Dong J, McCaffery JM, Bevis B, et al. (2010) Prion induction involves an ancient system for the sequestration of aggregated proteins and heritable changes in prion fragmentation. *Proc Natl Acad Sci USA* 107: 8633-8638.
46. Ross ED, Baxa U, Wickner RB (2004) Scrambled prion domains form prions and amyloid. *Mol Cell Biol* 24: 7206-7213.
47. Ross ED, Edskes HK, Terry MJ, Wickner RB (2005) Primary sequence independence for prion formation. *Proc Natl Acad Sci USA* 102: 12825-12830.
48. Couthouis J, Hart MP, Shorter J, DeJesus-Hernandez M, Erion R, et al. (2011) A yeast functional screen predicts new candidate ALS disease genes. *Proc Natl Acad Sci USA* 108: 20881-20890.
49. Harrison AF, Shorter J (2017) RNA-binding proteins with prion-like domains in health and disease. *Biochem J* 474: 1417-1438.
50. Li YR, King OD, Shorter J, Gitler AD (2013) Stress granules as crucibles of ALS pathogenesis. *J Cell Biol* 201: 361-372.
51. Banfi S, Servadio A, Chung M-y, Kwiatkowski TJ, McCall AE, et al. (1994) Identification and characterization of the gene causing type 1 spinocerebellar ataxia. *Nat Genet* 7: 513-520.
52. Orr HT, Zoghbi HY (2007) Trinucleotide repeat disorders. *Annu Rev Neurosci* 30: 575-621.
53. Cummings CJ, Mancini MA, Antalffy B, DeFranco DB, Orr HT, et al. (1998) Chaperone suppression of aggregation and altered subcellular proteasome localization imply protein misfolding in SCA1. *Nat Genet* 19: 148-154.
54. Lorenzetti D, Bohlega S, Zoghbi HY (1997) The expansion of the CAG repeat in ataxin-2 is a frequent cause of autosomal dominant spinocerebellar ataxia. *Neurology* 49: 1009-1013.
55. Guo L, Shorter J (2016) Biology and pathobiology of TDP-43 and emergent therapeutic strategies. *Cold Spring Harb Perspect Med*: a024554.
56. Neumann M, Sampathu DM, Kwong LK, Truax AC, Micsenyi MC, et al. (2006) Ubiquitinated TDP-43 in frontotemporal lobar degeneration and amyotrophic lateral sclerosis. *Science* 314: 130-133.

57. Ling SC, Polymenidou M, Cleveland DW (2013) Converging mechanisms in ALS and FTD: disrupted RNA and protein homeostasis. *Neuron* 79: 416-438.
58. Polymenidou M, Lagier-Tourenne C, Hutt KR, Bennett CF, Cleveland DW, et al. (2012) Misregulated RNA processing in amyotrophic lateral sclerosis. *Brain research* 1462: 3-15.
59. Bhardwaj A, Myers MP, Buratti E, Baralle FE (2013) Characterizing TDP-43 interaction with its RNA targets. *Nucleic Acids Research* 41: 5062-5074.
60. Lukavsky PJ, Daujotyte D, Tollervey JR, Ule J, Stuani C, et al. (2013) Molecular basis of UG-rich RNA recognition by the human splicing factor TDP-43. *Nat Struct Mol Biol* 20: 1443-1449.
61. Polymenidou M, Lagier-Tourenne C, Hutt KR, Huelga SC, Moran J, et al. (2011) Long pre-mRNA depletion and RNA missplicing contribute to neuronal vulnerability from loss of TDP-43. *Nat Neurosci* 14: 459-468.
62. Tollervey JR, Curk T, Rogelj B, Briese M, Cereda M, et al. (2011) Characterizing the RNA targets and position-dependent splicing regulation by TDP-43. *Nat Neurosci* 14: 452-458.
63. Ling JP, Pletnikova O, Troncoso JC, Wong PC (2015) TDP-43 repression of nonconserved cryptic exons is compromised in ALS-FTD. *Science* 349: 650-655.
64. Wider C, Dickson DW, Jon Stoessel A, Tsuboi Y, Chapon F, et al. (2009) Pallidonigral TDP-43 pathology in Perry syndrome. *Parkinsonism & related disorders* 15: 281-286.
65. Kabashi E, Valdmanis PN, Dion P, Spiegelman D, McConkey BJ, et al. (2008) TARDBP mutations in individuals with sporadic and familial amyotrophic lateral sclerosis. *Nat Genet* 40: 572-574.
66. Pesiridis GS, Lee VM, Trojanowski JQ (2009) Mutations in TDP-43 link glycine-rich domain functions to amyotrophic lateral sclerosis. *Hum Mol Genet* 18: R156-162.
67. Rutherford NJ, Zhang Y, Baker M, Gass JM, Finch NA, et al. (2008) Novel mutations in TARDBP (TDP-43) in patients with familial amyotrophic lateral sclerosis. *PLoS Genet* 4: e1000193.
68. Sreedharan J, Blair IP, Tripathi VB, Hu X, Vance C, et al. (2008) TDP-43 mutations in familial and sporadic amyotrophic lateral sclerosis. *Science* 319: 1668-1672.
69. Van Deerlin VM, Leverenz JB, Bekris LM, Bird TD, Yuan W, et al. (2008) TARDBP mutations in amyotrophic lateral sclerosis with TDP-43 neuropathology: a genetic and histopathological analysis. *Lancet Neurol* 7: 409-416.
70. Borroni B, Bonvicini C, Alberici A, Buratti E, Agosti C, et al. (2009) Mutation within TARDBP leads to frontotemporal dementia without motor neuron disease. *Hum Mutat* 30: E974-983.
71. Floris G, Borghero G, Cannas A, Di Stefano F, Murru MR, et al. (2015) Clinical phenotypes and radiological findings in frontotemporal dementia related to TARDBP mutations. *J Neurol* 262: 375-384.
72. Lagier-Tourenne C, Polymenidou M, Cleveland DW (2010) TDP-43 and FUS/TLS: emerging roles in RNA processing and neurodegeneration. *Hum Mol Genet* 19: R46-64.
73. Kawahara Y, Mieda-Sato A (2012) TDP-43 promotes microRNA biogenesis as a component of the Drosha and Dicer complexes. *Proc Natl Acad Sci USA* 109: 3347-3352.

74. Buratti E, Brindisi A, Giombi M, Tisminetzky S, Ayala YM, et al. (2005) TDP-43 binds heterogeneous nuclear ribonucleoprotein A/B through its C-terminal tail: an important region for the inhibition of cystic fibrosis transmembrane conductance regulator exon 9 splicing. *J Biol Chem* 280: 37572-37584.
75. D'Ambrogio A, Buratti E, Stuani C, Guarnaccia C, Romano M, et al. (2009) Functional mapping of the interaction between TDP-43 and hnRNP A2 in vivo. *Nucleic Acids Research* 37: 4116-4126.
76. Bentmann E, Neumann M, Tahirovic S, Rodde R, Dormann D, et al. (2012) Requirements for stress granule recruitment of fused in sarcoma (FUS) and TAR DNA-binding protein of 43 kDa (TDP-43). *J Biol Chem* 287: 23079-23094.
77. Ash PE, Zhang YJ, Roberts CM, Saldi T, Hutter H, et al. (2010) Neurotoxic effects of TDP-43 overexpression in *C. elegans*. *Hum Mol Genet* 19: 3206-3218.
78. Johnson BS, McCaffery JM, Lindquist S, Gitler AD (2008) A yeast TDP-43 proteinopathy model: Exploring the molecular determinants of TDP-43 aggregation and cellular toxicity. *Proc Natl Acad Sci USA* 105: 6439-6444.
79. Johnson BS, Snead D, Lee JJ, McCaffery JM, Shorter J, et al. (2009) TDP-43 is intrinsically aggregation-prone, and amyotrophic lateral sclerosis-linked mutations accelerate aggregation and increase toxicity. *J Biol Chem* 284: 20329-20339.
80. Saini A, Chauhan VS (2011) Delineation of the core aggregation sequences of TDP-43 C-terminal fragment. *Chembiochem* 12: 2495-2501.
81. Elden AC, Kim HJ, Hart MP, Chen-Plotkin AS, Johnson BS, et al. (2010) Ataxin-2 intermediate-length polyglutamine expansions are associated with increased risk for ALS. *Nature* 466: 1069-1075.
82. Voigt A, Herholz D, Fiesel FC, Kaur K, Müller D, et al. (2010) TDP-43-mediated neuron loss *in vivo* requires RNA-binding activity. *PLoS ONE* 5: e12247.
83. Peters OM, Ghasemi M, Brown RH, Jr. (2015) Emerging mechanisms of molecular pathology in ALS. *J Clin Invest* 125: 2548.
84. Benajiba L, Le Ber I, Camuzat A, Lacoste M, Thomas-Anterion C, et al. (2009) TARDBP mutations in motoneuron disease with frontotemporal lobar degeneration. *Ann Neurol* 65: 470-473.
85. Borroni B, Archetti S, Del Bo R, Papetti A, Buratti E, et al. (2010) TARDBP mutations in frontotemporal lobar degeneration: frequency, clinical features, and disease course. *Rejuvenation Res* 13: 509-517.
86. Chiò A, Calvo A, Moglia C, Restagno G, Ossola I, et al. (2010) Amyotrophic lateral sclerosis-frontotemporal lobar dementia in 3 families with p.Ala382Thr TARDBP mutations. *Arch Neurol* 67: 1002-1009.
87. Driver-Dunckley E, Connor D, Hentz J, Sabbagh M, Silverberg N, et al. (2009) No evidence for cognitive dysfunction or depression in patients with mild restless legs syndrome. *Mov Disord* 24: 1840-1842.
88. Millecamps S, Salachas F, Cazeneuve C, Gordon P, Bricka B, et al. (2010) SOD1, ANG, VAPB, TARDBP, and FUS mutations in familial amyotrophic lateral sclerosis: genotype-phenotype correlations. *J Med Genet* 47: 554-560.
89. Moreno F, Rabinovici GD, Karydas A, Miller Z, Hsu SC, et al. (2015) A novel mutation P112H in the TARDBP gene associated with frontotemporal lobar degeneration without motor neuron disease and abundant neuritic amyloid plaques. *Acta Neuropathol Commun* 3: 19.

90. Soong BW, Lin KP, Guo YC, Lin CC, Tsai PC, et al. (2014) Extensive molecular genetic survey of Taiwanese patients with amyotrophic lateral sclerosis. *Neurobiol Aging* 35: 2423 e2421-2426.
91. Winton MJ, Van Deerlin VM, Kwong LK, Yuan W, Wood EM, et al. (2008) A90V TDP-43 variant results in the aberrant localization of TDP-43 in vitro. *FEBS Lett* 582: 2252-2256.
92. Chiang HH, Andersen PM, Tysnes OB, Gredal O, Christensen PB, et al. (2012) Novel TARDBP mutations in Nordic ALS patients. *J Hum Genet* 57: 316-319.
93. Cady J, Allred P, Bali T, Pestronk A, Goate A, et al. (2015) Amyotrophic lateral sclerosis onset is influenced by the burden of rare variants in known amyotrophic lateral sclerosis genes. *Ann Neurol* 77: 100-113.
94. Cirulli ET, Lasseigne BN, Petrovski S, Sapp PC, Dion PA, et al. (2015) Exome sequencing in amyotrophic lateral sclerosis identifies risk genes and pathways. *Science* 347: 1436-1441.
95. Lek M, Karczewski KJ, Minikel EV, Samocha KE, Banks E, et al. (2016) Analysis of protein-coding genetic variation in 60,706 humans. *Nature* 536: 285-291.
96. Quadri M, Cossu G, Saddi V, Simons EJ, Murgia D, et al. (2011) Broadening the phenotype of TARDBP mutations: the TARDBP Ala382Thr mutation and Parkinson's disease in Sardinia. *Neurogenetics* 12: 203-209.
97. Buratti E (2015) Chapter One - Functional significance of TDP-43 mutations in disease. In: Friedmann T, Dunlap JC, Goodwin SF, editors. *Advances in Genetics*: Academic Press. pp. 1-53.
98. Abel O, Shatunov A, Jones AR, Andersen PM, Powell JF, et al. (2013) Development of a smartphone app for a genetics website: The Amyotrophic Lateral Sclerosis Online Genetics Database (ALSoD). *JMIR Mhealth Uhealth* 1: e18.
99. Ju S, Tardiff DF, Han H, Divya K, Zhong Q, et al. (2011) A yeast model of FUS/TLS-dependent cytotoxicity. *PLoS Biol* 9: e1001052.
100. Schwartz JC, Cech TR, Parker RR (2015) Biochemical properties and biological functions of FET proteins. *Annu Rev Biochem* 84: 355-379.
101. Qiu H, Lee S, Shang Y, Wang WY, Au KF, et al. (2014) ALS-associated mutation FUS-R521C causes DNA damage and RNA splicing defects. *J Clin Invest* 124: 981-999.
102. Corrado L, Del Bo R, Castellotti B, Ratti A, Cereda C, et al. (2010) Mutations of FUS gene in sporadic amyotrophic lateral sclerosis. *J Med Genet* 47: 190-194.
103. Kwiatkowski TJ, Bosco DA, LeClerc AL, Tamrazian E, Vanderburg CR, et al. (2009) Mutations in the FUS/TLS gene on chromosome 16 cause familial amyotrophic lateral sclerosis. *Science* 323: 1205-1208.
104. Rademakers R, Stewart H, DeJesus-Hernandez M, Krieger C, Graff-Radford N, et al. (2010) Fus gene mutations in familial and sporadic amyotrophic lateral sclerosis. *Muscle Nerve* 42: 170-176.
105. Vance C, Rogelj B, Hortobagyi T, De Vos KJ, Nishimura AL, et al. (2009) Mutations in FUS, an RNA processing protein, cause familial amyotrophic lateral sclerosis type 6. *Science* 323: 1208-1211.
106. Fecto F, Siddique T (2011) Making connections: pathology and genetics link amyotrophic lateral sclerosis with frontotemporal lobe dementia. *J Mol Neurosci* 45: 663-675.

107. Neumann M, Rademakers R, Roeber S, Baker M, Kretzschmar HA, et al. (2009) A new subtype of frontotemporal lobar degeneration with FUS pathology. *Brain* 132: 2922-2931.
108. Neumann M, Roeber S, Kretzschmar HA, Rademakers R, Baker M, et al. (2009) Abundant FUS-immunoreactive pathology in neuronal intermediate filament inclusion disease. *Acta Neuropathol* 118: 605-616.
109. Seelaar H, Klijnsma KY, de Koning I, van der Lugt A, Chiu WZ, et al. (2010) Frequency of ubiquitin and FUS-positive, TDP-43-negative frontotemporal lobar degeneration. *J Neurol* 257: 747-753.
110. Sun Z, Diaz Z, Fang X, Hart MP, Chesi A, et al. (2011) Molecular determinants and genetic modifiers of aggregation and toxicity for the ALS disease protein FUS/TLS. *PLoS Biol* 9: e1000614.
111. Urwin H, Josephs KA, Rohrer JD, Mackenzie IR, Neumann M, et al. (2010) FUS pathology defines the majority of tau- and TDP-43-negative frontotemporal lobar degeneration. *Acta Neuropathol* 120: 33-41.
112. Dormann D, Rodde R, Edbauer D, Bentmann E, Fischer I, et al. (2010) ALS-associated fused in sarcoma (FUS) mutations disrupt Transportin-mediated nuclear import. *EMBO J* 29: 2841-2857.
113. Daigle JG, Lanson NA, Jr., Smith RB, Casci I, Maltare A, et al. (2013) RNA-binding ability of FUS regulates neurodegeneration, cytoplasmic mislocalization and incorporation into stress granules associated with FUS carrying ALS-linked mutations. *Hum Mol Genet* 22: 1193-1205.
114. Sun S, Ling SC, Qiu J, Albuquerque CP, Zhou Y, et al. (2015) ALS-causative mutations in FUS/TLS confer gain and loss of function by altered association with SMN and U1-snRNP. *Nat Commun* 6: 6171.
115. Lattante S, Rouleau GA, Kabashi E (2013) TARDBP and FUS mutations associated with amyotrophic lateral sclerosis: summary and update. *Hum Mutat* 34: 812-826.
116. Blair IP, Williams KL, Warraich ST, Durnall JC, Thoeng AD, et al. (2010) FUS mutations in amyotrophic lateral sclerosis: clinical, pathological, neurophysiological and genetic analysis. *J Neurol Neurosurg Psychiatry* 81: 639-645.
117. Broustal O, Camuzat A, Guillot-Noel L, Guy N, Millecamps S, et al. (2010) FUS mutations in frontotemporal lobar degeneration with amyotrophic lateral sclerosis. *J Alzheimers Dis* 22: 765-769.
118. Huey ED, Ferrari R, Moreno JH, Jensen C, Morris CM, et al. (2012) FUS and TDP43 genetic variability in FTD and CBS. *Neurobiol Aging* 33: 1016 e1019-1017.
119. Ticozzi N, Silani V, LeClerc AL, Keagle P, Gellera C, et al. (2009) Analysis of FUS gene mutation in familial amyotrophic lateral sclerosis within an Italian cohort. *Neurology* 73: 1180-1185.
120. Van Langenhove T, van der Zee J, Sleegers K, Engelborghs S, Vandenberghe R, et al. (2010) Genetic contribution of FUS to frontotemporal lobar degeneration. *Neurology* 74: 366-371.
121. Yan J, Deng HX, Siddique N, Fecto F, Chen W, et al. (2010) Frameshift and novel mutations in FUS in familial amyotrophic lateral sclerosis and ALS/dementia. *Neurology* 75: 807-814.

122. Belzil VV, Valdmanis PN, Dion PA, Daoud H, Kabashi E, et al. (2009) Mutations in FUS cause FALS and SALS in French and French Canadian populations. *Neurology* 73: 1176-1179.
123. Exome Variant Server, NHLBI GO Exome Sequencing Project, Seattle, WA (URL: <http://evs.gs.washington.edu/EVS/>).
124. Groen EJ, van Es MA, van Vught PW, Spliet WG, van Engelen-Lee J, et al. (2010) FUS mutations in familial amyotrophic lateral sclerosis in the Netherlands. *Arch Neurol* 67: 224-230.
125. Hewitt C, Kirby J, Highley JR, Hartley JA, Hibberd R, et al. (2010) Novel FUS/TLS mutations and pathology in familial and sporadic amyotrophic lateral sclerosis. *Arch Neurol* 67: 455-461.
126. Belzil VV, Daoud H, St-Onge J, Desjarlais A, Bouchard JP, et al. (2011) Identification of novel FUS mutations in sporadic cases of amyotrophic lateral sclerosis. *Amyotroph Lateral Scler* 12: 113-117.
127. Couthouis J, Hart MP, Erion R, King OD, Diaz Z, et al. (2012) Evaluating the role of the FUS/TLS-related gene EWSR1 in amyotrophic lateral sclerosis. *Hum Mol Genet* 21: 2899-2911.
128. Neumann M, Bentmann E, Dormann D, Jawaid A, DeJesus-Hernandez M, et al. (2011) FET proteins TAF15 and EWS are selective markers that distinguish FTLD with FUS pathology from amyotrophic lateral sclerosis with FUS mutations. *Brain* 134: 2595-2609.
129. Ticozzi N, Vance C, Leclerc AL, Keagle P, Glass JD, et al. (2011) Mutational analysis reveals the FUS homolog TAF15 as a candidate gene for familial amyotrophic lateral sclerosis. *Am J Med Genet B Neuropsychiatr Genet* 156B: 285-290.
130. Lee BJ, Cansizoglu AE, Süel KE, Louis TH, Zhang Z, et al. (2006) Rules for nuclear localization sequence recognition by karyopherin β 2. *Cell* 126: 543-558.
131. Zakaryan RP, Gehring H (2006) Identification and characterization of the nuclear localization/retention signal in the EWS proto-oncoprotein. *J Mol Biol* 363: 27-38.
132. Couthouis J, Raphael AR, Daneshjou R, Gitler AD (2014) Targeted exon capture and sequencing in sporadic amyotrophic lateral sclerosis. *PLoS Genet* 10: e1004704.
133. Marko M, Vlassis A, Guialis A, Leichter M (2012) Domains involved in TAF15 subcellular localisation: dependence on cell type and ongoing transcription. *Gene* 506: 331-338.
134. Kim HJ, Kim NC, Wang YD, Scarborough EA, Moore J, et al. (2013) Mutations in prion-like domains in hnRNPA2B1 and hnRNPA1 cause multisystem proteinopathy and ALS. *Nature* 495: 467-473.
135. Watts GD, Wymer J, Kovach MJ, Mehta SG, Mumm S, et al. (2004) Inclusion body myopathy associated with Paget disease of bone and frontotemporal dementia is caused by mutant valosin-containing protein. *Nat Genet* 36: 377-381.
136. Nalbandian A, Donkervoort S, Dec E, Badadani M, Katheria V, et al. (2011) The multiple faces of valosin-containing protein-associated diseases: inclusion body myopathy with Paget's disease of bone, frontotemporal dementia, and amyotrophic lateral sclerosis. *J Mol Neurosci* 45: 522-531.
137. Benatar M, Wu J, Fernandez C, Weihl CC, Katzen H, et al. (2013) Motor neuron involvement in multisystem proteinopathy. *Neurology* 80: 1874-1880.

138. Shi Z, Hayashi YK, Mitsuhashi S, Goto K, Kaneda D, et al. (2012) Characterization of the Asian myopathy patients with VCP mutations. *Eur J Neurol* 19: 501-509.
139. Chung PY, Beyens G, de Freitas F, Boonen S, Geusens P, et al. (2011) Indications for a genetic association of a VCP polymorphism with the pathogenesis of sporadic Paget's disease of bone, but not for TNFSF11 (RANKL) and IL-6 polymorphisms. *Mol Genet Metab* 103: 287-292.
140. Kim NC, Tresse E, Kolaitis RM, Molliex A, Thomas RE, et al. (2013) VCP is essential for mitochondrial quality control by PINK1/Parkin and this function is impaired by VCP mutations. *Neuron* 78: 65-80.
141. Johnson JO, Mandrioli J, Benatar M, Abramzon Y, Van Deerlin VM, et al. (2010) Exome sequencing reveals VCP mutations as a cause of familial ALS. *Neuron* 68: 857-864.
142. Buchan JR, Kolaitis R-M, Taylor JP, Parker R (2013) Eukaryotic stress granules are cleared by granulophagy and Cdc48/VCP function. *Cell* 153: 1461-1474.
143. Jean-Philippe J, Paz S, Caputi M (2013) hnRNP A1: the Swiss army knife of gene expression. *Int J Mol Sci* 14: 18999-19024.
144. Campillos M, Lamas JR, Garcia MA, Bullido MJ, Valdivieso F, et al. (2003) Specific interaction of heterogeneous nuclear ribonucleoprotein A1 with the -219T allelic form modulates APOE promoter activity. *Nucleic Acids Res* 31: 3063-3070.
145. Hay DC, Kemp GD, Dargemont C, Hay RT (2001) Interaction between hnRNPA1 and I κ B α is required for maximal activation of NF- κ B-dependent transcription. *Mol Cell Biol* 21: 3482-3490.
146. Xia H (2005) Regulation of gamma-fibrinogen chain expression by heterogeneous nuclear ribonucleoprotein A1. *J Biol Chem* 280: 13171-13178.
147. Han Siew P, Tang Yue H, Smith R (2010) Functional diversity of the hnRNPs: past, present and perspectives. *Biochemical Journal* 430: 379-392.
148. Huelga SC, Vu AQ, Arnold JD, Liang TY, Liu PP, et al. (2012) Integrative genome-wide analysis reveals cooperative regulation of alternative splicing by hnRNP proteins. *Cell Rep* 1: 167-178.
149. Barreau C, Paillard L, Osborne HB (2005) AU-rich elements and associated factors: are there unifying principles? *Nucleic Acids Res* 33: 7138-7150.
150. Bonnal S, Pileur F, Orsini C, Parker F, Pujol F, et al. (2005) Heterogeneous nuclear ribonucleoprotein A1 is a novel internal ribosome entry site trans-acting factor that modulates alternative initiation of translation of the fibroblast growth factor 2 mRNA. *J Biol Chem* 280: 4144-4153.
151. Cammas A, Pileur F, Bonnal S, Lewis SM, Leveque N, et al. (2007) Cytoplasmic relocalization of heterogeneous nuclear ribonucleoprotein A1 controls translation initiation of specific mRNAs. *Mol Biol Cell* 18: 5048-5059.
152. LaBranche H, Dupuis S, Ben-David Y, Bani M-R, Wellinger RJ, et al. (1998) Telomere elongation by hnRNP A1 and a derivative that interacts with telomeric repeats and telomerase. *Nat Genet* 19: 199-202.
153. Guil S, Caceres JF (2007) The multifunctional RNA-binding protein hnRNP A1 is required for processing of miR-18a. *Nat Struct Mol Biol* 14: 591-596.
154. Michlewski G, Caceres JF (2010) Antagonistic role of hnRNP A1 and KSRP in the regulation of let-7a biogenesis. *Nat Struct Mol Biol* 17: 1011-1018.

155. Goina E, Skoko N, Pagani F (2008) Binding of DAZAP1 and hnRNPA1/A2 to an exonic splicing silencer in a natural BRCA1 exon 18 mutant. *Mol Cell Biol* 28: 3850-3860.
156. Martinez-Contreras R, Cloutier P, Shkreta L, Fiset JF, Revil T, et al. (2007) hnRNP proteins and splicing control. *Adv Exp Med Biol* 623: 123-147.
157. Martinez FJ, Pratt GA, Van Nostrand EL, Batra R, Huelga SC, et al. (2016) Protein-RNA networks regulated by normal and ALS-associated mutant hnRNPA2B1 in the nervous system. *Neuron* 92: 780-795.
158. Moran-Jones K, Wayman L, Kennedy DD, Reddel RR, Sara S, et al. (2005) hnRNP A2, a potential ssDNA/RNA molecular adapter at the telomere. *Nucleic Acids Res* 33: 486-496.
159. Tanaka E, Fukuda H, Nakashima K, Tsuchiya N, Seimiya H, et al. (2007) HnRNP A3 binds to and protects mammalian telomeric repeats in vitro. *Biochem Biophys Res Commun* 358: 608-614.
160. Hoek KS, Kidd GJ, Carson JH, Smith R (1998) hnRNP A2 selectively binds the cytoplasmic transport sequence of myelin basic protein mRNA. *Biochemistry* 37: 7021-7029.
161. Shan J, Munro TP, Barbarese E, Carson JH, Smith R (2003) A molecular mechanism for mRNA trafficking in neuronal dendrites. *J Neurosci* 23: 8859-8866.
162. Mitchell J, Paul P, Chen HJ, Morris A, Payling M, et al. (2010) Familial amyotrophic lateral sclerosis is associated with a mutation in D-amino acid oxidase. *Proc Natl Acad Sci USA* 107: 7556-7561.
163. Sasabe J, Miyoshi Y, Suzuki M, Mita M, Konno R, et al. (2012) D-amino acid oxidase controls motoneuron degeneration through D-serine. *Proc Natl Acad Sci USA* 109: 627-632.
164. Goldschmidt L, Teng PK, Riek R, Eisenberg D (2010) Identifying the amyloids, proteins capable of forming amyloid-like fibrils. *Proc Natl Acad Sci USA* 107: 3487-3492.
165. Paul KR, Molliex A, Cascarina S, Boncella AE, Taylor JP, et al. (2017) The effects of mutations on the aggregation propensity of the human prion-like protein hnRNPA2B1. *Mol Cell Biol*.
166. Thandapani P, O'Connor TR, Bailey TL, Richard S (2013) Defining the RGG/RG motif. *Mol Cell* 50: 613-623.
167. Jean-Philippe J, Paz S, Lu ML, Caputi M (2014) A truncated hnRNP A1 isoform, lacking the RGG-box RNA binding domain, can efficiently regulate HIV-1 splicing and replication. *Biochim Biophys Acta* 1839: 251-258.
168. Liu Q, Shu S, Wang RR, Liu F, Cui B, et al. (2016) Whole-exome sequencing identifies a missense mutation in hnRNPA1 in a family with flail arm ALS. *Neurology* 87: 1763-1769.
169. Salajegheh M, Pinkus JL, Taylor JP, Amato AA, Nazareno R, et al. (2009) Sarcoplasmic redistribution of nuclear TDP-43 in inclusion body myositis. *Muscle Nerve* 40: 19-31.
170. Pinkus JL, Amato AA, Taylor JP, Greenberg SA (2014) Abnormal distribution of heterogeneous nuclear ribonucleoproteins in sporadic inclusion body myositis. *Neuromuscul Disord* 24: 611-616.

171. Neumann M, Igaz LM, Kwong LK, Nakashima-Yasuda H, Kolb SJ, et al. (2007) Absence of heterogeneous nuclear ribonucleoproteins and survival motor neuron protein in TDP-43 positive inclusions in frontotemporal lobar degeneration. *Acta Neuropathologica* 113: 543-548.
172. Anderson P, Kedersha N (2008) Stress granules: the Tao of RNA triage. *Trends Biochem Sci* 33: 141-150.
173. Bosco DA, Lemay N, Ko HK, Zhou H, Burke C, et al. (2010) Mutant FUS proteins that cause amyotrophic lateral sclerosis incorporate into stress granules. *Hum Mol Genet* 19: 4160-4175.
174. Buchan JR, Parker R (2009) Eukaryotic stress granules: the ins and outs of translation. *Mol Cell* 36: 932-941.
175. Wolozin B (2012) Regulated protein aggregation: stress granules and neurodegeneration. *Mol Neurodegener* 7: 56-68.
176. Kedersha N, Stoecklin G, Ayodele M, Yacono P, Lykke-Andersen J, et al. (2005) Stress granules and processing bodies are dynamically linked sites of mRNP remodeling. *J Cell Biol* 169: 871-884.
177. Jain S, Parker R (2013) The discovery and analysis of P bodies. In: Chan EKL, Fritzler MJ, editors. *Ten Years of Progress in GW/P Body Research*. New York, NY: Springer New York. pp. 23-43.
178. Guo L, Shorter J (2015) It's raining liquids: RNA tunes viscoelasticity and dynamics of membraneless organelles. *Mol Cell* 60: 189-192.
179. Mayeda A, Munroe SH, Cáceres JF, Krainer AR (1994) Function of conserved domains of hnRNP A1 and other hnRNP A/B proteins. *EMBO J* 13: 5483-5495.
180. Siomi H, Dreyfuss G (1995) A nuclear localization domain in the hnRNP A1 protein. *J Cell Biol* 129: 551-560.
181. Burke KA, Janke AM, Rhine CL, Fawzi NL (2015) Residue-by-residue view of in vitro FUS granules that bind the C-terminal domain of RNA polymerase II. *Mol Cell* 60: 231-241.
182. Liu-Yesucevitz L, Bilgutay A, Zhang YJ, Vanderweyde T, Citro A, et al. (2010) Tar DNA binding protein-43 (TDP-43) associates with stress granules: analysis of cultured cells and pathological brain tissue. *PLoS ONE* 5: e13250.
183. Gilks N, Kedersha N, Ayodele M, Shen L, Stoecklin G, et al. (2004) Stress granule assembly is mediated by prion-like aggregation of TIA-1. *Mol Biol Cell* 15: 5383-5398.
184. Reijns MA, Alexander RD, Spiller MP, Beggs JD (2008) A role for Q/N-rich aggregation-prone regions in P-body localization. *J Cell Sci* 121: 2463-2472.
185. Seydoux G, Braun RE (2006) Pathway to totipotency: lessons from germ cells. *Cell* 127: 891-904.
186. Hennig S, Kong G, Mannen T, Sadowska A, Kobelke S, et al. (2015) Prion-like domains in RNA binding proteins are essential for building subnuclear paraspeckles. *J Cell Biol* 210: 529-539.
187. Mannen T, Yamashita S, Tomita K, Goshima N, Hirose T (2016) The Sam68 nuclear body is composed of two RNase-sensitive substructures joined by the adaptor HNRNPL. *J Cell Biol* 214: 45-59.
188. Boke E, Mitchison TJ (2017) The balbiani body and the concept of physiological amyloids. *Cell Cycle* 16: 153-154.

189. Boke E, Ruer M, Wuhr M, Coughlin M, Lemaitre R, et al. (2016) Amyloid-like self-assembly of a cellular compartment. *Cell* 166: 637-650.
190. Ford AF, Shorter J (2015) Fleeting amyloid-like forms of Rim4 ensure meiotic fidelity. *Cell* 163: 275-276.
191. Berchowitz LE, Kabachinski G, Walker MR, Carlile TM, Gilbert WV, et al. (2015) Regulated formation of an amyloid-like translational repressor governs gametogenesis. *Cell* 163: 406-418.
192. Ritz AM, Trautwein M, Grassinger F, Spang A (2014) The prion-like domain in the exomer-dependent cargo Pin2 serves as a trans-Golgi retention motif. *Cell Rep* 7: 249-260.
193. Gal J, Zhang J, Kwinter DM, Zhai J, Jia H, et al. (2011) Nuclear localization sequence of FUS and induction of stress granules by ALS mutants. *Neurobiol Aging* 32: 2323 e2327-2340.
194. Lenzi J, De Santis R, de Turreis V, Morlando M, Laneve P, et al. (2015) ALS mutant FUS proteins are recruited into stress granules in induced pluripotent stem cell-derived motoneurons. *Dis Model Mech* 8: 755-766.
195. Kim HJ, Raphael AR, LaDow ES, McGurk L, Weber RA, et al. (2014) Therapeutic modulation of eIF2alpha phosphorylation rescues TDP-43 toxicity in amyotrophic lateral sclerosis disease models. *Nat Genet* 46: 152-160.
196. Swisher KD, Parker R (2010) Localization to, and effects of Pbp1, Pbp4, Lsm12, Dhh1 and Pab1 on stress granules in *Saccharomyces cerevisiae*. *PLoS ONE* 5: e10006.
197. Daoud H, Belzil V, Martins S, et al. (2011) Association of long atxn2 cag repeat sizes with increased risk of amyotrophic lateral sclerosis. *Archives of Neurology* 68: 739-742.
198. Lu HP, Gan SR, Chen S, Li HF, Liu ZJ, et al. (2015) Intermediate-length polyglutamine in ATXN2 is a possible risk factor among Eastern Chinese patients with amyotrophic lateral sclerosis. *Neurobiol Aging* 36: 1603 e1611-1604.
199. Ross OA, Rutherford NJ, Baker M, Soto-Ortolaza AI, Carrasquillo MM, et al. (2011) Ataxin-2 repeat-length variation and neurodegeneration. *Hum Mol Genet* 20: 3207-3212.
200. Mitchell SF, Jain S, She M, Parker R (2013) Global analysis of yeast mRNPs. *Nat Struct Mol Biol* 20: 127-133.
201. Segal SP, Dunckley T, Parker R (2006) Sbp1p affects translational repression and decapping in *Saccharomyces cerevisiae*. *Mol Cell Biol* 26: 5120-5130.
202. Beggs JD (2005) Lsm proteins and RNA processing. *Biochemical Society Transactions* 33: 433-438.
203. Chowdhury A, Mukhopadhyay J, Tharun S (2007) The decapping activator Lsm1p-7p-Pat1p complex has the intrinsic ability to distinguish between oligoadenylated and polyadenylated RNAs. *RNA* 13: 998-1016.
204. He W, Parker R (2001) The yeast cytoplasmic Lsm1/Pat1p complex protects mRNA 3' termini from partial degradation. *Genetics* 158: 1445-1455.
205. Luhtala N, Parker R (2009) LSM1 over-expression in *Saccharomyces cerevisiae* depletes U6 snRNA levels. *Nucleic Acids Res* 37: 5529-5536.
206. Pannone BK, Kim SD, Noe DA, Wolin SL (2001) Multiple functional interactions between components of the Lsm2-Lsm8 complex, U6 snRNA, and the yeast La protein. *Genetics* 158: 187-196.

207. Kufel J, Bousquet-Antonelli C, Beggs JD, Tollervey D (2004) Nuclear pre-mRNA decapping and 5' degradation in yeast require the Lsm2-8p complex. *Mol Cell Biol* 24: 9646-9657.
208. Buchan JR, Muhlrad D, Parker R (2008) P bodies promote stress granule assembly in *Saccharomyces cerevisiae*. *The Journal of Cell Biology* 183: 441-455.
209. Kedersha N, Anderson P (2009) Chapter 4 Regulation of translation by stress granules and processing bodies. In: Hershey JWB, editor. *Prog Mol Biol Transl Sci*: Academic Press. pp. 155-185.
210. Nonhoff U, Ralser M, Welzel F, Piccini I, Balzereit D, et al. (2007) Ataxin-2 interacts with the DEAD/H-box RNA helicase DDX6 and interferes with P-bodies and stress granules. *Mol Biol Cell* 18: 1385-1396.
211. Hackman P, Sarparanta J, Lehtinen S, Vihola A, Evilä A, et al. (2013) Welander distal myopathy is caused by a mutation in the RNA-binding protein TIA1. *Annals of Neurology* 73: 500-509.
212. Klar J, Sobol M, Melberg A, Mabert K, Ameer A, et al. (2013) Welander distal myopathy caused by an ancient founder mutation in TIA1 associated with perturbed splicing. *Hum Mutat* 34: 572-577.
213. Elbaum-Garfinkle S, Brangwynne CP (2015) Liquids, fibers, and gels: the many phases of neurodegeneration. *Dev Cell* 35: 531-532.
214. Shorter J (2016) Membraneless organelles: phasing in and out. *Nat Chem* 8: 528-530.
215. Shin Y, Berry J, Pannucci N, Haataja MP, Toettcher JE, et al. (2017) Spatiotemporal control of intracellular phase transitions using light-activated optodroplets. *Cell* 168: 159-171 e114.
216. Brangwynne CP, Eckmann CR, Courson DS, Rybarska A, Hoesge C, et al. (2009) Germline P granules are liquid droplets that localize by controlled dissolution/condensation. *Science* 324: 1729-1732.
217. Kroschwald S, Maharana S, Mateju D, Malinowska L, Nuske E, et al. (2015) Promiscuous interactions and protein disaggregases determine the material state of stress-inducible RNP granules. *eLife* 4: e06807.
218. Banani SF, Rice AM, Peeples WB, Lin Y, Jain S, et al. (2016) Compositional control of phase-separated cellular bodies. *Cell* 166: 651-663.
219. Hyman AA, Weber CA, Julicher F (2014) Liquid-liquid phase separation in biology. *Annu Rev Cell Dev Biol* 30: 39-58.
220. Nott TJ, Craggs TD, Baldwin AJ (2016) Membraneless organelles can melt nucleic acid duplexes and act as biomolecular filters. *Nat Chem* 8: 569-575.
221. Brangwynne CP, Tompa P, Pappu RV (2015) Polymer physics of intracellular phase transitions. *Nat Phys* 11: 899-904.
222. Molliex A, Temirov J, Lee J, Coughlin M, Kanagaraj AP, et al. (2015) Phase separation by low complexity domains promotes stress granule assembly and drives pathological fibrillization. *Cell* 163: 123-133.
223. Nott TJ, Petsalaki E, Farber P, Jervis D, Fussner E, et al. (2015) Phase transition of a disordered nuage protein generates environmentally responsive membraneless organelles. *Mol Cell* 57: 936-947.
224. Kato M, Han TW, Xie S, Shi K, Du X, et al. (2012) Cell-free formation of RNA granules: low complexity sequence domains form dynamic fibers within hydrogels. *Cell* 149: 753-767.

225. Murakami T, Qamar S, Lin JQ, Schierle GS, Rees E, et al. (2015) ALS/FTD mutation-induced phase transition of FUS liquid droplets and reversible hydrogels into irreversible hydrogels impairs RNP granule function. *Neuron* 88: 678-690.
226. Jain S, Wheeler JR, Walters RW, Agrawal A, Barsic A, et al. (2016) ATPase-modulated stress granules contain a diverse proteome and substructure. *Cell* 164: 487-498.
227. Patel A, Lee HO, Jawerth L, Maharana S, Jahnel M, et al. (2015) A liquid-to-solid phase transition of the ALS protein FUS accelerated by disease mutation. *Cell* 162: 1066-1077.
228. DeJesus-Hernandez M, Mackenzie IR, Boeve BF, Boxer AL, Baker M, et al. (2011) Expanded GGGGCC hexanucleotide repeat in noncoding region of C9ORF72 causes chromosome 9p-linked FTD and ALS. *Neuron* 72: 245-256.
229. Lee K-H, Zhang P, Kim Hong J, Mitrea DM, Sarkar M, et al. (2016) C9orf72 dipeptide repeats impair the assembly, dynamics, and function of membrane-less organelles. *Cell* 167: 774-788.e717.
230. Lin Y, Mori E, Kato M, Xiang S, Wu L, et al. (2016) Toxic PR poly-dipeptides encoded by the C9orf72 repeat expansion target LC domain polymers. *Cell* 167: 789-802.e712.
231. Vashist S, Cushman M, Shorter J (2010) Applying Hsp104 to protein-misfolding disorders. *Biochem Cell Biol* 88: 1-13.
232. Sweeny EA, Shorter J (2008) Prion proteostasis: Hsp104 meets its supporting cast. *Prion* 2: 135-140.
233. Sweeny EA, Shorter J (2016) Mechanistic and structural insights into the prion-disaggregase activity of Hsp104. *J Mol Biol* 428: 1870-1885.
234. Jackrel ME, Shorter J (2014) Potentiated Hsp104 variants suppress toxicity of diverse neurodegenerative disease-linked proteins. *Dis Model Mech* 7: 1175-1184.
235. Jackrel ME, DeSantis ME, Martinez BA, Castellano LM, Stewart RM, et al. (2014) Potentiated Hsp104 variants antagonize diverse proteotoxic misfolding events. *Cell* 156: 170-182.
236. Halfmann R, Jarosz DF, Jones SK, Chang A, Lancaster AK, et al. (2012) Prions are a common mechanism for phenotypic inheritance in wild yeasts. *Nature* 482: 363-368.
237. Shorter J, Lindquist S (2004) Hsp104 catalyzes formation and elimination of self-replicating Sup35 prion conformers. *Science* 304: 1793-1797.
238. DeSantis ME, Leung EH, Sweeny EA, Jackrel ME, Cushman-Nick M, et al. (2012) Operational plasticity enables hsp104 to disaggregate diverse amyloid and nonamyloid clients. *Cell* 151: 778-793.
239. DeSantis ME, Shorter J (2012) Hsp104 drives "protein-only" positive selection of Sup35 prion strains encoding strong [PSI(+)]. *Chem Biol* 19: 1400-1410.
240. Vacher C, Garcia-Oroz L, Rubinsztein DC (2005) Overexpression of yeast hsp104 reduces polyglutamine aggregation and prolongs survival of a transgenic mouse model of Huntington's disease. *Hum Mol Genet* 14: 3425-3433.
241. Jackrel ME, Shorter J (2014) Reversing deleterious protein aggregation with re-engineered protein disaggregases. *Cell Cycle* 13: 1379-1383.

242. Jackrel ME, Shorter J (2015) Engineering enhanced protein disaggregases for neurodegenerative disease. *Prion* 9: 90-109.
243. Jackrel ME, Yee K, Tariq A, Chen AI, Shorter J (2015) Disparate mutations confer therapeutic gain of Hsp104 function. *ACS Chem Biol* 10: 2672-2679.
244. Shorter J (2011) The mammalian disaggregase machinery: Hsp110 synergizes with Hsp70 and Hsp40 to catalyze protein disaggregation and reactivation in a cell-free system. *PLoS ONE* 6: e26319.
245. Torrente MP, Shorter J (2013) The metazoan protein disaggregase and amyloid depolymerase system: Hsp110, Hsp70, Hsp40, and small heat shock proteins. *Prion* 7: 457-463.
246. Duennwald ML, Echeverria A, Shorter J (2012) Small heat shock proteins potentiate amyloid dissolution by protein disaggregases from yeast and humans. *PLoS Biol* 10: e1001346.
247. Poepsel S, Sprengel A, Sacca B, Kaschani F, Kaiser M, et al. (2015) Determinants of amyloid fibril degradation by the PDZ protease HTRA1. *Nat Chem Biol* 11: 862-869.
248. Ali YO, Allen HM, Yu L, Li-Kroeger D, Bakhshizadehmahmoudi D, et al. (2016) NMNAT2:HSP90 complex mediates proteostasis in proteinopathies. *PLoS Biol* 14: e1002472.
249. Shorter J (2016) Engineering therapeutic protein disaggregases. *Mol Biol Cell* 27: 1556-1560.
250. Foury F (1997) Human genetic diseases: a cross-talk between man and yeast. *Gene* 195: 1-10.
251. Armakola M, Higgins MJ, Figley MD, Barmada SJ, Scarborough EA, et al. (2012) Inhibition of RNA lariat debranching enzyme suppresses TDP-43 toxicity in ALS disease models. *Nat Genet* 44: 1302-1309.
252. Trojanowski JQ (2008) PENN neurodegenerative disease research – in the spirit of Benjamin Franklin. *Neurosignals* 16: 5-10.
253. Spillantini MG, Schmidt ML, Lee VMY, Trojanowski JQ, Jakes R, et al. (1997) [alpha]-Synuclein in Lewy bodies. *Nature* 388: 839-840.
254. Gitler AD, Bevis BJ, Shorter J, Strathearn KE, Hamamichi S, et al. (2008) The Parkinson's disease protein alpha-synuclein disrupts cellular Rab homeostasis. *Proc Natl Acad Sci USA* 105: 145-150.
255. Meriin AB, Zhang X, He X, Newnam GP, Chernoff YO, et al. (2002) Huntington toxicity in yeast model depends on polyglutamine aggregation mediated by a prion-like protein Rnq1. *J Cell Biol* 157: 997-1004.
256. Outeiro TF, Lindquist S (2003) Yeast cells provide insight into alpha-synuclein biology and pathobiology. *Science* 302: 1772-1775.
257. Treusch S, Hamamichi S, Goodman JL, Matlack KES, Chung CY, et al. (2011) Functional links between A β toxicity, endocytic trafficking and Alzheimer's disease risk factors in yeast. *Science* 334: 1241-1245.
258. Shorter J, Taylor JP (2013) Disease mutations in the prion-like domains of hnRNP A1 and hnRNP A2/B1 introduce potent steric zippers that drive excess RNP granule assembly. *Rare Diseases* 1: e25200.
259. Burd CG, Dreyfuss G (1994) RNA binding specificity of hnRNP A1: significance of hnRNP A1 high-affinity binding sites in pre-mRNA splicing. *EMBO J* 13: 1197-1204.

260. Mayeda A, Munroe SH, Xu RM, Krainer AR (1998) Distinct functions of the closely related tandem RNA-recognition motifs of hnRNP A1. *RNA* 4: 1111-1123.
261. Cobianchi F, Karpel RL, Williams KR, Notario V, Wilson SH (1988) Mammalian heterogeneous nuclear ribonucleoprotein complex protein A1. *J Biol Chem* 263: 1063-1071.
262. Süel KE, Gu H, Chook YM (2008) Modular organization and combinatorial energetics of proline-tyrosine nuclear localization signals. *PLoS Biol* 6: e137.
263. Truant R, Fridell RA, Benson RE, Bogerd H, Cullen BR (1998) Identification and functional characterization of a novel nuclear localization signal present in the yeast Nab2 poly(A)(+) RNA binding protein. *Mol Cell Biol* 18: 1449-1458.
264. Kryndushkin DS, Alexandrov IM, Ter-Avanesyan MD, Kushnirov VV (2003) Yeast [PSI⁺] prion aggregates are formed by small Sup35 polymers fragmented by Hsp104. *J Biol Chem* 278: 49636-49643.
265. Sondheimer N, Lindquist S (2000) Rnq1: an epigenetic modifier of protein function in yeast. *Mol Cell* 5: 163-172.
266. Bagriantsev S, Liebman SW (2004) Specificity of prion assembly in vivo. [PSI⁺] and [PIN⁺] form separate structures in yeast. *J Biol Chem* 279: 51042-51048.
267. Douglas PM, Treusch S, Ren HY, Halfmann R, Duennwald ML, et al. (2008) Chaperone-dependent amyloid assembly protects cells from prion toxicity. *Proc Natl Acad Sci USA* 105: 7206-7211.
268. Treusch S, Lindquist S (2012) An intrinsically disordered yeast prion arrests the cell cycle by sequestering a spindle pole body component. *J Cell Biol* 197: 369-379.
269. Corley SM, Gready JE (2008) Identification of the RGG box motif in shadoo: RNA-binding and signaling roles? *Bioinform Biol Insights* 2: 383-400.
270. Morgan CE, Meagher JL, Levengood JD, Delproposto J, Rollins C, et al. (2015) The first crystal structure of the UP1 domain of hnRNP A1 bound to RNA reveals a new look for an old RNA binding protein. *J Mol Biol* 427: 3241-3257.
271. Buratti E, Baralle FE (2001) Characterization and functional implications of the RNA binding properties of nuclear factor TDP-43, a novel splicing regulator of CFTR exon 9. *J Biol Chem* 276: 36337-36343.
272. Melamed D, Young DL, Gamble CE, Miller CR, Fields S (2013) Deep mutational scanning of an RRM domain of the *Saccharomyces cerevisiae* poly(A)-binding protein. *RNA* 19: 1537-1551.
273. Caponigro G, Parker R (1996) Mechanisms and control of mRNA turnover in *Saccharomyces cerevisiae*. *Microbiol Rev* 60: 233-249.
274. Mangus DA, Evans MC, Jacobson A (2003) Poly(A)-binding proteins: multifunctional scaffolds for the post-transcriptional control of gene expression. *Genome Biology* 4: 223-223.
275. Raju KK, Natarajan S, Kumar NS, Kumar DA, NM R (2015) Role of cytoplasmic deadenylation and mRNA decay factors in yeast apoptosis. *FEMS Yeast Res* 15: fou006.
276. Sachs AB, Davis RW (1989) The poly(A) binding protein is required for poly(A) shortening and 60S ribosomal subunit-dependent translation initiation. *Cell* 58: 857-867.
277. Brengues M, Parker R (2007) Accumulation of polyadenylated mRNA, Pab1p, eIF4E, and eIF4G with P-Bodies in *Saccharomyces cerevisiae*. *Mol Biol Cell* 18: 2592-2602.

278. Buchan JR, Yoon JH, Parker R (2011) Stress-specific composition, assembly and kinetics of stress granules in *Saccharomyces cerevisiae*. *J Cell Sci* 124: 228-239.
279. Montero-Lomelí M, Morais BLB, Figueiredo DL, Neto DCS, Martins JRP, et al. (2002) The initiation factor eIF4A is involved in the response to lithium stress in *Saccharomyces cerevisiae*. *J Biol Chem* 277: 21542-21548.
280. Sen ND, Zhou F, Ingolia NT, Hinnebusch AG (2015) Genome-wide analysis of translational efficiency reveals distinct but overlapping functions of yeast DEAD-box RNA helicases Ded1 and eIF4A. *Genome Research* 25: 1196-1205.
281. Mazroui R, Sukarieh R, Bordeleau M-E, Kaufman RJ, Northcote P, et al. (2006) Inhibition of ribosome recruitment induces stress granule formation independently of eukaryotic initiation factor 2 α phosphorylation. *Mol Biol Cell* 17: 4212-4219.
282. Teixeira D, Parker R (2007) Analysis of P-body assembly in *Saccharomyces cerevisiae*. *Mol Biol Cell* 18: 2274-2287.
283. Ralser M, Albrecht M, Nonhoff U, Lengauer T, Lehrach H, et al. (2005) An integrative approach to gain insights into the cellular function of human Ataxin-2. *J Mol Biol* 346: 203-214.
284. Anderson JT, Paddy MR, Swanson MS (1993) PUB1 is a major nuclear and cytoplasmic polyadenylated RNA-binding protein in *Saccharomyces cerevisiae*. *Mol Cell Biol* 13: 6102-6113.
285. Duttagupta R, Tian B, Wilusz CJ, Khounh DT, Soteropoulos P, et al. (2005) Global analysis of Pub1p targets reveals a coordinate control of gene expression through modulation of binding and stability. *Mol Cell Biol* 25: 5499-5513.
286. Spiller MP, Boon K-L, Reijns MAM, Beggs JD (2007) The Lsm2-8 complex determines nuclear localization of the spliceosomal U6 snRNA. *Nucleic Acids Res* 35: 923-929.
287. Khalid MF, Damha MJ, Shuman S, Schwer B (2005) Structure-function analysis of yeast RNA debranching enzyme (Dbr1), a manganese-dependent phosphodiesterase. *Nucleic Acids Res* 33: 6349-6360.
288. Warde-Farley D, Donaldson SL, Comes O, Zuberi K, Badrawi R, et al. (2010) The GeneMANIA prediction server: biological network integration for gene prioritization and predicting gene function. *Nucleic Acids Res* 38: W214-W220.
289. Ingelfinger D, Arndt-Jovin DJ, Lührmann R, Achsel T (2002) The human LSm1-7 proteins colocalize with the mRNA-degrading enzymes Dcp1/2 and Xrn1 in distinct cytoplasmic foci. *RNA* 8: 1489-1501.
290. Tharun S, He W, Mayes AE, Lennertz P, Beggs JD, et al. (2000) Yeast Sm-like proteins function in mRNA decapping and decay. *Nature* 404: 515-518.
291. Wang Q, He J, Lynn B, Rymond BC (2005) Interactions of the yeast SF3b splicing factor. *Mol Cell Biol* 25: 10745-10754.
292. Crotti LB, Bačíková D, Horowitz DS (2007) The Prp18 protein stabilizes the interaction of both exons with the U5 snRNA during the second step of pre-mRNA splicing. *Genes Dev* 21: 1204-1216.
293. Saha D, Khandelia P, O'Keefe RT, Vijayraghavan U (2012) *Saccharomyces cerevisiae* NineTeen Complex (NTC)-associated factor Bud31/Ycr063w assembles on pre-catalytic spliceosomes and improves first and second step pre-mRNA splicing efficiency. *J Biol Chem* 287: 5390-5399.

294. van Roon A-MM, Yang J-C, Mathieu D, Bermel W, Nagai K, et al. (2015) (113)Cd NMR experiments reveal an unusual metal cluster in the solution structure of the yeast splicing protein Bud31p. *Angewandte Chemie (International Ed in English)* 54: 4861-4864.
295. Saha D, Banerjee S, Bashir S, Vijayraghavan U (2012) Context dependent splicing functions of Bud31/Ycr063w define its role in budding and cell cycle progression. *Biochem Biophys Res Commun* 424: 579-585.
296. Fica SM, Oubridge C, Galej WP, Wilkinson ME, Bai X-C, et al. (2017) Structure of a spliceosome remodelled for exon ligation. *Nature* 542: 377-380.
297. Flom G, Weekes J, Johnson JL (2005) Novel interaction of the Hsp90 chaperone machine with Ssl2, an essential DNA helicase in *Saccharomyces cerevisiae*. *Curr Genet* 47: 368-380.
298. Schmid AB, Lagleder S, Gräwert MA, Röhl A, Hagn F, et al. (2012) The architecture of functional modules in the Hsp90 co-chaperone Sti1/Hop. *EMBO J* 31: 1506-1517.
299. Shaner L, Wegele H, Buchner J, Morano KA (2005) The yeast Hsp110 Sse1 functionally interacts with the Hsp70 chaperones Ssa and Ssb. *J Biol Chem* 280: 41262-41269.
300. Mandal AK, Nillegoda NB, Chen JA, Caplan AJ (2008) Ydj1 protects nascent protein kinases from degradation and controls the rate of their maturation. *Mol Cell Biol* 28: 4434-4444.
301. Francis BR, Thorsness PE (2011) Hsp90 and mitochondrial proteases Yme1 and Yta10/12 participate in ATP synthase assembly in *Saccharomyces cerevisiae*. *Mitochondrion* 11: 587-600.
302. Borkovich KA, Farrelly FW, Finkelstein DB, Taulien J, Lindquist S (1989) hsp82 is an essential protein that is required in higher concentrations for growth of cells at higher temperatures. *Mol Cell Biol* 9: 3919-3930.
303. Nathan DF, Vos MH, Lindquist S (1997) In vivo functions of the *Saccharomyces cerevisiae* Hsp90 chaperone. *Proc Natl Acad Sci USA* 94: 12949-12956.
304. Taipale M, Jarosz DF, Lindquist S (2010) HSP90 at the hub of protein homeostasis: emerging mechanistic insights. *Nat Rev Mol Cell Biol* 11: 515-528.
305. Grandin N, Charbonneau M (2001) Hsp90 levels affect telomere length in yeast. *Mol Genet Genomics* 265: 126-134.
306. Lancaster DL, Dobson CM, Rachubinski RA (2013) Chaperone proteins select and maintain [PIN(+)] prion conformations in *Saccharomyces cerevisiae*. *J Biol Chem* 288: 1266-1276.
307. Wegele H, Haslbeck M, Reinstein J, Buchner J (2003) Sti1 is a novel activator of the Ssa proteins. *J Biol Chem* 278: 25970-25976.
308. Lee C-T, Graf C, Mayer FJ, Richter SM, Mayer MP (2012) Dynamics of the regulation of Hsp90 by the co-chaperone Sti1. *EMBO J* 31: 1518-1528.
309. Röhl A, Toppel F, Bender E, Schmid AB, Richter K, et al. (2015) Hop/Sti1 phosphorylation inhibits its co-chaperone function. *EMBO Reports* 16: 240-249.
310. Hoseini H, Pandey S, Jores T, Schmitt A, Franz-Wachtel M, et al. (2016) The cytosolic cochaperone Sti1 is relevant for mitochondrial biogenesis and morphology. *FEBS J* 283: 3338-3352.

311. Moosavi B, Wongwigkarn J, Tuite MF (2010) Hsp70/Hsp90 co-chaperones are required for efficient Hsp104-mediated elimination of the yeast [PSI⁺] prion but not for prion propagation. *Yeast* 27: 167-179.
312. Reidy M, Masison DC (2010) Sti1 regulation of Hsp70 and Hsp90 is critical for curing of *Saccharomyces cerevisiae* [PSI(+)] prions by Hsp104. *Mol Cell Biol* 30: 3542-3552.
313. Raviol H, Sadlish H, Rodriguez F, Mayer MP, Bukau B (2006) Chaperone network in the yeast cytosol: Hsp110 is revealed as an Hsp70 nucleotide exchange factor. *EMBO J* 25: 2510-2518.
314. Shaner L, Trott A, Goeckeler JL, Brodsky JL, Morano KA (2004) The function of the yeast molecular chaperone Sse1 is mechanistically distinct from the closely related Hsp70 family. *J Biol Chem* 279: 21992-22001.
315. O'Driscoll J, Clare D, Saibil H (2015) Prion aggregate structure in yeast cells is determined by the Hsp104-Hsp110 disaggregase machinery. *J Cell Biol* 211: 145-158.
316. Moran C, Kinsella GK, Zhang Z-R, Perrett S, Jones GW (2013) Mutational analysis of Sse1 (Hsp110) suggests an integral role for this chaperone in yeast prion propagation in vivo. *G3: Genes|Genomes|Genetics* 3: 1409-1418.
317. Reidy M, Sharma R, Shastry S, Roberts B-L, Albino-Flores I, et al. (2014) Hsp40s specify functions of Hsp104 and Hsp90 protein chaperone machines. *PLoS Genet* 10: e1004720.
318. Flom GA, Lemieszek M, Fortunato EA, Johnson JL (2008) Farnesylation of Ydj1 is required for in vivo interaction with Hsp90 client proteins. *Mol Biol Cell* 19: 5249-5258.
319. Sharma D, Stanley RF, Masison DC (2009) Curing of yeast [URE3] prion by the Hsp40 cochaperone Ydj1p is mediated by Hsp70. *Genetics* 181: 129-137.
320. Caplan AJ, Cyr DM, Douglas MG (1992) YDJ1p facilitates polypeptide translocation across different intracellular membranes by a conserved mechanism. *Cell* 71: 1143-1155.
321. Becker J, Walter W, Yan W, Craig EA (1996) Functional interaction of cytosolic hsp70 and a DnaJ-related protein, Ydj1p, in protein translocation in vivo. *Mol Cell Biol* 16: 4378-4386.
322. Lee DH, Sherman MY, Goldberg AL (1996) Involvement of the molecular chaperone Ydj1 in the ubiquitin-dependent degradation of short-lived and abnormal proteins in *Saccharomyces cerevisiae*. *Mol Cell Biol* 16: 4773-4781.
323. Glover JR, Lindquist S (1998) Hsp104, Hsp70, and Hsp40: a novel chaperone system that rescues previously aggregated proteins. *Cell* 94: 73-82.
324. Lian H-Y, Zhang H, Zhang Z-R, Loovers HM, Jones GW, et al. (2007) Hsp40 interacts directly with the native state of the yeast prion protein Ure2 and inhibits formation of amyloid-like fibrils. *J Biol Chem* 282: 11931-11940.
325. Cary GA, Vinh DBN, May P, Kuestner R, Dudley AM (2015) Proteomic analysis of Dhh1 complexes reveals a role for Hsp40 chaperone Ydj1 in yeast P-body assembly. *G3: Genes|Genomes|Genetics* 5: 2497-2511.
326. Walters RW, Muhlrad D, Garcia J, Parker R (2015) Differential effects of Ydj1 and Sis1 on Hsp70-mediated clearance of stress granules in *Saccharomyces cerevisiae*. *RNA* 21: 1660-1671.

327. Wilusz JE, Sunwoo H, Spector DL (2009) Long noncoding RNAs: functional surprises from the RNA world. *Genes Dev* 23: 1494-1504.
328. Yamashita A, Shichino Y, Yamamoto M (2016) The long non-coding RNA world in yeasts. *Biochim Biophys Acta, Gene Regul Mech* 1859: 147-154.
329. Hong E-JE, Roeder GS (2002) A role for Ddc1 in signaling meiotic double-strand breaks at the pachytene checkpoint. *Genes Dev* 16: 363-376.
330. Fingerman IM, Sutphen K, Montano SP, Georgiadis MM, Vershon AK (2004) Characterization of critical interactions between Ndt80 and MSE DNA defining a novel family of Ig-fold transcription factors. *Nucleic Acids Res* 32: 2947-2956.
331. Murata S, Yashiroda H, Tanaka K (2009) Molecular mechanisms of proteasome assembly. *Nat Rev Mol Cell Biol* 10: 104-115.
332. Horowitz DS, Krainer AR (1997) A human protein required for the second step of pre-mRNA splicing is functionally related to a yeast splicing factor. *Genes Dev* 11: 139-151.
333. Morales JC, Richard P, Rommel A, Fattah FJ, Motea EA, et al. (2014) Kub5-Hera, the human Rtt103 homolog, plays dual functional roles in transcription termination and DNA repair. *Nucleic Acids Res.*
334. Jäntti J, Lahdenranta J, Olkkonen VM, Söderlund H, Keränen S (1999) SEM1, a homologue of the split hand/split foot malformation candidate gene Dss1, regulates exocytosis and pseudohyphal differentiation in yeast. *Proc Natl Acad Sci USA* 96: 909-914.
335. Wang Y, Niu Y, Li B (2015) Balancing acts of SRI and an auto-inhibitory domain specify Set2 function at transcribed chromatin. *Nucleic Acids Res.*
336. Cherry JM, Hong EL, Amundsen C, Balakrishnan R, Binkley G, et al. (2012) *Saccharomyces Genome Database: the genomics resource of budding yeast.* *Nucleic Acids Res* 40: D700-D705.
337. Huh W-K, Falvo JV, Gerke LC, Carroll AS, Howson RW, et al. (2003) Global analysis of protein localization in budding yeast. *Nature* 425: 686-691.
338. Silva A, Sampaio-Marques B, Fernandes Â, Carreto L, Rodrigues F, et al. (2013) Involvement of yeast HSP90 isoforms in response to stress and cell death induced by acetic acid. *PLoS ONE* 8: e71294.
339. Lin Y, Protter DS, Rosen MK, Parker R (2015) Formation and maturation of phase-separated liquid droplets by RNA-binding proteins. *Mol Cell* 60: 208-219.
340. Bolognesi B, Lorenzo Gotor N, Dhar R, Cirillo D, Baldrighi M, et al. (2016) A concentration-dependent liquid phase separation can cause toxicity upon increased protein expression. *Cell Rep* 16: 222-231.
341. Altmann M, Müller PP, Wittmer B, Ruchti F, Lanker S, et al. (1993) A *Saccharomyces cerevisiae* homologue of mammalian translation initiation factor 4B contributes to RNA helicase activity. *EMBO J* 12: 3997-4003.
342. Park E-H, Walker SE, Zhou F, Lee JM, Rajagopal V, et al. (2013) Yeast eukaryotic initiation factor 4B (eIF4B) enhances complex assembly between eIF4A and eIF4G in vivo. *J Biol Chem* 288: 2340-2354.
343. Matsuo R, Mizobuchi S, Nakashima M, Miki K, Ayusawa D, et al. (2017) Central roles of iron in the regulation of oxidative stress in the yeast *Saccharomyces cerevisiae*. *Curr Genet*: 1-13.

344. Puig S, Askeland E, Thiele DJ (2005) Coordinated remodeling of cellular metabolism during iron deficiency through targeted mRNA degradation. *Cell* 120: 99-110.
345. Castells-Roca L, Pijuan J, Ferrezuelo F, Bellí G, Herrero E (2016) Cth2 protein mediates early adaptation of yeast cells to oxidative stress conditions. *PLoS ONE* 11: e0148204.
346. Rendl LM, Bieman MA, Smibert CA (2008) *S. cerevisiae* Vts1p induces deadenylation-dependent transcript degradation and interacts with the Ccr4p-Pop2p-Not deadenylase complex. *RNA* 14: 1328-1336.
347. Kessler MM, Henry MF, Shen E, Zhao J, Gross S, et al. (1997) Hrp1, a sequence-specific RNA-binding protein that shuttles between the nucleus and the cytoplasm, is required for mRNA 3'-end formation in yeast. *Genes Dev* 11: 2545-2556.
348. Haimovich G, Medina Daniel A, Causse Sebastien Z, Garber M, Millán-Zambrano G, et al. (2013) Gene expression is circular: factors for mRNA degradation also foster mRNA synthesis. *Cell* 153: 1000-1011.
349. Sayani S, Chanfreau GF (2012) Sequential RNA degradation pathways provide a fail-safe mechanism to limit the accumulation of unspliced transcripts in *Saccharomyces cerevisiae*. *RNA* 18: 1563-1572.
350. Abisambra JF, Jinwal UK, Suntharalingam A, Arulselvam K, Brady S, et al. (2012) DnaJA1 antagonizes constitutive Hsp70-mediated stabilization of tau. *J Mol Biol* 421: 653-661.
351. Evans CG, Wisen S, Gestwicki JE (2006) Heat shock proteins 70 and 90 inhibit early stages of amyloid beta-(1-42) aggregation in vitro. *J Biol Chem* 281: 33182-33191.
352. Duennwald ML, Jagadish S, Muchowski PJ, Lindquist S (2006) Flanking sequences profoundly alter polyglutamine toxicity in yeast. *Proc Natl Acad Sci USA* 103: 11045-11050.
353. Wolfe KJ, Ren HY, Trepte P, Cyr DM (2013) The Hsp70/90 cochaperone, Sti1, suppresses proteotoxicity by regulating spatial quality control of amyloid-like proteins. *Mol Biol Cell* 24: 3588-3602.
354. Wang H, Lu M, Yao M, Zhu W (2016) Effects of treatment with an Hsp90 inhibitor in tumors based on 15 phase II clinical trials. *Mol Clin Oncol* 5: 326-334.
355. Waza M, Adachi H, Katsuno M, Minamiyama M, Sang C, et al. (2005) 17-AAG, an Hsp90 inhibitor, ameliorates polyglutamine-mediated motor neuron degeneration. *Nat Med* 11: 1088-1095.
356. Auluck PK, Bonini NM (2002) Pharmacological prevention of Parkinson disease in *Drosophila*. *Nat Med* 8: 1185-1186.
357. Gietz RD, Schiestl RH (2007) High-efficiency yeast transformation using the LiAc/SS carrier DNA/PEG method. *Nat Protoc* 2: 31-34.
358. Halfmann R, Lindquist S (2008) Screening for amyloid aggregation by semi-denaturing detergent-agarose gel electrophoresis. *Journal of Visualized Experiments : JoVE*: 838.
359. Seither Katelyn M, McMahan Heather A, Singh N, Wang H, Cushman-Nick M, et al. (2014) Specific aromatic foldamers potently inhibit spontaneous and seeded A β 42 and A β 43 fibril assembly. *Biochem J* 464: 85-98.

360. Tong AH, Boone C (2006) Synthetic genetic array analysis in *Saccharomyces cerevisiae*. *Methods Mol Biol* 313: 171-192.
361. Tong AHY, Evangelista M, Parsons AB, Xu H, Bader GD, et al. (2001) Systematic genetic analysis with ordered arrays of yeast deletion mutants. *Science* 294: 2364-2368.
362. Tong AHY, Lesage G, Bader GD, Ding H, Xu H, et al. (2004) Global mapping of the yeast genetic interaction network. *Science* 303: 808-813.
363. Armakola M, Hart MP, Gitler AD (2011) TDP-43 toxicity in yeast. *Methods* 53: 238-245.
364. Collins SR, Schuldiner M, Krogan NJ, Weissman JS (2006) A strategy for extracting and analyzing large-scale quantitative epistatic interaction data. *Genome Biology* 7: R63-R63.
365. Jinek M, Chylinski K, Fonfara I, Hauer M, Doudna JA, et al. (2012) A programmable dual-RNA-guided DNA endonuclease in adaptive bacterial immunity. *Science* 337: 816-821.
366. Perrimon N, Ni JQ, Perkins L (2010) In vivo RNAi: today and tomorrow. *Cold Spring Harb Perspect Biol* 2: a003640.
367. Chery J (2016) RNA therapeutics: RNAi and antisense mechanisms and clinical applications. *Postdoc journal: a journal of postdoctoral research and postdoctoral affairs* 4: 35-50.
368. Chapman KB, Boeke JD (1991) Isolation and characterization of the gene encoding yeast debranching enzyme. *Cell* 65: 483-492.
369. Wilusz JE, Sharp PA (2013) Molecular biology. A circuitous route to noncoding RNA. *Science* 340: 440-441.
370. Parenteau J, Durand M, Véronneau S, Lacombe A-A, Morin G, et al. (2008) Deletion of many yeast introns reveals a minority of genes that require splicing for function. *Mol Biol Cell* 19: 1932-1941.
371. Ben-Aroya S, Coombes C, Kwok T, O'Donnell KA, Boeke JD, et al. (2008) Toward a comprehensive temperature-sensitive mutant repository of the essential genes of *Saccharomyces cerevisiae*. *Mol Cell* 30: 248-258.
372. Wheeler JR, Matheny T, Jain S, Abrisch R, Parker R (2016) Distinct stages in stress granule assembly and disassembly. *eLife* 5: e18413.
373. Vieira NM, Naslavsky MS, Licinio L, Kok F, Schlesinger D, et al. (2014) A defect in the RNA-processing protein HNRPD1 causes limb-girdle muscular dystrophy 1G (LGMD1G). *Hum Mol Genet* 23: 4103-4110.